The detection of dynamic voltage collapse and transfer margin estimation

by

Bo Long

A thesis submitted to the graduate faculty

in partial fulfillment of the requirements for the degree of

MASTER OF SCIENCE

Major: Electrical Engineering

Major Professor: Venkataramana Ajjarapu

Iowa State University

Ames, Iowa

1997

Graduate College
Iowa State University

This is to certify that the Master's thesis of

Bo Long

has met the thesis requirements of Iowa State University

Signatures have been redacted for privacy

DEDICATED TO MY PARENTS

TABLE OF CONTENTS

LIST OF FIGURES

1 INTRODUCTION

The North American interconnected power system is the largest machine ever devised. It is truly amazing that such a system has operated with a high degree of reliability for over a century.

People in the power industry have always been trying to make full use of the interconnected system for economy and security. For instance, it is always desired to transfer power between different parties in the system for economic reasons. However, there are limitations on this transfer. Some of these limitations are listed below:

- Thermal loading capacity of transmission lines
- Bus voltage levels
- Stability constraints
  - Transient stability
  - Small signal (dynamic) stability
    - Oscillatory stability
    - Aperiodic stability

In the operation of power systems, stability has always been, and will remain a challenge for a foreseeable future and, indeed, is likely to increase in importance.

Power system stability [1] may be generally defined as that property of a power system that enables it to remain in a stable operating equilibrium under normal operating conditions and regain an acceptable state of equilibrium after being subjected to a disturbance.

Power transmission capability has traditionally been limited either by rotor angle (synchronous) stability or by thermal loading capacities. The blackout problem has been associated with transient stability; fortunately this problem is now diminished by fast short circuit clearing, powerful excitation systems, and various special stability controls.

Voltage (load) stability, however, is now a major concern in planning and operating electric power systems. The main factor causing instability is the inability of the power system to meet the demand for reactive power. The heart of the issue is usually the voltage drop that occurs when active power and reactive power flow through the inductive reactances associated with the transmission network. Many electric utilities are facing voltage-imposed limits. One reason is the need for more intensive use of available transmission facilities as a consequence of load growth coupled with the economies of long distance energy exchange. This usually leads to a typical scenario of voltage collapse. Things became even more critical with the advent of power industry deregulation.

During 1993, the electric power industry in the US started a series of unprecedented changes as a result of the Energy Policy Act of 1992. It promotes wholesale competition through open access and encourages non-discriminatory transmission services by public utilities. As a consequence, the transmission systems are being required to accommodate flow patterns for which they were not originally designed. The resultant increased use of existing transmission is made possible in part, by reactive power compensation which is inherently less robust than "wire-in-the-air" [2]. Therefore, this newly formed competitive environment may lead to frequent violations of transfer capability limits. The two recent western blackouts [3] in late 1996 have been recognized as voltage related. The blackouts revealed the importance of incorporating dynamic voltage stability constraints in operation and planning studies.

With these considerations, this thesis concentrates on the aspect of small signal (dynamic) stability constraints on the transfer capability of transmission systems, particularly, from a voltage stability (collapse type) point of view.

1.1 Solution of Nonlinear Equations

A power system is a typical nonlinear dynamic system which can be described by a set of differential and algebraic equations(DAEs). The steady state description, therefore, is typically a set of nonlinear algebraic equations. In power system analysis, one often needs to solve these equations. Part of this set of nonlinear algebraic equations usually come in the form of power flow. Providing a robust numerical solver for these nonlinear power flow equations is crucial. The existence of a complete steady state solution of the DAE model essentially rests upon the existence of a power flow solution. Power system optimization is yet another example which often leads to the problem of solving some nonlinear algebraic equations.

The most frequently used algorithms in solving nonlinear algebraic equations are those of the Newton type. The fast (quadratic) convergence of Newton's method is the reason for its unchallengeable popularity. However, though an unquestionable powerful tool, it needs a good starting point. The initial guess of the solution to start the iteration needs to be within the so-called radius of convergence. Sometimes, looking for a good initial guess is not a trivial task. A second problem is the ill-conditioning of the iterative Jacobian for a heavily loaded network. This often leads to poor convergence of the method since the Jacobian may become nearly singular.

Fortunately, these problems, as will be addressed in chapter 2, can be overcome by some advanced numerical techniques, namely, the homotopy and continuation methods.

1.2 Detection of Voltage Collapse

A brief qualitative description of voltage collapse phenomena is given in section 1.1. However, a robust quantitative measure to identify voltage collapse in planning and operation studies is needed. Before going into a discussion about voltage collapse detection, let us first review some of the definitions related to voltage stability as developed by the IEEE and the CIGRÉ [4, 5, 2]:

- *Small disturbance voltage stable*

  A power system at a given operating state is *small-disturbance voltage stable* if, following

any small disturbance, voltages near loads are identical or close to the pre-disturbance values. (Small-disturbance voltage stability corresponds to a related linearized dynamic model with eigenvalues having negative real parts. This dynamic model will be introduced in chapter 3.)

- *Voltage collapse*

  A power system enters a state of *voltage collapse* when a disturbance, increase in load demand, or change in system condition causes a progressive and uncontrollable drop in voltage. Voltage collapse may be total (blackout) or partial.

With these definitions in mind, we will briefly touch upon the different techniques used in recent years for voltage collapse identification. As mentioned earlier, a power system, as a typical nonlinear dynamic system, is described by a set of DAEs. The different methods for stability analysis, based on how the DAE model is treated, can be classified into the following three groups.

1.2.1 Power Flow Based Approach

In this approach, the dynamic part of the DAE model is ignored. The point of the singularity of the power flow Jacobian is deemed the point of voltage collapse. There are unreasonable (slack bus and PV bus) assumptions used in representing the system by the power flow model. In general, the singularity of the power flow Jacobian does not indicate instability. This will be further explained in chapter 3.

1.2.2 Nonlinear Large Disturbance Analysis

When the power system is subjected to large perturbations such as short circuits, nonlinear analysis with the DAE model is needed. Time domain simulation has to be applied to capture the true picture of the phenomenon. The first step in this approach is to find the numerical solutions for the state variables after the system is subjected to certain disturbances. The initial conditions usually come from the power flow, which is a part of the complete steady state description of the whole system. The second phase in time domain simulation involves

extensive output analysis using the data generated from the simulation programs. Important quantities such as voltages at critical buses or system frequency are displayed. By observing the selected system states evolution curves, one can identify the area of voltage problems. Information like stability margin is determined at the end of simulation.

Time domain simulation, in which appropriate modeling is included, captures the events and their chronology leading to instability and, thus, is useful for detailed study of specific voltage collapse situations, coordination of protection and controls, and testing of remedial measures. However it is very time consuming and requires extensive output analysis. It also does not readily provide sensitivity information and the degree of instability.

1.2.3 Small Signal (Dynamic) Voltage Stability Analysis

When the system is under small disturbances, such as gradual increase of load, the original nonlinear DAE model can be linerized around the specified operating point. When the algebraic constraints are incorporated into the differential part of the model, dynamic stability can be analyzed by checking the eigenvalues of the system state matrix (to be defined in chapter 3). The problems with this approach is that eigenvalue computation is very expensive and thus is very demanding for large power system studies.

1.2.4 Need for Alternatives

The power flow based approach often masks some important dynamics associated with voltage instability. Nonlinear time domain simulation or eigenvalue computation based dynamic analysis is too cost intensive. Even if the computational burden would not be of concern, there is still another problem with either the time domain simulation or the eigen-analysis approach. It is that the power flow is used to generate the steady state solution of the complete DAE system. As will be shown later, the power flow description of the system is very different from that in dynamic analysis. This inconsistent description may give wrong results. Therefore, it is of great interest to develop a methodology in which the system dynamics is reasonably represented and the associated analysis does not require too much computational burden, and

the problem of inconsistent description of the system can be rectified. A new approach has been developed to overcome these shortcomings. It is addressed in chapter 3.

1.3 Sensitivity Analysis and Transfer Margin Estimation

In power system planning and operation studies, the detection of voltage collapse is only part of the work facing the engineers. To avoid voltage collapse, it is necessary to investigate the contributing factors that lead to instability. Effective controls need to be designed to prevent the system from collapsing. Information about what controls are effective and where to locate them is very useful. Sensitivity based approaches are very useful in addressing the above problem.

Sometimes sensitivity is defined for evaluating general system performance, such as parametric sensitivity. It indirectly relates to stability since system degradation eventually will lead to collapse if no preventive measures are applied. More often the sensitivity is defined with respect to certain stability indices which are intended for determining the degree of stability. The stability index can be given state based, requiring only information from the current operating point, or large deviation based, which also requires a knowledge about the critical point. The latter accounts for nonlinearities caused by larger disturbances or load increases. A link between a given state index and a large deviation based index is needed if it is desired that the sensitivity can be used quantitatively to predict the effectiveness of the particular controls applied. Using this kind of quantitative sensitivity measure, one will then be able to further apply the methodology to estimate transfer margin as limited by voltage collapse, without actually re-computing the P-V curves. Further, if system dynamics are of concern, the sensitivity of a stability index should be defined with respect to the DAE model of the power system. In chapter 4, these issues are addressed in detail. A new sensitivity measure is developed and used to estimate the transfer margin as limited by dynamic voltage collapse.

1.4 Scope of The Work and Thesis Outline

An effective approach to identify dynamic voltage collapse is developed here. It is called the simultaneous equilibria tracing technique. Eigenvalue computation is avoided while a full dynamic analysis is conducted on the DAE model of the power system. The inconsistency of the power flow description of the dynamic part of the system when producing the equilibria for nonlinear or small signal stability analysis is resolved in the new approach. An effective way of incorporating system limits is introduced and it is shown that the total system Jacobian is valid for both Newton-Raphson iteration and voltage collapse identification.

The *invariant subspace parametric sensitivity (ISPS)* is a general sensitivity measure which can be applied to identify the critical components of the system that most affect voltage stability. A sparse formulation is derived for computing the measure of ISPS. A quantitative sensitivity index is further derived from the measure of ISPS. It is used to estimate the transfer margin. This index makes it possible to quantify the effectiveness of controls in terms of real power transfer margin increase.

The outline of the thesis is as follows. In chapter 2, a critical review of the application of two robust numerical methods for solving nonlinear algebraic equations, namely, homotopy and continuation, is given. Clarification of conceptual differences is made to give a clear picture of potential applications of the methods to power system analysis. In chapter 3, a further extension of the continuation technique is given to detect dynamic voltage collapse. This methodology does not require the formation of the system state matrix and the computation of its eigenvalues. In chapter 4, a quantitative sensitivity index is derived and applied to voltage stability margin estimation. Conclusions and suggestions for future work are given in chapter 5.

2 NUMERICAL METHODS FOR NONLINEAR EQUATIONS

As mentioned in chapter 1, many problems in power system analysis involve the solution of nonlinear algebraic equations. Examples are those from power flow related or optimization problems. A robust numerical solver is indispensable and sometimes determines the success of the whole solution to the problem. To this end, we may apply some advanced numerical techniques, namely, homotopy and continuation, with which the drawbacks of conventional methods can be overcome. This chapter first briefly presents the basic concepts, principles, and methods of homotopy and continuation. Their interplay is also clearly described so that one can understand and grasp the essence of both the methods. Then a critical review of the application of these methods to the power system problems is given.

2.1 Problem Statement

The problem of determining the roots of nonlinear equations is of frequent occurrence in scientific work. Such equations typically arise in connection with equilibrium problems. When describing a real life problem, the nonlinear equations usually involve one or more parameters. Denoting one such parameter by α, the nonlinear equations read:

$$f(y, \alpha) = 0 \tag{2.1}$$

where f: $R^n \times R \rightarrow R^n$ is a mapping which is assumed to be smooth. In equation 2.1, $\alpha = 0$ usually corresponds to the base case solution. If a priori knowledge concerning zero points of f is available, it is advisable to calculate y via a Newton type algorithm defined by an iteration formula such as:

$$y_{i+1} = y_i - A_i^{-1} f(y_i, 0) \tag{2.2}$$

where A_i is some reasonable approximation of the Jacobian $f_y(y_i, 0)$. However, if an adequate starting value for a Newton type iteration method is not available, we must seek other remedies. In section 2.2, we will introduce how this lack of knowledge for an initial guess can be tackled by the homotopy method.

Because the systems described by 2.1 depend on α, we speak of a family of nonlinear equations. Solutions now depend on the parameter α, i.e., $y(\alpha)$. Upon varying the parameter α, we will get a series of solutions. This is often called a solution curve. At each point corresponding to a certain α_k, if we keep solving 2.1 via the conventional Newton type iteration, i.e., by formula 2.2, we may run into difficulty due to the singularity of the Jacobian $f_y(y, \alpha_k)$. The singularity occurs at a so-called turning point when the equation is parameterized with respect to α. In the subsequent sections, we will discuss the interesting topic of curve tracing via the continuation method. We will show how the problem of singularity of the Jacobian can be resolved, namely, by switching the continuation parameter. Section 2.4 will give an illustration of how the principles discussed in section 2.2 and 2.3 can be applied to power system analysis.

2.2 Homotopy Method

We center our discussion on obtaining a solution to a system of n nonlinear equations in n variables described by equation 2.1 when α is a fixed value. The homotopy method first defines an easy problem for which a solution is known. Then it defines a path between this easy problem and the problem we actually want to solve. This easy problem, with which the homotopy method starts, is gradually transformed to the solution of the hard problem. Mathematically, this means that one has to define a homotopy or deformation: $R^n \times R \to R^n$ such that

$$H(y, 0) = g(y) \qquad H(y, 1) = f(y) \tag{2.3}$$

where g is a trivial smooth map having known zero points and H is also smooth. Typically one may choose a convex homotopy such as

$$H(y, t) = (1 - t)g(y) + tf(y) \quad 0 \leq t \leq 1 \tag{2.4}$$

The problem $H(y,t) = 0$ is then solved for values t between 0 and 1. This is equivalent to tracing an implicitly defined curve (i.e. $H(y(t)) = 0$) from a starting point $(y^0, 0)$ to a solution point $(y^n, 1)$. Under certain conditions, $y(t)$ can be defined as (see Fig. 2.1):

$$\dot{y}(t) = -(H_y(t, y(t)))^{-1} H_t(t, y(t)) \tag{2.5}$$

If this succeeds, then a zero point of f is obtained, i.e. $H(y,1) = f(y)$. However, one may suspect that this is an unnatural approach, since 2.5 seems to be a more complicated problem to solve than $H(y(t)) = 0$. But we should not lose sight of the fact that the solution curve $y(t)$ consists of zero points of H, and as such it enjoys the powerful local contractive properties with respect to iterative methods such as those of Newton type. Hence, one is led to numerically integrate 2.5 very coarsely, and then locally use an iterative method for solving $H(y(t)) = 0$ as a stabilizer. This is the general idea in the continuation methods with a predictor and corrector tracing scheme.

The relationship 2.4, which embeds the original problem in a family of problems, gives an

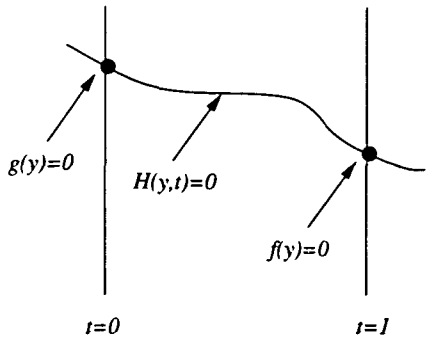

Figure 2.1 Homotopy curve

example of a homotopy that connects the two functions f and g. In general a homotopy can be any continuous connection between f and g. If such a map H exists, we say that f is homotopic to g. A good introduction to homotopy methods can be found in references [6, 7, 8, 9]. A simple two-dimensional nonlinear problem is given in Appendix A to illustrate how the homotopy method works.

Whether or not the tracing of a curve can succeed depends on the continuation strategy

employed. Whenever a homotopy is introduced, one will then need to to trace the homotopy curve from the easy start and arrive at the solution to the original problem. Figure 2.2 shows the relationship between homotopy and continuation. If the curve can be parameterized with respect to the parameter t, then the classical embedding algorithm [6] can be applied. In the following sections, we will discuss how a parameterization is done and how vital this procedure is to the continuation, or say to the curve tracing process. Particularly, we will show how the continuation is carried on even when the curve is not parameterizable with respect to a certain parameter.

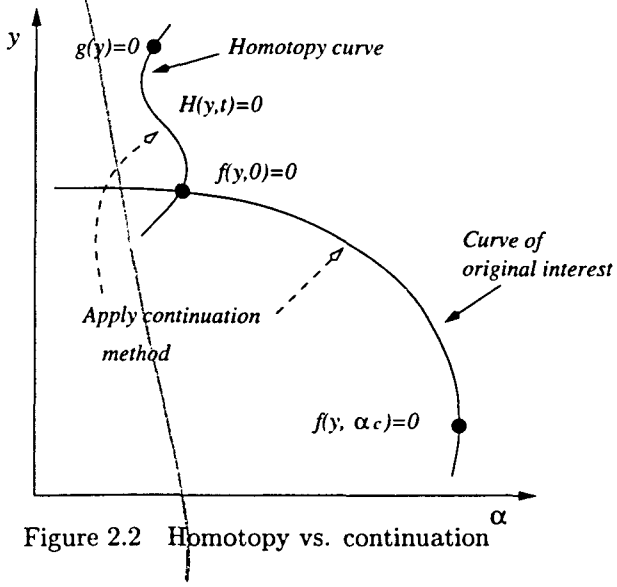

Figure 2.2 Homotopy vs. continuation

2.3 Continuation Methods

A general description of the different aspects of continuation methods in curve tracing is given below. [6, 10, 8, 11, 12] are good references for a detailed explanation of these methods. Brief but more pertinent exploration of applying the methodology to power system studies is given in section 2.4. The system of nonlinear equations in the form of equation 2.1 serves as a basis for discussion. One note is that, for the tracing of a curve defined by 2.4, the discussion is the same as for the curve defined by 2.1. Here, y denotes an n-dimensional vector.

Continuation methods usually consist of the following [12]: predictor, parameterization strategy, corrector, and step length control. Assume that at least one solution of equation

2.1 (for a particular α) has been calculated, for instance, by the homotopy method. For the tracing of a curve defined by 2.4, this corresponds to the assumption that g has a known zero point. The jth continuation step starts from a solution (y_j, α_j) of equation 2.1 and attempts to calculate the next solution (y_{j+1}, α_{j+1}) for the next α, namely, α_{j+1}. With a predictor-corrector method, the step j to step $j+1$ is split into two parts, with $(\overline{y}_j, \overline{\alpha}_j)$ produced in between by the prediction. In general, the predictor merely provides an initial guess for the corrector iterations that home in a solution of equation 2.1. The distance between two consecutive solutions is called the step size. In addition to equation 2.1, a relation that identifies the location of a solution on the branch is needed. This identification is closely related to the kind of parameterization strategy chosen to trace the curve.

In the curve tracing process, at some critical points (e.g. turning points), the singularity of the Jacobian matrix f_y often causes trouble either in the prediction or in the correction process. This means that the current continuation parameter has become ill-suited for parameterizing the curve. One way of overcoming this difficulty at turning points is to parameterize the curve by arclength. The augmented Jacobian can be nonsingular throughout the tracing process. However, in practical power system analysis, we always want to get as much useful information as possible during the continuation process. The arclength usually has a geometrical rather than a physical meaning, therefore we are often more interested in another important ODE-based predictor, i.e., the tangent predictor and the corresponding corrector with the curve locally parameterized at each step. This is deferred to section 2.4 with the power system example.

The efficiency in curve tracing is closely related to the step length control strategy. It is not difficult to choose a workable step size in practice, though some trial and error work is often required before the appropriate step size can be found. Step control often can be based on the estimates of the convergence quality of the corrector iteration. Reference [464] in [13] selects step size according to the number of corrector iterations. In general, the step length control scheme is problem dependent.

In a practical situation, such as in power systems, saddle node bifurcations, to which our

attention will mainly be given, are generic with the collapse type voltage problems. However, in some other situations, other bifurcations might occur more frequently and thus will be of greater interest. For instance, the type of bifurcation that connects equilibria with periodic motion, i.e., hopf bifurcation, is also generic. Problems, such as how to locate a hopf bifurcation point on the traced branch and the related topics are thoroughly treated in reference [13].

2.4 Applications to Power Systems

The first paper applying the curve tracing technique based on Davidenko's method [14] to power system analysis appeared in 1971 [15]. The authors in that reference used the ordinary differential equations method to trace the curve via the following formula:

$$\frac{dy}{d\alpha} = -f_y^{-1} f_\alpha \tag{2.6}$$

However, here, the singularity of f_y creates numerical problem. Continuation methods can well alleviate this problem. In recent years, many papers were published that applied the homotopy and continuation methods to power systems. To name a few, [16, 17, 18, 19, 20, 21], [22], [23], [24, 25, 26], [27, 28], [29, 30], [31, 32, 33, 34, 35], [36], [37], [38, 39], [40], [41], [42], [43], [15], [44]. The following section concentrates on the main aspects of these papers.

2.4.1 The Continuation Power Flow for Static Voltage Stability Analysis

The purpose of the continuation power flow is to find a continuum of power flow solutions for a given load change scenario. The CPF [19] is based on reference [11]. In order to incorporate the load and generation variation parameter α, the power flow equations are reformulated as follows:

$$\Delta P_i = P_{Gi0}(1 + \alpha K_{Gpi}) - P_{Li0}(1 + \alpha K_{lpi}) - P_{Ti} \tag{2.7}$$

$$\Delta Q_i = Q_{Gi} - Q_{Li0}(1 + \alpha K_{lqi}) - Q_{Ti} \tag{2.8}$$

where quantities with subscript 0 denote the base case generation and load. K_{Gpi}, K_{lpi}, and K_{lqi}, are multipliers corresponding to the rate of load change and generation following scenario. They usually vary with different load models and generation sharing schemes.

If f in 2.1 is used to denote the complete set of power flow equations, then to solve the problem, the continuation algorithm in CPF starts from a known solution and uses a predictor-corrector scheme to find the subsequent solutions at different loading levels.

Predictor: Once a base solution has been found ($\alpha = 0$), a prediction of the next solution can be made by taking appropriately sized steps in a direction tangential to the solution path. The tangent T is the solution of the linear system:

$$-\begin{bmatrix} f_y & f_\alpha \\ & e_k^T \end{bmatrix}\begin{bmatrix} dy \\ d\alpha \end{bmatrix} = \begin{bmatrix} 0 \\ \pm 1 \end{bmatrix} \tag{2.9}$$

Provided the full rank condition $\text{rank}(f_y, f_\alpha) = n$ holds along the whole branch, the above equation has a unique solution at any point on the branch (k may have to be changed to select a different continuation parameter at a particular step, especially at or near the turning point). It is known from [19] that a stability index and identification of weak buses can also be obtained from the tangent vector. Once the tangent vector has been found, the prediction can be easily made as:

$$(\overline{y}_{j+1}, \overline{\alpha}_{j+1}) = (y_j, \alpha_j) + \sigma_j T \tag{2.10}$$

where σ_j designates the step size.

Parameterization and the corrector: Now that a prediction has been made, a method of correcting the approximate solution is needed. Actually the best way to present this corrector is to expand on parameterization, which is vital to the process. Local parameterization looks promising here and thus is employed. In local parameterization, the local original set of equations is augmented by one equation that specifies the value of one of the state variables. In the case of the power system example, this means specifying either a bus voltage magnitude, a bus voltage angle, or the load parameter α as shown by the following equations:

$$\begin{bmatrix} f(\theta, v, \alpha) \\ Y_k - \eta \end{bmatrix} = 0 \qquad \textit{and} \qquad -\begin{bmatrix} f_y & f_\alpha \\ & e_k^T \end{bmatrix}\begin{bmatrix} \Delta\theta \\ \Delta v \\ \Delta\alpha \end{bmatrix} = \begin{bmatrix} f(\theta, v, \alpha) \\ 0 \end{bmatrix} \tag{2.11}$$

where $Y = (\theta, v, \alpha)$, $y = (\theta, v)$ and k is locally selected to make the continuation algorithm flexible. In the CPF, selection of the continuation parameter corresponds to the state variable

that has the largest tangent vector component. More simply put, this means to choose the state variable that has the greatest rate of change near a given solution as the next continuation parameter. Accordingly, a slightly modified Newton-Raphson iterative process can be used to solve the corrector equations. The corrector Jacobian can be seen to have the same form as the predictor Jacobian. This continuation parameter switching strategy can solve the singular Jacobian problem appearing at the critical points on the traced curve. The CPF is a powerful tool in static voltage stability studies. It has the ability to find a set of solutions from a base case up to the critical point in a single program run. Unlike conventional power flow programs, it can compute the power flow solution at or near the critical loading point where traditional programs often fail to converge or take longer times to find a solution. It also provides intermediate results which provide valuable insights into the voltage stability of the system and the areas prone to voltage collapse. Different variations of the continuation methods applied to the power system problems can be found in references [24, 28]. A one dimensional nonlinear problem is used in Appendix A to show the basic steps involved in continuation.

2.4.2 Homotopy Related Continuation in Voltage Stability Analysis

In section 2.2, we have given the basic ideas on when homotopy is needed, how it can be employed, and how it is related to continuation. Next we will discuss the application of homotopy related continuation in power flow curve tracing.

In power system analysis, specifically, in power flow studies, one could find a homotopy [40] which relates the power flow solutions to the variation of load and generation scenario parameters. The load and generation scenario from a base case condition is defined as:

$$Y_s(t) = Y_{s0} + tY_d \tag{2.12}$$

where

Y_{s0} : *specified base load*

Y_d : *load/generation pattern*

t : *homotopy scalar parameter*

By substituting equation 2.12 into the load flow equation, the homotopy equation is defined as:

$$H(x,t) = Y(x) - Y_s(t) \tag{2.13}$$

$$= Y(x) - Y_{s0} - tY_d = 0 \tag{2.14}$$

The solution of $H(x,t) = 0$ also provides a load flow solution for specified value $Y_s(t)$. To estimate a solution $(x_0 + \Delta x, t_0 + \Delta t)$ that adjoins a known solution (x_0, t_0), the linearized relations between Δx and Δt should satisfy equation 2.16, where J_{LF} means the Jacobian matrix used in conventional power flow problem.

$$H(x_0 + \Delta x, t_0 + \Delta t) = H(x_0, t_0) + H_x \Delta x + H_t \Delta t = 0 \tag{2.15}$$

$$H_x \Delta x + H_t \Delta t = 0 \qquad J_{LF} \Delta x - Y_d t = 0 \tag{2.16}$$

The intention here is to trace the curve of solutions from a base load condition at $t = 0$ to a critical load condition at $t = t_{max}$. As noted by the discusser of [40], however, in order to overcome the numerical difficulties at the turning point, one must rely on the different parameterizations of the nose curve to avoid small step sizes near the critical point and to allow the drawing of the nose curve to continue around the critical point. Here the homotopy function, which incorporates a load/generation parameter, is built in such a way that it corresponds to the original power flow equations at different load/generation levels. So the tracing of $H(x,t)$ will yield the PV or QV curve, which is the solution curve being sought. As stated in section 2.2, homotopy itself does not relate to any particular continuation method, rather, it leads to the problem of continuation or parameter study of the introduced homotopy function. Whether the homotopy function corresponds to the curve of original interest depends on how one formulates the problem. In most cases, unlike the above example, the homotopy continuation is led from a known solution of an easy problem not of original interest to the solution of the more difficult problem being studied. Therefore, a homotopy continuation process usually yields only one solution on the solution path of the original problem (see Fig. 2.2).

2.4.3 Direct Method in Computing the Saddle Node Bifurcation Point: A One Step Continuation

In section 2.3, discussion has been given to show that the tracing of a curve can be done via continuation. In subsection 2.4.1, we've shown how this is related to voltage stability studies, also there, we've noticed that, on the traced curve, a particular point, namely, the critical point, or sometimes called the saddle node bifurcation point, is often of greater interest. If we are only interested in locating this point with respect to α_c, or say, we are interested in the maximum allowable variation of α where the corresponding linearization (Jacobian) is singular, we have yet another approach available, i.e., the direct method [18, 21, 24, 25, 26, 27].

Saddle node bifurcations, as opposed to other kind of bifurcations, are typical in practice, and are mathematically characterized by the steady state Jacobian f_y having a simple and unique zero eigenvalue, with nonzero right eigenvector u and left eigenvector w. This condition can be summarized by the set of vector equations 2.17 for the right and left eigenvectors.

$$\begin{bmatrix} f(y,\alpha) \\ f_y(y,\alpha)u \\ u_k - 1 \end{bmatrix} = 0 \qquad or \qquad \begin{bmatrix} f(y,\alpha) \\ wf_y(y,\alpha) \\ w_k - 1 \end{bmatrix} = 0 \tag{2.17}$$

In 2.17, the original system of equations is augmented in such a way that for the enlarged system, the turning point becomes regular. Solving for 2.17 will yield the desired turning point.

Advantages: The direct method can find the critical point where the Jacobian is singular by solving the enlarged system of power flow equations in one step. The left and right eigenvectors produced in the direct approach carry very important information. For instance, it was shown that, at saddle node bifurcations, the right eigenvector corresponding to the zero eigenvalue gives the trajectory of the system state variables [35]. The left eigenvector can be used to construct a normal vector [31, 32, 33, 34] on the bifurcation hypersurface. This will be discussed in the next subsection.

Limitations: In the direct approach, for a successful convergence, a good initial guess is needed. This method basically doubles the number of equations to be solved. However, some

of these shortcomings can be overcome by following the approach proposed in reference [45]. In that paper, the authors explored the structure of equation 2.17. It was shown that the whole system can be resolved into four linear subsystems, each with the same coefficient matrix. Reference [21] applied this method to power system voltage stability studies. Reference [24] gives a comparison of the continuation method with the direct method.

2.4.4 Continuation Towards a Closest Saddle Node Bifurcation

In subsections 2.4.1 and 2.4.2, we have shown how to trace a PV curve. For instance, starting from a known solution, employing the CPF algorithm, we may trace the entire PV curve without any numerical difficulty. We may also choose the direct method to locate the critical point if we don't need the entire curve. However, one might have found that the produced PV curve must correspond to a particular load increase and generation sharing scheme. But in practical power system operations, the load increase and generation sharing scheme may change at will, and thus it's often more preferable to find a closest saddle node bifurcation point [31, 32, 33, 34, 23, 42, 44] at which the critical loading is met without the need for specifying the scenario. It is even so when transmission systems become more open, resulting an increase in potentially harmful third party transactions of which the operator may have little knowledge or control.

In computing the closest saddle node bifurcation point, an iterative method [31, 32, 33] can be used. The iteration to compute a closest saddle node bifurcation has two main steps (see Fig. 2.3): In the first step, the standard methods for finding the saddle node bifurcations along a given ray of operation direction, e.g., by the CPF method, direct method, or the homotopy method can be used. In the second step, the direction of the ray is updated, which is parallel to the normal vector n defined as [31]:

$$n = w f_L \tag{2.18}$$

where w is the left eigenvector corresponding to the zero eigenvalue at the bifurcation point and f_L the Jacobian of f with respect to L, the loading vector. Based on the information gathered at the ith iteration, n_i is updated to n_{i+1} so that a closer saddle node bifurcation point can be

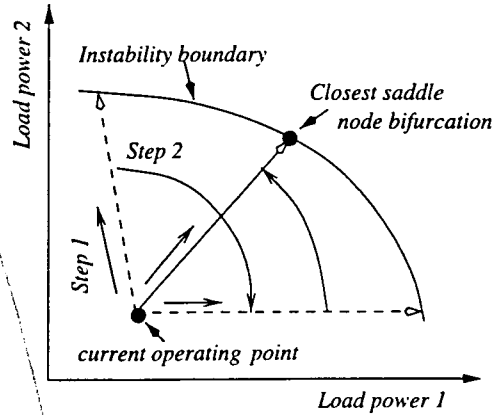

Figure 2.3 Closest bifurcation

found. Hopefully the iteration will succeed, and the ray will converge to a direction in which a locally closest saddle node bifurcation will be met. The way to update the ray direction is not unique, which leads to different algorithms. Some methods use the normal vector to the hypersurface Σ of saddle node bifurcation points at $L(n_i)$ as the new ray direction n_{i+1} [31], while others use quasi-Newton approach to update n_i [42]. It is shown in [42] that the former approach may result in slow convergence. This is because only the first order derivatives of the function denoting the distance between the operating point at L_0 and a saddle node bifurcation point at $L(n)$ along n_i are used. In the latter method, a quadratic function $s_i(n)$ denoting the distance is constructed. Finding the local closest saddle node bifurcation will correspond to a constrained optimization problem of minimizing $s_i(n)$. Because the latter approach in updating the direction of the ray is based on the approximations to the second order as well as the first order derivatives of the distance function $s_i(n)$, it may give better convergence.

In reference [44], the authors used the multiple power flow method to approximate a closest loadability limit.

Advantages: The normal vector to the bifurcation surface in the parameter space provides very valuable information for designing preventive and corrective controls. There have been reports about its applications to power systems [29, 30]. When the current operating point is close to the instability boundary, the above mentioned iteration usually can well converge to the closest saddle node bifurcation points. And with this information, the system operator

can then take appropriate measures to prevent the system from approaching the possible worst case voltage collapse.

Limitations: In practical operations, the system topological structure will change during system contingencies that will change the security boundary greatly. For successful convergence of the iterative method, it is often required that it starts from a point close to the instability boundary. And the boundary should not be too curved, otherwise divergence may occur. Also, the worst case load/generation scenario might be the one which would not be chosen by the system operator for economical or other secure operation considerations. The optimal corrective control direction [33], related to the closest bifurcation, might still be impractical. This is because it often involves changes in power injections at a large percentage of system buses, and further, in implementing such preventive control, neither cost nor the availability of such control measures has been considered. In other words, it almost always involves the load shedding at junction buses with no actual load, or requires reactive power support at buses with no reactive compensation devices available. However, one can consider these constraints, but in that case the solution may be sub-optimal but still very meaningful for system analysis and operations.

2.4.5 The Optimal Continuation Power Flow: Continuation in OPF Studies

An optimal power flow (OPF) solution gives the optimal active and reactive power dispatch, and the optimal settings of all controllable variables for a static power system loading condition. The OCPF method [16, 17] uses the systematic approach of the continuation technique to provide a series of solutions for the increased transfer or load level. The OCPF starts at the given base load using a gradient based optimization technique. It consists of the following two parts: the continuation process and the optimization process, the first of which is nearly the same as in the CPF and its corrected output is fed into the optimization process. During the optimization process, the corrected solution is iteratively optimized in steps via a gradient based optimization technique. Once the optimal solution is obtained, the output is fed back into the continuation process so that the next solution can be predicted. This procedure

continues until a critical point corresponding to voltage collapse is obtained.

2.4.6 Homotopy Related Continuation in Optimal Power Flow (OPF) Studies

As a mathematical tool, homotopy related continuation methods can also be applied to the optimal power flow problems. As already indicated, a homotopy usually leads one to the study of curve tracing. The text here is given only to show how one links the homotopy continuation method to the OPF problems [22, 36, 38, 39, 43].

The essential idea of homotopy continuation applied in any particular situation is to construct a series (the discrete version) or a continuum of infinitely many (the continuous version, e.g., the differential homotopy continuation) equations during which the complexity of the problems is increased gradually. And in most cases, the ultimate solution of the difficult problem is of original interest, and the usefulness of intermediate results are dependent upon how one formulates the problem. In solving OPF problems, one would be led to reconstruct the problem and build a ladder of complexity to approach the original problem. This can be done as follows: deform the complete OPF problem by constructing a sub-problem first. This sub-problem can be constructed by ignoring some functional constraints in the original problem. Then deform the sub-problem such that at a value of the continuation parameter $t = 0$, the solution to the resulting deformed sub-problem is trivially found. This will mark the beginning of a tracing process, which, when successful, will provide the solution to the sub-problem. If at the solution to the sub-problem, functional constraints previously ignored in its construction prove to be within bounds, the solution to the sub-problem will be the solution to the complete OPF problem. If not, a further sub-problem should be created. That is, incorporate the violated functional variables as active constraints into the new sub-problem, and solve the problem as above. This procedure is repeated until all functional violations at hand are removed at which time the solution at hand will be the solution to the complete OPF problem. In the continuation process, a sequence of closely spaced loads is fed into the nonlinear optimization. This produces a discrete OPF solution strategy as an output. The initial guess for each new optimal solution is the optimal solution of the previous load. Once

this load tracing procedure is initiated, the solution times for the individual OPF solutions are greatly reduced, because this kind of algorithms execute quickly when presented with good initial guesses.

By recalling why one introduces homotopy, it would be easy to observe the property of the homotopy continuation method that it does not require a feasible starting point. As discussed in subsection 2.4.2, in tracing the homotopy function curve, numerical difficulties due to singularity of the Jacobian may arise. In homotopy based OPF, if the formulation still involves the solution of the original set of load flow equations, it will give rise to numerical problems at certain critical points.

2.4.7 Some Remarks About Applications

When one is beset with the lack of good starting points for the Newton type iterative methods in solving nonlinear equations, or when one needs to lead a parameter study of nonlinear system equilibrium problems, it would probably be advisable to turn to homotopy and continuation methods. Applications in recent years have manifested the great potential of the techniques to engineering problems. This chapter does not present an exhaustive survey but a compact text on continuation and its application to power system analysis. Continuation, bifurcation, and related numerical methods are very well addressed in [6, 10, 13].

3 SIMULTANEOUS EQUILIBRIA TRACING AND DYNAMIC VOLTAGE COLLAPSE DETECTION

In power system analysis, it is frequently of interest to find solutions of the system at an equilibrium point. For instance, the solution of the power flow equations are needed in system planning and static security analysis. In stability analysis, a power flow is used to calculate the voltages and angles at all buses, and then the dynamic state variables are evaluated using the device equations. This procedure causes some problems as will be shown in the following sections. To overcome these problems, we will further extend the continuation technique to simultaneously trace the total system equilibria of the structure preserving power system model, which is described by a set of nonlinear differential and algebraic equations (DAEs). Physical interpretations of the new approach will give insights into some issues which are important to a good understanding of the power system. An immediate application of the new strategy is the identification of dynamic voltage collapse without eigenvalue computations.

3.1 Equilibria Tracing in Power System Analysis

Unlike in power flow analysis, a detailed dynamic representation of the power system is required to analyze the system's stability behavior. As a typical nonlinear dynamic system, with the multiple time-scale property, a set of nonlinear DAEs can be employed to describe the behavior of the power system, i.e.,

$$\dot{X} = F(X,Y,P) \tag{3.1}$$

$$0 = G(X,Y,P) \tag{3.2}$$

where X includes the dynamic states, Y includes the algebraic state variables, and P consists of all parameters explicitly appearing in F or G. Some of these parameters can be control input settings.

3.1.1 Total Solution at Equilibrium

A system equilibrium solution is needed for the evaluation of the stability, the solution X_0 and Y_0 of equations 3.1 and 3.2 at steady state, i.e., when $\dot{X} = 0$, constitute the equilibrium point. Setting the differential to zero indicates a state of equilibrium of the system. In small signal stability analysis, the right hand side of the DAEs is first linearized, and then the system state matrix A_{sys} (see Equation 3.26) is evaluated at (X_0, Y_0). Its eigenvalues give dynamic stability information of the current equilibrium point. In nonlinear time domain analysis, the equilibrium solution (X_0, Y_0) gives the initial conditions to start numerical integration. In direct Lyapunov type stability analysis, this solution is also required.

3.1.2 Traditional Approach

In equation 3.2, G corresponds to the power balance equations at all buses in the system. Therefore its dimension is larger than that of the power flow. In power flow, it is assumed that the voltages at PV buses and voltage and angle at the slack bus(es) are known and constant. Consequently, for a network of N buses, if there are N_G generators, N_s of which are designated as slack, then the number of equations in the power flow formulation will be $2N - N_G - N_s$ (for polar coordinates). For a constant generator terminal voltage, it is assumed that the static gain of the excitation system is infinite. No limitations on the slack bus generation can be enforced during the solution process. Once a power flow is solved, together with the pre-specified generation and voltages for PV and slack buses, the X_0 values will be updated using equation 3.1 at steady state. The control parameter settings in P corresponding to this X_0 are then computed. This procedure of solving for (X_0, Y_0, P_0) is termed as the two-step approach. With this total system equilibrium solution, further stability analysis can then be conducted.

The above procedure has some drawbacks. Firstly, if control limits are enforced, a solution (X_0, Y_0, P_0) satisfying these limits may not exist. The slack bus generation might also exceed limits after the power flow. In this case, the state which is limited would need to be fixed at its limiting value and a corresponding new steady state equilibrium solution would have to be found. This would require a new power flow, for each specified value of PV bus generation or terminal voltage, or possibly generator reactive power injection. For the last case, the generator voltage becomes part of the power flow solution. For a heavily loaded system, this trial and error procedure may have to be repeated several times, each time requiring a new power flow solution. Secondly, even after a set of (X_0, Y_0, P_0) values satisfying all limits are found, there still exists another problem which is inevitable in using the power flow based two-step approach to produce equilibria solution for stability analysis. That is, the description of the generators in the power flow is very different from that in the dynamic response. How the generators behave in a dynamic process depends on the dynamic characteristics of the synchronous machines and the control systems associated with them. These controls are not represented for the PV bus generators and the slack bus generators are simply left out in the power flow. Therefore, it may not be unusual that this discrepancy in representation leads to erroneous results.

3.2 Power Flow Methodology and Assumptions

Before introducing the simultaneous equilibria tracing technique, let us first have a closer look at the assumptions used in the power flow, particularly the reasons why they are needed. With a clearer understanding of these assumptions, we will then be able to devise a procedure in which the problems encountered in the traditional approach can be avoided.

3.2.1 Nonlinearity in Power Flow

In normal electrical network analysis, the voltages and/or currents of power sources are given as known quantities. In order to find the voltages at various nodes and currents in all branches, one simply needs to solve the network nodal equations which are linear. Corre-

spondingly, for power network, this refers to the nodal representation, given in phaser notation as

$$Y\overline{V} = \overline{I} \tag{3.3}$$

where Y is the network admittance matrix, $\overline{V}$ is the vector of phaser voltages at all buses, and $\overline{I}$ is the nodal phaser injection currents. The conditions for 3.3 to have a solution with a specified set of injection currents $\overline{I}$ are

- Y is nonsingular
- rank$(Y|\overline{I})$ = rank(Y) if Y is singular

Were the injection currents known, the power flow would have involved no nonlinear equations. However, in power system analysis, the nodal voltages and injection currents are both unknown before a power flow is solved. Instead, the generation and load powers are given as the known quantities. They are related to the nodal voltages and injection currents as shown below.

$$\begin{aligned} \overline{I}_i &= \frac{S_{Gi} - S_{Li}}{\overline{V}_i^*} \\ &= \frac{(P_{Gi} - P_{Li}) + j(Q_{Gi} - Q_{Li})}{\overline{V}_i^*} \end{aligned}$$

The '*' sign indicates the complex conjugate. With the real and imaginary parts separated, equation 3.3 is transformed into the following form:

$$0 = P_{Ei} - P_{Li} - P_{Ti} \quad i = 1, \cdots, N \tag{3.4}$$

$$0 = Q_{Ei} - Q_{Li} - Q_{Ti} \quad i = 1, \cdots, N \tag{3.5}$$

where

$$P_{Ti} = V_i \sum_{k=1}^{N} V_k y_{ik} cos(\theta_i - \theta_k - \gamma_{ik}) \tag{3.6}$$

$$Q_{Ti} = V_i \sum_{k=1}^{N} V_k y_{ik} sin(\theta_i - \theta_k - \gamma_{ik}) \tag{3.7}$$

The two nonlinear equations 3.4 and 3.5 correspond to the algebraic part of the DAE formulation given in 3.2. With the powers specified at the terminal buses, X variables are not of concern in the power flow equations.

3.2.2 Slack Bus Assumption

The unknowns in equations 3.4 and 3.5 are $(\underline{V}, \underline{\theta})$, the number of which is $2N$. The underline sign is used to denote vectors. If we want to solve these unknowns directly using the Newton's method, we have to specify the generations and load powers at all buses. And most probably, with a starting point $(\underline{V}^0, \underline{\theta}^0)$ close to normal operating conditions, this approach will lead to divergence. A closer look of the structure of the power balance equations will give more insight into the problem. Designating the generator at the Nth bus as the slack, summing up the first $N-1$ equations in 3.4 and 3.5 and then adding them to the Nth and $2Nth$ equations respectively will yield

$$P_{Gs} = \sum_{i=1}^{N} P_{Li} + P_{loss}(\underline{V}, \underline{\theta}) - \sum_{i=1}^{N-1} P_{Ei} \tag{3.8}$$

$$Q_{Gs} = \sum_{i=1}^{N} Q_{Li} + Q_{loss}(\underline{V}, \underline{\theta}) - \sum_{i=1}^{N-1} Q_{Ei} \tag{3.9}$$

since we know that

$$\sum_{i=1}^{N} P_{Ti} = P_{loss}(\underline{V}, \underline{\theta})$$

$$\sum_{i=1}^{N} Q_{Ti} = Q_{loss}(\underline{V}, \underline{\theta})$$

These two equations can be put together with the first $N-1$ equations from 3.4 and 3.5 respectively to represent the complete network. Equations 3.8 and 3.9 show that, if a solution $(\underline{V}^*, \underline{\theta}^*)$ exists, for a possible successful convergence, we must specify the generations subject to the constraints given in 3.8 and 3.9. Since the losses as a function of the network solution are unknown before the power flow is solved, it is practically impossible to do so. Therefore, it is very likely that, if we have to specify the power generations for all generators, constraints 3.8 and 3.9 may be greatly violated, and correspondingly the starting point $(\underline{V}^0, \underline{\theta}^0)$ might be well out of the radius of convergence of the Newton's method. Also, there is a possibility that a *real* solution simply does not exist corresponding to this set of specified generations. (From algebraic equations theory, we know that a solution always exists if we also consider complex roots.) If one can devise a scheme so that there is freedom of adjusting the generation during

the course of iteratively solving the power flow equations, then convergence performance might be much better. Referring to this, an immediate thought would be to eliminate equations 3.8 and 3.9 altogether from the power flow iteration. Consequently, the slack bus generation need not be specified. To do so, we must remove two unknowns from $(\underline{V}, \underline{\theta})$. This is no difficulty at all. Because the goal of a power flow is to give a dispatch of the generation so that the system load can be served with the bus voltages being close to normal operating conditions, usually close to 1.0 per unit, we can reasonably assign 1.0 to V_s and 0^0 to θ_s, the latter of which is simply to set a reference for the angle measurement, and thus it is arbitrary. After the power flow converges, we then calculate the losses and assign all of them to the slack generators. This procedure makes sure that the loss-generation imbalance does not cause convergence trouble during iteration. And this imbalance is fixed *only* after the power flow is solved. The above discussion shows that the slack bus assumption is a mathematical requirement for possible/good convergence of the Newton's iterative algorithm.

3.2.3 PV Bus Assumption

In order to maintain the system voltage levels, the generators are equipped with automatic voltage regulators (AVR) so that terminal voltages are within limits during system load increase or other disturbances. With the power flow description of the system, the only way to reflect this fact is to force the terminal voltages at the generator buses as constant since AVR is not represented. To achieve this, the reactive power balance equations for generator buses must be removed. As a consequence, Q_{Ei} no longer needs to be specified as input, it is released as a variable. Physically, this means that reactive support from generators helps maintain a relatively high and steady terminal voltage. Numerically, this possibly also leads to better convergence characteristics of the Newton-Raphson power flow algorithm.

After the above discussion, we are now ready to devise a new strategy that eliminates the unreasonable assumptions used in the power flow. It solves for a reasonable set of (X, Y) values with control limits automatically implemented. This leads us to the topic of simultaneous equilibria tracing technique.

3.3 Total Power System Equilibria Solutions

From the discussion given in section 3.2, we can make two conclusions about the assumptions used in the power flow:

- *Slack bus methodology* provides a means of "automatically" adjusting real and reactive power generations "during" the iterations, not at all buses, but only for the slack, so that at any iteration the losses are not causing the point to be too far away from the true solution, therefore making Newton's iterative method possible to converge.

- *The PV bus assumption* is used to reflect the need of maintaining the system voltage levels by AVRs and it also possibly helps improve the convergence rate of the Newton-Raphson algorithm.

In the following sections, we will study how these assumptions, which cause the problems mentioned in subsection 3.1.2, can be removed, while the goals they are made to achieve are not sacrificed.

Before we introduce the simultaneous equilibria tracing technique, let us first give a detailed representation of the structure-preserving power system model.

3.3.1 System Modeling

The dynamic models adopted from reference [46] include a two-axis synchronous machine with the IEEE type DC-I exciter and a simplified boiler-governor model (first order model each for boiler and governor).

- The 2-axis synchronous machine model:

$$\begin{aligned}
\dot{\delta}_i &= (\omega_i - \omega_s)\omega_B && (3.10)\\
\dot{\omega}_i &= M_{Gi}^{-1}(P_{Mi} - D_{Gi}(\omega_i - \omega_s) - (E'_{qi} - X'_{di}I_{di})I_{qi} - (E'_{di} + X'_{qi}I_{qi})I_{di}) && (3.11)\\
\dot{E}'_{qi} &= \frac{1}{T'_{d0i}}(E_{fdi} - E'_{qi} - (X_{di} - X'_{di})I_{di}) && (3.12)\\
\dot{E}'_{di} &= \frac{1}{T'_{q0i}}(-E'_{di} + (X_{qi} - X'_{qi})I_{qi}) && (3.13)\\
i &= 1, \cdots, N_G
\end{aligned}$$

ω_s is the system frequency, and ω_B is the base value frequency (377.0 rad/s).

- Interface voltage equations to the network

$$\begin{aligned} E'_{qi} &= V_i cos(\delta_i - \theta_i) + R_{si} I_{qi} + X'_{di} I_{di} \\ E'_{di} &= V_i sin(\delta_i - \theta_i) + R_{si} I_{di} - X'_{qi} I_{qi} \end{aligned}$$

This gives the generator injection currents as

$$\begin{aligned} I_{di} &= d_i^{-1}(R_{si} E'_{di} + E'_{qi} X'_{qi} - R_{si} V_i sin(\delta_i - \theta_i) - X'_{qi} V_i cos(\delta_i - \theta_i)) \\ I_{qi} &= d_i^{-1}(R_{si} E'_{qi} - E'_{di} X'_{di} - R_{si} V_i cos(\delta_i - \theta_i) + X'_{di} V_i sin(\delta_i - \theta_i)) \\ d_i &= R_{si}^2 + X'_{di} X'_{qi} \end{aligned}$$

In order to get a minimum representation of the system, the rotor angle differential equation from 3.10 for the reference machine is first subtracted from the equations for the remaining $N_G - 1$ generators and eliminated afterwards. This reference machine is chosen solely for the sake of angle reference, so it is arbitrary. The bus voltage angles are then measured with respect to the rotor axis of this selected reference machine.

- Excitation system

The IEEE type DC-I exciter is shown in Figure 3.1 and the dynamic model is

$$\dot{E}_{fdi} = \frac{1}{T_{Ei}}(V_{Ri} - (K_{Ei} + S_{Ei}(E_{fdi}))E_{fdi}) \tag{3.14}$$

$$\dot{V}_{Ri} = \frac{1}{T_{Ai}}(-V_{Ri} + K_{Ai}(V_{REFi}^{EX} - V_i - R_{Fi}), \quad V_{pss} = 0 \tag{3.15}$$

$$\dot{R}_{Fi} = \frac{1}{T_{Fi}}(-R_{Fi} - (K_{Ei} + S_{Ei}(E_{fdi}))K_{Fi} E_{fdi}/T_{Ei} + K_{Fi} V_{Ri}/T_{Ei}) \tag{3.16}$$

where V_{REFi}^{EX} is the exciter reference voltage. V_{Ri} and R_{Fi} are the outputs of AVR and exciter soft feedback respectively. E_{fdi} is the excitation field winding voltage.

- Prime mover and speed governor

Figure 3.2 shows the block diagram of the prime mover and speed governor model used in this work.

$$\dot{P}_{Mi} = \frac{1}{T_{CHi}}(\mu_i - P_{Mi}) \tag{3.17}$$

$$\dot{\mu}_i = \frac{1}{T_{Gi}}(P_{Gsi} - (\omega_i - \omega_{ref})/R_{Gi} - \mu_i) \tag{3.18}$$

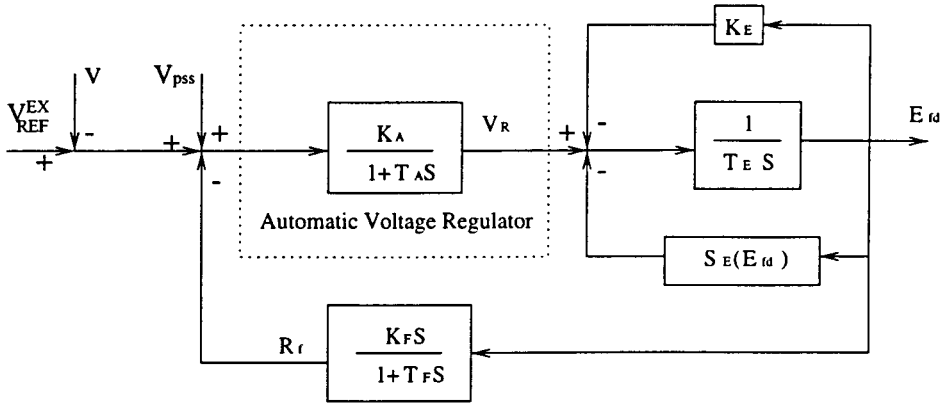

Figure 3.1 The IEEE type DC-I excitation system

P_{Gsi} is the governor real power setting for generator i. The speed-droop characteristics (see Fig. 3.3) determines the ultimate contribution of each machine to a change in the load and fixes the resulting system frequency.

- Network description

The network is basically described by equations 3.4 and 3.5. However, unlike in power flow, P_{Ei}'s and Q_{Ei}'s are no longer specified as constant inputs, but a function of system states X and Y, i.e.,

$$P_{Ei} = V_{di}I_{di} + V_{qi}I_{qi} \tag{3.19}$$
$$= V_i sin(\delta_i - \theta_i)I_{di} + V_i cos(\delta_i - \theta_i)I_{qi}$$
$$Q_{Ei} = V_{qi}I_{di} - V_{di}I_{qi} \tag{3.20}$$
$$= V_i cos(\delta_i - \theta_i)I_{di} - V_i sin(\delta_i - \theta_i)I_{qi}$$

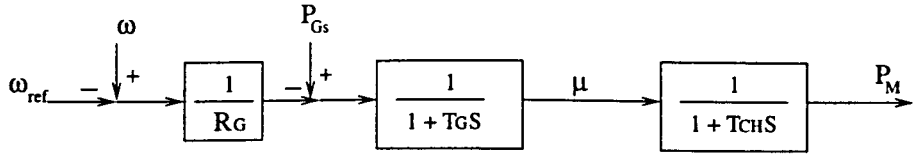

Figure 3.2 The prime mover and governor

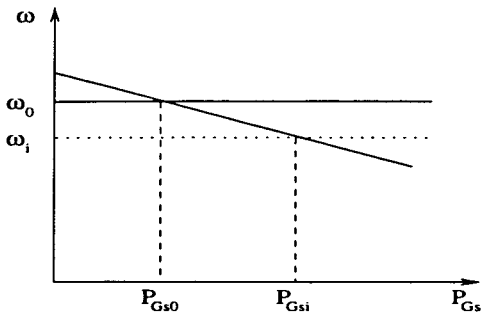

Figure 3.3 The governor speed-droop characteristic

Equations 3.10 - 3.18 together with 3.4 and 3.5 form the DAE description of the system, the abstract form of which is given in equations 3.1 and 3.2.

3.3.2 Simultaneously Solving for Total System Equilibria

Simultaneously solving for X and Y will enable us to avoid the assumptions used in power flow. This leads us to the question whether it is possible to solve for X and Y directly and simultaneously from equations 3.1 and 3.2 at equilibrium, i.e.,

$$0 = F(X, Y, P) \tag{3.21}$$

$$0 = G(X, Y, P) \tag{3.22}$$

The immediate concern is whether the Newton's method would work with as good convergence as that in the power flow.

As mentioned earlier, the release of slack bus generation is used in power flow so that network losses corresponding to a set of system voltages are not causing convergence trouble during iterations. In the complete description of the system at equilibrium state, this compensation becomes possible without the necessity of removing the slack bus power balance equations. With the description of the system at steady state by 3.21 and 3.22, generation at terminal interface to the network is now a function of system states (see equations 3.19 and 3.20). The governor frequency regulation together with the boiler valve control, as described by equations 3.18 and 3.17, interacts with the network real power balance constraints, through

mechanical power P_{Mi} (equations 3.11 and 3.17), to adjust the interface generation P_{Ei} so that real power losses are automatically compensated by regulating the system frequency. Similarly, the automatic voltage regulator (described by equations 3.14 to 3.16) interacts with the network reactive power balance constraints, through E_{fdi} to adjust Q_{Ei} so that reactive power losses are compensated by regulating terminal bus voltage V_i. In regard to PV bus assumption, it is not needed any more since AVR is actually represented.

Based on the above analysis, we claim that it is possible to solve for X and Y simultaneously by directly applying Newton's method to equations 3.21 and 3.22. Further, in the following section, we will show how we can incorporate this into continuation and apply the resultant simultaneous equilibria tracing technique to dynamic voltage collapse identification. Overall solution methodology is given in the sequel and the discussion of its numerical performance is reported in section 3.5.

3.4 Detection of Dynamic Voltage Collapse

As briefly introduced in chapter 1, the power flow has traditionally been the primary calculation to find the equilibrium and, thus, determine static voltage stability. This is because the power flow has always been considered the steady state description of the power system. As already shown that the existence of a total steady state/equilibrium solution X and Y rests essentially on the existence of a standard power flow solution if the two step approach is adopted. However, small signal/dynamic stability of the equilibrium solution is defined by a set of differential equations subject to the network algebraic constraints. In static voltage stability analysis, one is often led to find the maximum loading point, and this point has been historically deemed important for the assessment of voltage stability. At this point, the power flow Jacobian becomes singular, and it was once believed that the singularity of the power flow Jacobian signified voltage instability. But as shown in [46] that, only under very special circumstances, the power flow Jacobian has an explicit relationship with the system dynamic state matrix A_{sys} which will be defined shortly. The power flow singularity usually does not indicate instability. Hence, a power system operating state should be called steady state fea-

sible if it satisfies the full nonlinear AC power flow equations while meeting some operational constraints. This does not necessarily imply that the candidate operating point is stable in a dynamic sense. Voltage phenomena by itself are dynamic. The reason why the static power flow based analysis prevailed is due to the computational limitations and the slow properties of those dynamics influencing voltage stability. Based on the above discussion, we conclude that a power flow model is not adequate for assessing stability.

3.4.1 Eigenvalue-analysis Based Dynamic Voltage Stability Analysis

A strict dynamic voltage stability analysis will then require a full DAE formulation and eigenvalue analysis of the corresponding system state matrix at the interested equilibrium. In this thesis, dynamic stability means the system is stable under small disturbances. Therefore we can expand equations 3.1 and 3.2 into a Taylor series around the current equilibrium state. That is,

$$\dot{X}\mid_0 + \Delta\dot{X} = F(X_0, Y_0) + \frac{\partial F}{\partial X}\mid_0 \Delta X + \frac{\partial F}{\partial Y}\mid_0 \Delta Y \tag{3.23}$$

$$0 = G(X_0, Y_0) + \frac{\partial G}{\partial X}\mid_0 \Delta X + \frac{\partial G}{\partial Y}\mid_0 \Delta Y \tag{3.24}$$

which leads to

$$\begin{aligned} \begin{bmatrix} \Delta\dot{X} \\ 0 \end{bmatrix} &= \begin{bmatrix} F_X & F_Y \\ G_X & G_Y \end{bmatrix} \begin{bmatrix} \Delta X \\ \Delta Y \end{bmatrix} \\ &\hat{=} J \begin{bmatrix} \Delta X \\ \Delta Y \end{bmatrix} \end{aligned} \tag{3.25}$$

And we then have

$$\begin{aligned} \Delta\dot{X} &= (F_X - F_Y G_Y^{-1} G_X)\mid_0 \Delta X \\ &\hat{=} A_{sys}\Delta X \end{aligned} \tag{3.26}$$

Eigenvalue analysis of A_{sys}, which is termed the system (dynamic) state matrix, will give dynamic stability information of the current equilibrium point under small disturbances. At voltage collapse, the system loses the ability to supply enough power to a heavily loaded

network. At this point, the so-called saddle node bifurcation occurs which is described by the movement of one eigenvalue of A_{sys} on the real axis crossing the origin from the left half complex plane. Therefore an eigenvalue computation will help detect this movement, participation factor studies will show how bus voltages participate in this collapse mode, and sensitivity analysis will show the parameter influence on this critical eigenvalue. However, the above procedure is cost intensive since eigenvalue the computation is involved. Furthermore, the formation of A_{sys} also destroys sparsity of J.

3.4.2 Detection of Voltage Collapse Via Simultaneous Equilibria Tracing

At saddle node bifurcation which leads to voltage collapse, one of the eigenvalues of A_{sys} is zero. Equivalently, the determinant of A_{sys} is zero. From matrix theory, we know that,

$$\begin{aligned} det(J) &= det\begin{pmatrix} F_X & F_Y \\ G_X & G_Y \end{pmatrix} \\ &= det(F_X - F_Y G_Y^{-1} G_X) det(G_Y) \\ &= det(A_{sys}) det(G_Y) \end{aligned} \tag{3.27}$$

So if G_Y is nonsingular, the determinant of A_{sys} becomes zero if and only if the determinant of J is zero. The latter of which is the total system Jacobian which we are proposing to use for the simultaneous equilibria tracing. J is very sparse and thus allows efficient handling using sparsity techniques. Therefore the detection of the singularity of A_{sys} can be made while working on J. In the following section, we will show a simple procedure to detect the singularity of J. It does not need calculation of either eigenvalues or the determinant of J.

3.4.3 Solution Methodology

In the review given in chapter 2, we have shown how the continuation technique can be used for curve tracing in general, and detecting network loadability in particular. This method is now further extended to trace the total power system equilibria from the base case up to the point where dynamic voltage collapse occurs. That is, we apply the continuation method

to trace the curve defined by

$$0 = F(X, Y, \alpha) \tag{3.28}$$

$$0 = G(X, Y, \alpha) \tag{3.29}$$

where α is the bifurcation parameter. α denotes the system load/generation level and also can be used to parameterize the curve.

3.4.3.1 Continuation applied to simultaneous equilibria tracing

The bifurcation parameter α is incorporated into F and G to parameterize the curve. Since we are interested in tracing the equilibrium states when the system generation and load are increased, we parameterize the governor generation setting and system loads as

$$P_{Gsi}(\alpha) = P_{Gsi0} + K_{GPi}(\sum_{i=1}^{N} P_{Li}(\alpha) - \sum_{i=1}^{N} P_{Li0}) \tag{3.30}$$

$$P_{Li}(\alpha) = P_{Li0} + \alpha K_{Lpi} P_{Li0} \tag{3.31}$$

$$Q_{Li}(\alpha) = Q_{Li0} + \alpha K_{Lqi} Q_{Li0} \tag{3.32}$$

Equations 3.31 and 3.32 designate the load increase scenario. Eq. 3.30 gives the load increase sharing scheme for each generator selected from the system. P_{Gsi} is the generation setting point for the governor. As illustrated in chapter 2, the solution process is divided into prediction and correction. In the predictor step, the tangent vector is solved from

$$-\begin{bmatrix} F_X & F_Y & F_\alpha \\ G_X & G_Y & G_\alpha \\ & e_k^T & \end{bmatrix} \begin{bmatrix} dX \\ dY \\ d\alpha \end{bmatrix} = \begin{bmatrix} 0 \\ 0 \\ \pm 1 \end{bmatrix} \tag{3.33}$$

Once the prediction is made, the corrector is then computed to get back from the predicted point to the solution curve. The corrector is computed from equation 3.34.

$$-\begin{bmatrix} F_X & F_Y & F_\alpha \\ G_X & G_Y & G_\alpha \\ & e_k^T & \end{bmatrix} \begin{bmatrix} \Delta X \\ \Delta Y \\ \Delta \alpha \end{bmatrix} = \begin{bmatrix} F \\ G \\ 0 \end{bmatrix} \tag{3.34}$$

3.4.3.2 Detection of voltage collapse

The point where the Jacobian J becomes singular can be identified during the course of continuation. This is explained below.

Because α corresponds to the system generation and load level, it increases monotonically to the maximum value, at which voltage collapses. Therefore the tangent component $d\alpha$ is positive before the saddle node bifurcation, and negative afterwards. If we could exactly capture the point when $d\alpha$ is zero, then it is trivial to show the exact singularity of J. When $d\alpha = 0$, equation 3.33 reduces to

$$-\begin{bmatrix} F_X & F_Y \\ G_X & G_Y \end{bmatrix}\begin{bmatrix} dX \\ dY \end{bmatrix} = \begin{bmatrix} 0 \\ 0 \end{bmatrix} \tag{3.35}$$

Since one of the components from dX or dY is ± 1, $(dX, dY)^T$ is not a *null* vector, equation 3.35 therefore denotes singularity of J.

This technique captures the saddle node bifurcation by detecting the sign change of $d\alpha$, which is automatically done in the continuation process. Since J is very sparse, it is advantageous to apply a sparsity programming technique for solving 3.33 and 3.34. We thus achieve our aim of detecting dynamic voltage collapse without forming A_{sys} and computing its eigenvalues, neither do we need to compute the determinant of J.

3.4.4 Limits Implementation

It is very important to reasonably represent the system limits when studying voltage stability. In fact, voltage collapse occurs more than often as a consequence of limited local reactive power supply. When the system loses the ability to further meet the load demand in a heavily stressed network, the cascaded hitting of limits usually leads to system collapse. There are basically two types of limits to be considered. One is the governor limit, and the other is the AVR output limit. For voltage stability, the latter usually plays a more important role.

3.4.4.1 Governor limits

The governor limits are implemented by regulating the real power generation/load settings. Those generators which hit P_{Gsi}^{max} will then be forced to stay at maximum, and no longer allowed to further pick up the system load increase.

3.4.4.2 AVR limits

The automatic voltage regulator (AVR) controls the terminal voltage of the synchronous machine. It indirectly controls the reactive power output by regulating the AVR output voltage V_R. In the new formulation, we are able to directly implement the limits which are usually given to restrict the output of the voltage regulator. *Forcing the AVR output voltage at a particular value will directly control the rotor current to stay below limits and indirectly control the reactive generation.* This can be proven as follows. At an equilibrium state, the AVR output voltage is related to the synchronous machine rotor current as

$$V_{Ri} = (K_{Ei} + S_{Ei})E_{fdi} \tag{3.36}$$

$$= (K_{Ei} + S_{Ei})E_{qi} \tag{3.37}$$

$$= (K_{Ei} + S_{Ei})X_{adi}I_{fdi} \tag{3.38}$$

where E_{qi} is the generator's internal induced quadrature axis voltage [47]. So if we ignore the saturation effect, the rotor current is proportional to V_{Ri}, which proves the first half of the above statement. A machine's reactive power output can be written as

$$Q_{Ei} = \frac{V_i E_{qi}}{X_{di}} cos(\delta_i - \theta i) - V_i^2 (\frac{cos^2(\delta_i - \theta i)}{X_{di}} + \frac{sin^2(\delta_i - \theta i)}{X_{qi}}) \tag{3.39}$$

When V_{Ri} is fixed at a certain value, the reactive power will then be limited indirectly, at least not increase exponentially when approaching voltage collapse. This proves the second half of the previous statement.

Once the AVR of a generator hits the limit, it loses the ability to adjust V_{Ri} and thus Q_{Ei} to meet the load increase. The AVR has to be set so that V_{Ri} stays at the limiting value. Referring to equation 3.15, the dynamic differential equation will be dropped and will

not be included for stability analysis. This is obvious if one recalls the definition of stability from control theory. That is, the limited dynamic state will stay as a constant, and it no longer participates in the dynamic response of the system. If we solve the remaining equations which provide the DAE description of the system with the same control inputs, we may not be able to find a solution. This is because, when the system load further increases, in order to continuously keep V_{Ri} at the limiting value, the corresponding excitation reference voltage V_{REFi}^{EX} may have to be reduced. The decrease of the exciter reference voltage reflects the inability of the generator to keep pace with the load increase. In the conventional two-step based equilibria tracing approach, this would require a new power flow solution with a different set of generation and/or voltage specifications for the PV buses. After this, the X variables are then calculated and the control inputs including the exciter reference voltage will then be updated to a new smaller value in this case. As mentioned in the first section of this chapter, this causes the problem of inconsistent description of the generators. In the new formulation, when some new limits are hit, this update of control settings can be done automatically during continuation. To do so, we include the following equation, which is nothing but the right hand side of 3.15 with V_{Ri} at its maximum.

$$0 = \frac{1}{T_{Ai}}(-V_{Ri}^{max} + K_{Ai}(V_{REFi}^{EX} - V_i - R_{Fi}) \hat{=} f_i^{AVR+} \tag{3.40}$$

If a new limit is found to be violated at the end of the current correction, the following Jacobian will then be used in the immediate correction to update the input exciter reference voltage.

$$-\begin{bmatrix} \overline{F}_{\overline{X}} & \overline{F}_Y & 0 & \overline{F}_\alpha \\ G_{\overline{X}i} & G_Y & 0 & G_\alpha \\ f_{i\overline{X}}^{AVR+} & f_{iY}^{AVR+} & f_{iV_{ref}}^{AVR+} & 0 \\ & e_k^T & & \end{bmatrix} \begin{bmatrix} \Delta\overline{X} \\ \Delta Y \\ \Delta V_{REFi}^{EX} \\ \Delta\alpha \end{bmatrix} = \begin{bmatrix} \overline{F} \\ G \\ f_i^{AVR+} \\ 0 \end{bmatrix} \tag{3.41}$$

where $\overline{F}$ ={F}-{f_i^{AVR}} and $\overline{X}$ ={X}-{V_{Ri}} and $f_{iV_{ref}}^{AVR+} \hat{=} \partial f_i^{AVR+}/\partial V_{REFi}^{EX}$. After this, if no

new limits are violated, the following equation will then be used for subsequent correctors:

$$-\begin{bmatrix} \overline{F}_{\overline{X}} & \overline{F}_Y & 0 & \overline{F}_\alpha \\ G_{\overline{X}} & G_Y & 0 & G_\alpha \\ f_{i\overline{X}}^{AVR+} & f_{iY}^{AVR+} & 10^{15} & 0 \\ & e_k^T & & \end{bmatrix} \begin{bmatrix} \Delta\overline{X} \\ \Delta Y \\ \Delta V_{Ri} \\ \Delta\alpha \end{bmatrix} = \begin{bmatrix} \overline{F} \\ G \\ 0 \\ 0 \end{bmatrix} \tag{3.42}$$

Once the limit is hit, the predictor equation from then on is changed to

$$-\begin{bmatrix} \overline{F}_{\overline{X}} & \overline{F}_Y & 0 & \overline{F}_\alpha \\ G_{\overline{X}} & G_Y & 0 & G_\alpha \\ f_{i\overline{X}}^{AVR+} & f_{iY}^{AVR+} & 10^{15} & 0 \\ & e_k^T & & \end{bmatrix} \begin{bmatrix} d\overline{X} \\ dY \\ dV_{Ri} \\ d\alpha \end{bmatrix} = \begin{bmatrix} 0 \\ 0 \\ 0 \\ \pm 1 \end{bmatrix} \tag{3.43}$$

The large number is used to keep the size of the matrix unchanged which provides programming ease. And by using this Jacobian, we observe that neither the AVR output voltage nor the input exciter reference voltage is updated during the prediction process. This makes sure that we get the tangent of the equilibrium curve corresponding to the current input settings while satisfying the limits already encountered. The above analysis is illustrated in Figure 3.4.

When $d\alpha$ is zero, from equation 3.43,

$$det\begin{pmatrix} \overline{F}_{\overline{X}} & \overline{F}_Y & 0 \\ G_{\overline{X}} & G_Y & 0 \\ f_{\overline{X}}^{AVR+} & f_Y^{AVR+} & 10^{15}I \end{pmatrix} = 0 \tag{3.44}$$

And we have

$$det\begin{pmatrix} \overline{F}_{\overline{X}} & \overline{F}_Y & 0 \\ G_{\overline{X}} & G_Y & 0 \\ f_{\overline{X}}^{AVR+} & f_Y^{AVR+} & 10^{15}I \end{pmatrix} = det\begin{pmatrix} \overline{F}_{\overline{X}} & \overline{F}_Y \\ G_{\overline{X}} & G_Y \end{pmatrix} det\left(10^{15}I\right) \tag{3.45}$$

Thus we observe that $d\alpha = 0$ again signifies saddle node bifurcation of the DAE model.

The above derivation proves the validity of using the iterative continuation Jacobian (in Eq. 3.43) in simultaneous equilibria tracing to identify dynamic voltage collapse, both before and after hitting AVR limits. In chapter 4, we will see that the continuation Jacobian can also be used for studying the sensitivity of the saddle node bifurcation of the DAE model.

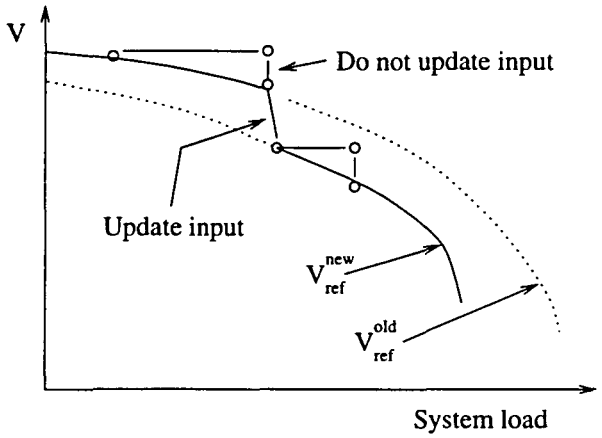

Figure 3.4 Limits implementation during continuation

3.4.4.3 Overall Procedure

The flow chart given in Figure 3.5 shows the overall solution strategy for identifying dynamic voltage collapse via simultaneous equilibria tracing.

3.5 Test System Studies

The proposed method was applied to the IEEE New England 39-Bus system and the Iowa 162-bus network. They include 10 and 17 generators respectively. Both governor limits and AVR output voltage limits were considered, the latter of which indirectly controls the reactive output.

3.5.1 The New England System

The system consists of 10 generators (at buses 31, 30 and 32-39), 17 load nodes (at buses 3, 4, 7, 8, 15, 16, 18, 20-21, 23-29, 39), and the remaining junction buses. The generation/load increase scenario is defined as: the real and reactive loads are increased at constant power factor and at the same rate among all load buses. Each generator is assigned a portion of the system load pick-up according to the base case generation (see Appendix E).

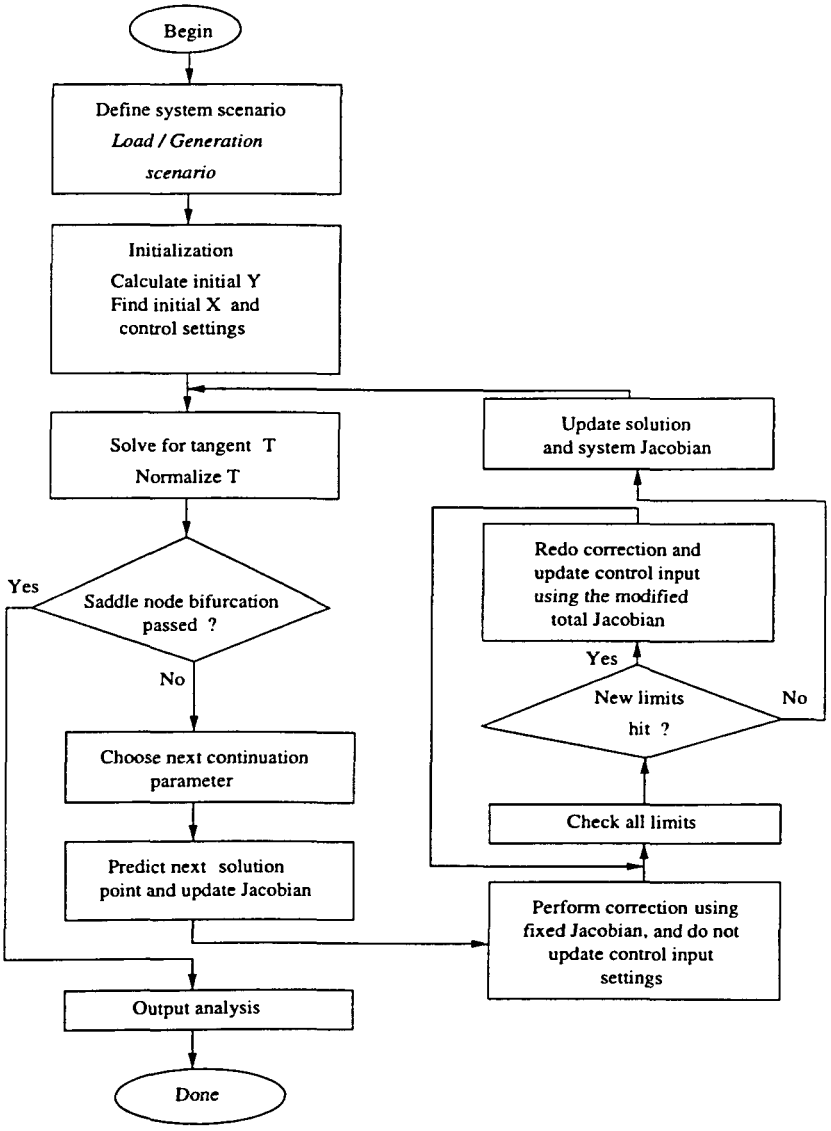

Figure 3.5 The overall flowchart

3.5.1.1 General description of test results

As explained in the previous sections, the automatic voltage regulator regulates the generator terminal voltage and its reactive power output to the network. The speed governor adjusts the real power generation and system frequency to meet load increase. Because all these devices are modeled in detail, we are able to observe how the synchronous machines interact with the network, both before and after hitting the limits. The inability of indefinitely supplying power through the network to the load centers, as a consequence of control system or machine capacity limitations and network loadability restrictions, will ultimately lead to system voltage collapse as will be shown in the sequel.

The system experiences voltage collapse (saddle node bifurcation) at a loading level of 8776 MW. All governors hit limits before reaching voltage instability. The generators at buses 30, 32 and 35 hit their AVR limits. The buses which experience lowest voltages at various loading levels are nodes 8, 12, and 15.

3.5.1.2 Automatic voltage regulator responses

We observed that, for all the generators which hit their AVR output voltage limits, the terminal voltage, AVR output voltage, reactive power generation, and exciter reference voltage have similar response profiles. Therefore we take the generator at bus 30 as the example for analysis.

Figure 3.6 shows that, before hitting its AVR output limit, the voltage regulator can maintain a fairly high and steady terminal voltage. When the system total load exceeds 8223 MW, AVR output voltage (Figure 3.8) hits the maximum value of 1.45 p.u. and the terminal voltage experiences a noticeable drop.

Figure 3.7 shows the profile of reactive generation at bus 30. A sudden slowing down of the increase in the reactive generation occurs when the AVR output limit is hit. From this point on, fixing the AVR output voltage makes the terminal reactive power generation to increase at a much slower speed.

Figures 3.8 and 3.9 are the AVR output and exciter reference voltages of generator at bus

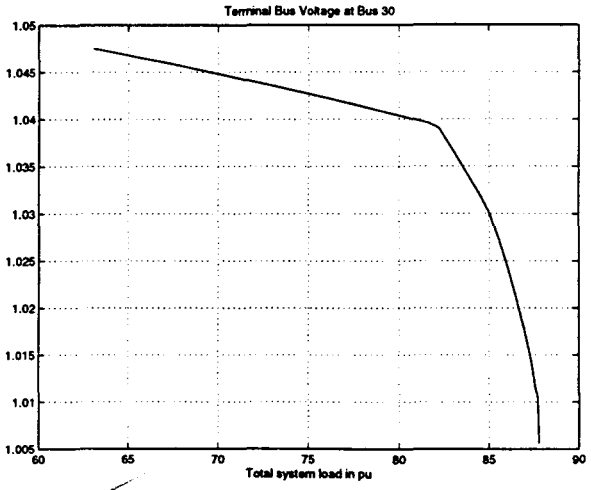

Figure 3.6 Voltage at bus 30

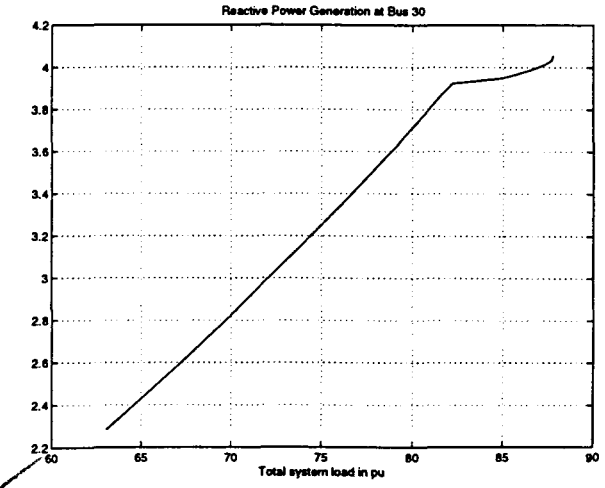

Figure 3.7 Reactive power generation at bus 30

30. The saturation of V_{R30} and drop of V_{REF30}^{EX} correspond to the hitting of the AVR limit.

3.5.1.3 Speed governor responses

The governor associated with generator at bus 35 is the first to reach its limit when the system loading level is 7621.0 MW. The dotted line (Fig. 3.10) shows the governor setting value and the solid line depicts the terminal real power generation. The terminal generation stays at an almost constant value after the governor hits the limit. However, at a system loading level of 7898.0 MW, when most of the governors hit their limits, the system frequency experiences a much larger sag (Fig. 3.11). This causes the terminal real power generation of generator at

bus 35 to increase further and eventually exceed the governor setting value.

3.5.2 The Iowa System

The system consists of 17 generators. The generation/load increase scenario is defined as: The real and reactive loads are increased at constant power factor and at the same rate at eleven load buses (at nodes 18, 20, 22, 30, 32, 52, 59, 80, 82, 87 and 89). Each generator is assigned a portion of the system load pick-up according to the base case generation (see Appendix E).

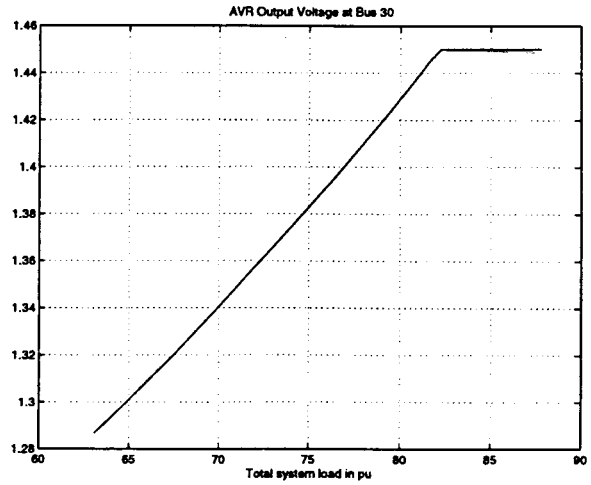

Figure 3.8 AVR output voltage V_R at bus 30

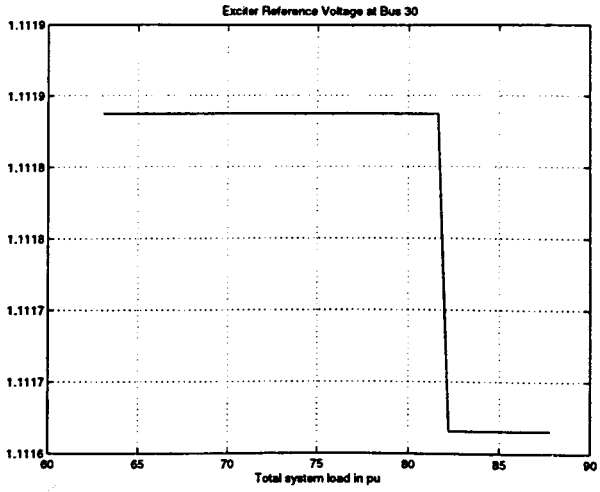

Figure 3.9 Exciter reference voltage V_{REF}^{EX} at bus 30

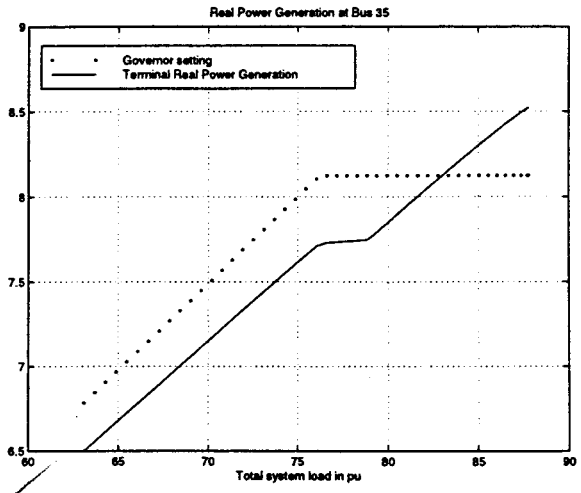

Figure 3.10 Governor response of generator at bus 35

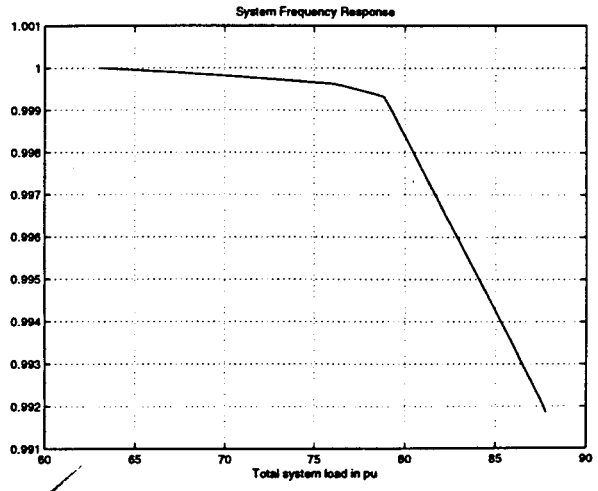

Figure 3.11 System frequency response

3.5.2.1 General description of test results

The system experiences a voltage collapse (saddle node bifurcation) at a loading level of 18500.0 MW. The governor of the generator at bus 125 hits its limit before reaching voltage instability. Generators at buses 76, 101, 108 and 126 hit their AVR limits.

3.5.2.2 Automatic voltage regulator responses

The first nonsmooth change of the terminal voltage at bus 126 (Figure 3.12) occurs when the AVR outputs of generators at buses 101 and 108 hit the maximum. When the system load

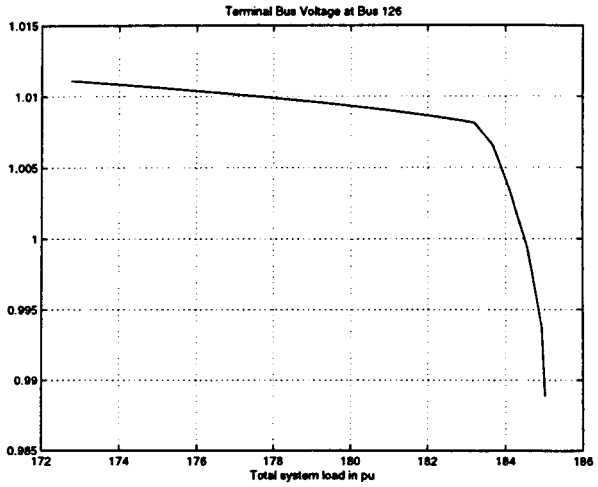

Figure 3.12 Voltage at bus 126

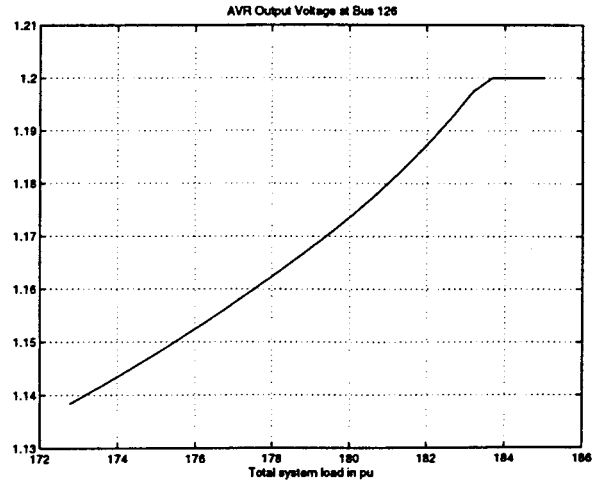

Figure 3.13 AVR output voltage V_R at bus 126

exceeds 18368.0 MW, V_{R126} itself hits the limit. From this point on, the terminal voltage at bus 126 experiences a much more abrupt decrease.

Figures 3.13 and 3.14 are the AVR output and exciter reference voltages of generator at bus 30. The saturation of V_{R126} and drop of V_{REF126}^{EX} correspond to the hitting of the AVR limit.

Figure 3.15 shows the profile of reactive generation at bus 76. A sudden decrease of the reactive generation occurs when its own AVR output limit is hit near the voltage collapse point.

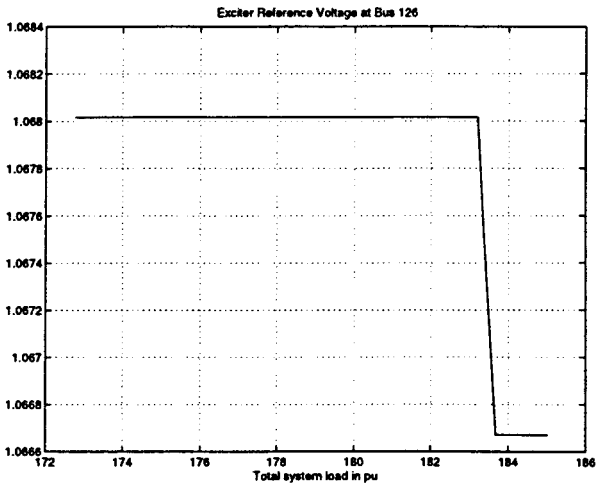

Figure 3.14 Exciter reference voltage V_{REF}^{EX} at bus 126

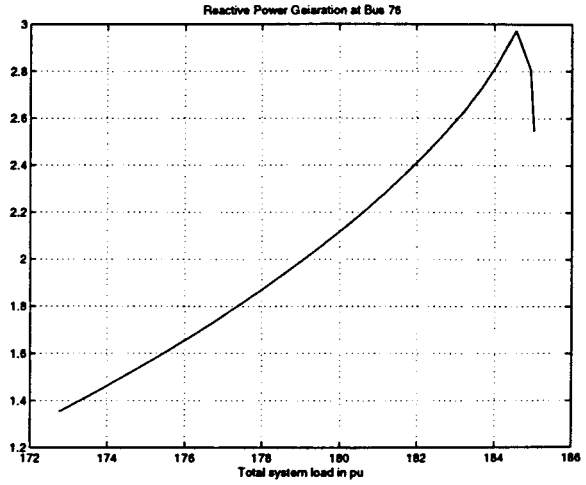

Figure 3.15 Reactive power generation at bus 76

3.5.2.3 Speed governor responses

The governor associated with the generator at bus 125 reaches its limit when the system loading level is 18064.0 MW. The dotted line shows the governor setting value and the solid line depicts the terminal real power generation (Fig. 3.16). After P_{Gs126} hits its maximum, the system frequency experiences a relatively faster drop (Fig. 3.17). This causes the terminal real power generation of generator at bus 125 to increase further and exceed the governor setting value.

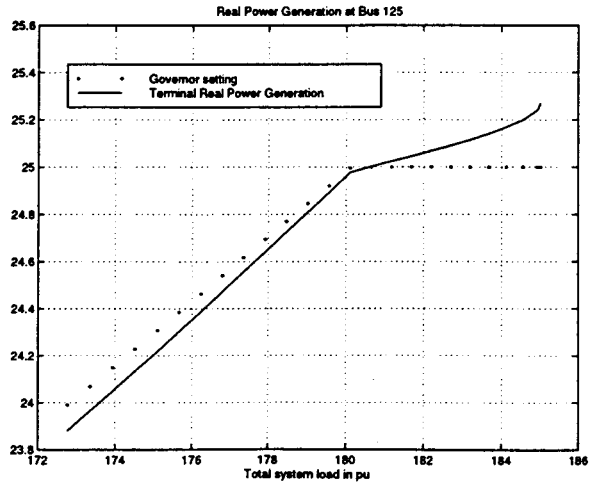

Figure 3.16 Governor response of generator at bus 125

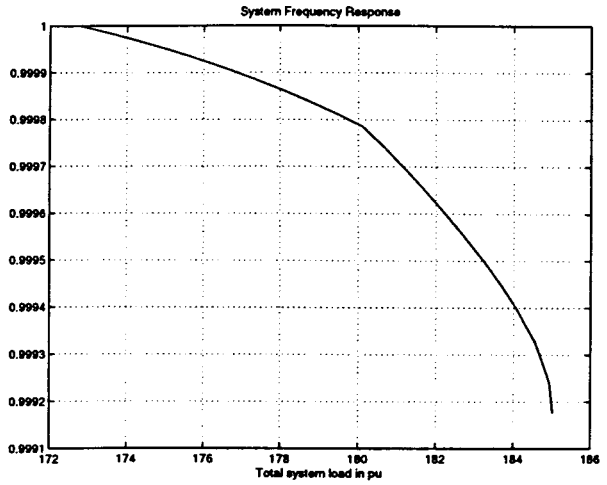

Figure 3.17 System frequency response

3.5.3 Conclusions

Traditional approaches for voltage stability analysis have concentrated mainly on using the power flow model, or the DAE model with eigenvalue analysis or time domain simulation studies. These methods either overly simplify the system or require too much computation. Further, even if computational costs were not of concern, in eigenvalue based or time domain simulation analysis, the inconsistent description of the synchronous machines between the power flow model and the dynamic model can lead to very different equilibrium solutions. This may give wrong stability results even though a strict dynamic model is used in time domain

simulation or small signal stability eigenvalue analysis. This is so because, from stability theory we know that, the initial equilibrium conditions determine the free motion of the system. This inherent problem with the conventional approach is avoided in the new framework.

Numerical results with the New England and the Iowa systems show that the proposed framework is well suited for dynamic voltage collapse identification. Modeling of the AVR and speed governor systems is indispensable in capturing the dynamic responses of the synchronous machines and identifying the mechanisms which lead to voltage collapse. Because the mid-term and long term dynamics are mainly dominated by the system quasi-steady state characteristics [48], i.e., equilibrium state characteristics, the new framework can replace the tedious time domain simulation for dynamic voltage stability analysis. Meanwhile, because system frequency is determined during continuation, a comprehensive synthetic system preventive control strategy can be developed, with due consideration given to both voltage and frequency regulations. The convergence rate of the continuation method applied to the total DAE system of equations is similar to the case when the system is described by the simple power flow model.

4 VOLTAGE STABILITY SENSITIVITY AND TRANSFER MARGIN ESTIMATION

In power system analysis, it is not enough to merely obtain the stability information. It is important to know the stability sensitivities. They provide the information related to parameters and controls that may influence the system stability. Since sensitivity is usually defined for some index relating to system performance, a review of some voltage stability indices is offered in section 4.1. Then a general description of sensitivity analysis follows in section 4.2. Providing a unified approach to combine stability results with sensitivity analysis is the subject of section 4.3, where the concept of invariant subspace parametric sensitivity (ISPS) is re-visited. An efficient computational procedure of the measure of ISPS through sparse formulation is proposed. Comparison of ISPS with eigenvalue sensitivity, and the σ_p vector which is the measure of ISPS, with the normal vector leads to further insights about parameter space and state space. In section 4.4, it is shown that the measure of ISPS can be further applied to estimate transfer margin as limited by dynamic voltage collapse. Numerical studies with the New England and Iowa systems show the effectiveness of the proposed sensitivity index.

4.1 Voltage Stability Indices

The intention of all indices is to give a measure of the margin between the current point of operation and the point where the system becomes unstable, thereby providing early warning of a potentially critical condition. The attributes of the indices in use are very different and it is convenient to classify the indices into two main classes (given-state based and large deviation based indices) as suggested by [49]. The following discussion about these indices should be thought of as independent of the model used in determining stability. The DAE model together

with the corresponding system state matrix A_{sys} provides true dynamic stability information. A static power flow based analysis does not directly give true stability information. Keeping this in mind, one should be clear that, for instance, the minimum eigenvalue can be that of A_{sys} or J_{LF}.

4.1.1 Given State Based Indices

These indices only use the information available at the current operating point. The operating point could be simulated for a desired power transfer condition. From this information, the system characteristic is calculated and system operation is classified.

- Reactive power reserve

  Automatically activated reactive power reserve at effective locations can serve as a simple, yet sensitive, voltage security index. And in addition to being a given state index, it can also serve as a large deviation index (MVAR distance to voltage collapse), with the assumption that instability occurs when the field current of a key generator reaches its limit or when a SVC reaches its boost limit.

- Voltage drop

  These indices are based on the principle that the voltage drops as the system is loaded. However this is sometimes masked by the effect of reactive power compensation devices and off-nominal tap setting of transformers.

- MW/MVAR losses

  The losses increase exponentially when a system approaches voltage collapse. The application of these losses used as indicators of voltage instability has been given in the literature.

- Incremental values

  These indices give information about the system state in the close vicinity of an operating point. Incremental values can provide a quantitative insight of weakness of a node. $\Delta Q/\Delta V$, for example, is sometimes used for assessing areas prone to voltage collapse.

- Incremental steady state margin (ISSM)

  This is an indicator calculated from a determinant of a special formulation of the system power flow Jacobian. After normalization, the maximum index value will be 1.0 and will reach 0.0 at critical load conditions. The earliest form of this index was proposed by Venikov [50].

- Minimum singular value or minimum eigenvalue

  Singular values have been employed in power systems because of the useful orthogonal decomposition of the Jacobian matrices. The singular value decomposition is typically used to determine the rank of a matrix, which is equal to the number of non-zero singular values of the matrix. Hence, its application to static voltage collapse analysis focuses on monitoring the smallest singular value up to the point where it becomes zero. Therefore it has been proposed as an index measuring stability. Similarly, the minimum eigenvalue could also be used as an index because it also becomes zero at the same time as the minimum singular value does.

When given state based indices are plotted against system load, most of their trajectories assume an exponential curvature. This makes it difficult to effectively predict voltage collapse using these indices [51].

4.1.2 Large Deviation Based Indices

Large deviation based indices account for nonlinearities caused by larger disturbances or load increases. These indices are normally more computationally demanding than the given state indices, but are more reliable. The margin is usually given in terms of the maximum increase in MW or MVAR load, and can either be based on a smooth increase in load from the normal operating conditions, or the load increase can be combined with contingencies in the system.

Methods based on large deviation indices in principle apply the same measure. However, the approach for calculation is very different. Some main classes are:

- Repeated power flows [49]

- Continuation methods [19]
- Optimization-based methods [52]
- Point-of-collapse methods [21, 25]
- Closest distance to maximum transfer boundary [23]
- Energy function methods [53]

4.2 Stability Studies Via Sensitivity Analysis

As introduced in chapter 3, the dynamic properties of the power system are characterized by the eigenproperties of the system state matrix A_{sys}. In practical situations, obtaining stability results is only part of the work. It is important to identify the key factors which affect stability, either beneficially or detrimentally. These factors can be described by the parameter influence on system performance and stability. The parameters can be operational or non-operational. A common approach in doing sensitivity analysis is to define a stability index and then study how the different parameters affect this index. By using sensitivity techniques, useful information about the relationships between state, control, and dependent variables can be established. These sensitivity signals are valid in the vicinity of the point of linearization. Sometimes the sensitivity might not be directly defined with respect to a certain stability index, and is thereof referred to as parametric sensitivity. Since system performance degradation often leads to loss of stability, parametric sensitivity is also used in sensitivity-based stability analysis. At a normal operating state, sensitivity analysis provides information about how different parameters influence stability. Certain control measures can be designed in order to prevent the system from instability. Should the system be in an emergency state under disturbances, effective controls must be applied to pull the system back to a normal state. Sensitivity analysis is well suited for evaluating the effectiveness of the controls.

4.2.1 Parametric Sensitivities

Near a given equilibrium solution (X_0, Y_0) of the structure preserving power system model as given in chapter 3 (equations 3.1 and 3.2), the derivatives $\partial X/\partial P$ and $\partial Y/\partial P$ at P_0 give a natural measure of the sensitivity of the solution. Here, P is a vector which includes all parameters explicitly appearing in F or G. From these derivatives, sensitivities of the dependent variables can be easily found. For instance, bus voltage sensitivity with respect to reactive power injections, transmission line loss sensitivity, or generator output sensitivity with respect to system load, can all be computed from $\partial X/\partial P$ and $\partial Y/\partial P$. From such sensitivities, a proper direction for adjusting the system control variables can be found.

4.2.2 Eigenvalue Sensitivity

As explained in section 3.4, eigenvalue analysis gives information about dynamic stability of the current operating point. Therefore the sensitivity of the critical eigenvalue(s) with respect to system parameters is often needed to design coordinated controls to prevent instability. Suppose λ_i is the critical eigenvalue of interest, its sensitivity with respect to any parameter p is [54]:

$$\frac{\partial \lambda_i}{\partial p} = \frac{v_i^T \frac{\partial A_{sys}}{\partial p} u_i}{v_i^T u_i} \tag{4.1}$$

where u_i and v_i are the right and left eigenvectors of A_{sys} corresponding to λ_i respectively. Eigenvalue sensitivity can be applied to any eigenvalue of critical interest, therefore oscillatory as well as collapse type instability can all be addressed by this approach. For voltage collapse analysis, one can apply this to the minimum zero crossing eigenvalue λ_{min}.

4.2.3 Invariant Subspace Parametric Sensitivity

A systematic sensitivity analysis procedure was developed at Iowa State University by Lee and Ajjarapu [41], which is called the invariant subspace parametric sensitivity (ISPS). It is obtained by properly projecting the parametric sensitivity onto the eigensubspaces corresponding to each eigenvalue. Even though it looks similar to eigenvalue sensitivity, it is different in the sense that one can derive a transfer margin sensitivity from the measure of ISPS. This

makes it possible to get sensitivity of a large deviation based index (MW/MVar distance to voltage collapse) from ISPS and utilize it to quantitatively predict the voltage collapse.

4.2.4 Qualitative Vs. Quantitative Sensitivities

Qualitative sensitivity refers to the fact that it only gives direction and relative magnitude of change of stability indices under parameter variations. Quantitative sensitivity can be used for the quantification of change of the stability index with respect to a change of some parameter. A good example of qualitative sensitivity is eigenvalue sensitivity. At an operating point, $\partial\lambda_i/\partial p$ gives qualitative information about the parameter's influence on the eigenvalue. Because the eigenvalue is a highly nonlinear function of system parameters, it is practically impossible to quantitatively estimate the change in the eigenvalue due to variations of some parameters. Recent work [55] made an attempt to predict eigenvalues using eigenvalue sensitivity (sensitivity of a given state index) computed at the current operating point. The results of the one machine against an infinite bus system are quite satisfactory when the parameters are varied by only 1% from nominal values. (The motivation is clear, since often the operators need to know how much control has to be applied to move the eigenvalue to the desired value in either preventive or corrective actions.) However, for a larger system, the proposed sensitivity could not predict the eigenvalues.

As mentioned in section 4.1.2, large deviation based indices account for the nonlinearities caused by larger disturbances. Since these indices are usually defined in the load power space, they characterize the critical operating condition from a parameter space point of view. On the other hand, the ISPS provides the parameter influence on the eigensubspaces in which the system dynamics is invariant. The measure of ISPS is further extended to derive transfer margin sensitivity. This sensitivity measure can be used for the quantitative prediction of voltage collapse.

4.3 The Invariant Subspace Parametric Sensitivity

Near a given state of equilibrium, the parametric sensitivity can be derived by taking the partial derivative of $F = 0$ and $G = 0$ with respect to the parameter vector P, i.e.,

$$\frac{\partial X}{\partial P} = A_{sys}^{-1}\left[\frac{\partial F}{\partial Y}\left[\frac{\partial G}{\partial Y}\right]^{-1}\frac{\partial G}{\partial P} - \frac{\partial F}{\partial P}\right] \tag{4.2}$$

$$\frac{\partial Y}{\partial P} = -\left[\frac{\partial G}{\partial Y}\right]^{-1}\left[\frac{\partial G}{\partial X}\frac{\partial X}{\partial P} + \frac{\partial G}{\partial P}\right] \tag{4.3}$$

These derivatives give a natural measure of the sensitivity of the solution $(X(P), Y(P))$ at the current operating point. However they do not necessarily directly relate to stability. This is explained in the sequel.

4.3.1 Eigenvalues, Eigenvectors and Modes of System Free Response

As shown in subsection 3.4.1, the dynamic behavior of the power system near an equilibrium point can be described by equation 3.26. The essential dynamic characteristics of the system are expressed in terms of the eigenproperties of the system state matrix A_{sys}.

The eigenvalues and associated left and right eigenvectors of A_{sys} can be computed from the following equations:

$$v_i^T A_{sys} = \lambda_i v_i^T \tag{4.4}$$

$$A_{sys} u_i = \lambda_i u_i \tag{4.5}$$

In the absence of an external input, the free motion of the system is

$$\Delta X(t) = \sum_{i=1}^{n} [e^{\lambda_i t}] u_i (v_i^T \Delta X_0) \tag{4.6}$$

If we use c_i to denote the scalar product $v_i^T \Delta X_0$, the time response of the kth state variable is given by

$$\Delta x_k(t) = u_{k1} c_1 e^{\lambda_1 t} + \cdots + u_{kn} c_n e^{\lambda_n t} \tag{4.7}$$

with the notation for the right and left eigenvectors as

$$u_i = (u_{1i} \cdots u_{ni})^T$$

$$v_i = (v_{1i} \cdots v_{ni})^T$$

Thus the free response (activated soly by initial conditions) is given by a linear combination of n dynamic modes corresponding to the n eigenvalues of A_{sys}. The scalar product $c_i = v_i^T \Delta X_0$ represents the magnitude of the excitation of the ith mode resulting from the initial conditions.

If the initial conditions lie on the jth eigenvector, the scalar product $v_i^T \Delta X_0$ for all $i \neq j$ are identically zero. Therefore only the jth mode is excited. If the vector representing the initial conditions is not an eigenvector, it can be represented by a linear combination of the n linearly independent eigenvectors of A_{sys}, which span the n dimensional *Euclidean* space and form a basis. The response of the entire system will be the sum of these n individual responses. If a component along an eigenvector of the initial condition is zero, the corresponding mode will not be excited. When the system is in a state of instability, one or more eigenvalues of A_{sys} will not be on the left half complex plane. Consequently, the modes associated with these eigenvalues are critical.

From the above discussion, we can see that in order to directly study how the parameters influence the critical modes, or any particular mode in general, a link between parametric sensitivity and the eigen-basis needs to be set up. The parametric sensitivity itself gives only scattered information about the parameter influence on all of the modes and can not filter out those critical ones affecting stability.

4.3.2 The Definition of ISPS

The aforementioned link can be built by projecting the total parametric sensitivity onto the particular eigensubspace of critical interest [41], thus producing the so-called invariant subspace parametric sensitivity (ISPS). The motivation of ISPS is to combine the stability and sensitivity information and to get a better understanding of the factors that contribute to instability. The invariance properties of the eigenbasis is exploited for linking the stability and sensitivity aspects of the system. In a small disturbance analysis, each eigenvalue belongs a particular eigenbasis. If a critical eigenbasis refers to a critical eigenvalue, then according to the invariance property of the eigenbasis, the system instabilities are governed by the dynamics on the critical eigenbasis. This is achieved by collapsing the entire state space onto the critical

eigenbasis. The parametric sensitivity is therefore projected onto the subspace (which is the span of the eigenbasis) corresponding to each eigenvalue. The link between the eigenvalues and the parameters is achieved through the projected parametric sensitivity (or ISPS). Before defining ISPS, let us first review some concepts from linear algebra. In the following discussion, for the sake of simplicity, we assume that the system state matrix has n distinct eigenvalues.

From matrix theory, it is known that on the reciprocal eigenbasis [56], the system state matrix can be written as

$$\begin{aligned} A_{sys} &= U\Lambda V \\ &= \sum_{i=1}^{n} \lambda_i M_i \end{aligned} \tag{4.8}$$

where

$$M_i = u_i v_i^T \tag{4.9}$$

$$U = [u_1, \cdots, u_n] = V^{-1} \tag{4.10}$$

$$u_i = (u_{1i} \cdots u_{ni})^T \tag{4.11}$$

$$V = [v_1, \cdots, v_n]^T = U^{-1} \tag{4.12}$$

$$v_i = (v_{1i} \cdots v_{ni})^T \tag{4.13}$$

$$\Lambda = diag(\lambda_1 \cdots \lambda_n) \tag{4.14}$$

And the inverse of A_{sys} can be similarly decomposed as

$$\begin{aligned} A_{sys}^{-1} &= [U\Lambda V]^{-1} \\ &= V^{-1}\Lambda^{-1}U^{-1} \\ &= U\Lambda^{-1}V \\ &= \sum_{i=1}^{n} \frac{M_i}{\lambda_i} \end{aligned} \tag{4.15}$$

Applying the above matrix decomposition technique, we can rewrite the parametric sensitivity in equation 4.2 as

$$\begin{aligned} \frac{\partial X}{\partial P} &= \left[\sum_{i=1}^{m} \frac{M_i}{\lambda_i}\right] \left[\frac{\partial F}{\partial Y}\left[\frac{\partial G}{\partial Y}\right]^{-1}\frac{\partial G}{\partial P} - \frac{\partial F}{\partial P}\right] \\ &= \left[\sum_{i=1}^{m} \frac{M_i}{\lambda_i}\right] S \end{aligned} \tag{4.16}$$

with S defined as

$$\begin{aligned} S &= \frac{\partial F}{\partial Y}\left[\frac{\partial G}{\partial Y}\right]^{-1}\frac{\partial G}{\partial P} - \frac{\partial F}{\partial P} \\ &= (S_1, \cdots, S_m) \end{aligned} \tag{4.17}$$

where m is the number of parameters of interest in the DAE model. S contains the the sensitivities of functions F and G with respect to the parameters in P. The inverse matrix A_{sys}^{-1} operating on S results in parametric sensitivity.

Premultiplying both sides of equation 4.16 by M_i,

$$M_i\frac{\partial X}{\partial P} = M_i\left(\left[\sum_{i=1}^{m}\frac{M_i}{\lambda_i}\right]S\right) \tag{4.18}$$

Since $M_iM_j = 0$ if $i \neq j$ and $M_iM_j = M_i$ if $i = j$, Eq 4.18 becomes

$$\begin{aligned} M_i\frac{\partial X}{\partial P} &= M_i\left(\frac{M_1}{\lambda_1} + \cdots + \frac{M_i}{\lambda_i} + \cdots + \frac{M_m}{\lambda_m}\right)S \\ &= \frac{M_i}{\lambda_i}S \end{aligned} \tag{4.19}$$

In the above equation (Eq 4.19), the vector S_j is the column of the sensitivity matrix S. Each term M_iS_j/λ_i represents the projection of parametric sensitivity onto the ith eigensubspace. This projected parametric sensitivity is defined as the ISPS. Then, the most sensitive parameter on a particular subspace can be obtained by taking the maximum of M_iS_j/λ_i, $j = 1, \cdots, m$.

In order to study the parameter influence on the eigensubspace associated with λ_i, we do not need to calculate the entire product of $\frac{M_i}{\lambda_i}S$. This is explained by the following two equations.

$$M_i\frac{\partial X}{\partial P} = \frac{M_i}{\lambda_i}S \tag{4.20}$$

$$= \frac{u_i\sigma_P}{\lambda_i} \tag{4.21}$$

where

$$\sigma_P = v_i^T S \tag{4.22}$$

On a particular eigensubspace, u_i/λ_i is the same for all the parameters. Therefore the σ_P vector gives complete information about the parameter influence on the eigensubspace. For this reason, σ_P is defined as *the measure of ISPS.*

4.3.3 Sparse Formulation of ISPS

With the above formulation, we need the inverse of $\partial G/\partial Y$. This procedure is neither numerically efficient nor stable. To overcome this, we work directly with Eqs 3.1 and 3.2, thus avoiding the use of A_{sys} and G_Y^{-1}. Consequently, sparsity will be restored. To this end, we compute the eigenvectors of A_{sys} from the total system Jacobian J. That is,

$$\begin{bmatrix} v_F^T & v_G^T \end{bmatrix} \begin{bmatrix} F_X & F_Y \\ G_X & G_Y \end{bmatrix} = \begin{bmatrix} \lambda_i v_F^T & 0 \end{bmatrix} \tag{4.23}$$

Equivalently,

$$v_F^T F_X + v_G^T G_X = \lambda_i v_F^T \tag{4.24}$$

$$v_F^T F_Y + v_G^T G_Y = 0 \tag{4.25}$$

This leads to

$$v_G^T = -v_F^T F_Y G_Y^{-1} \tag{4.26}$$

$$v_F^T (F_X - F_Y G_Y^{-1} G_X) = \lambda_i v_F^T \tag{4.27}$$

Eqs 4.4 and 4.27 show that v_F thus computed is the left eigenvector of A_{sys} corresponding to λ_i. The measure of ISPS in Eq 4.22 can then be computed as:

$$\begin{aligned} \sigma_P &= v_i^T S \\ &= v_i^T \left[F_Y G_Y^{-1} G_P - F_P \right] \\ &= v_F^T \left[F_Y G_Y^{-1} G_P - F_P \right] \\ &= v_F^T F_Y G_Y^{-1} G_P - v_F^T F_P \\ &= -v_F^T F_P - v_G^T G_P \\ &= -\begin{bmatrix} v_F^T & v_G^T \end{bmatrix} \begin{bmatrix} F_P \\ G_P \end{bmatrix} \end{aligned} \tag{4.28}$$

Here, no matrix inverse is involved. Details about how to compute the eigenvector from the total system Jacobian J by solving equation 4.23 can be found in [57, 58]. A brief introduction of this is given in Appendix B. We see that the intermediate result v_G, produced

while computing the eigenvector v_F from J, becomes meaningful. It can be interpreted as the weight which weighs the sensitivity of the algebraic equations. The above procedure can be applied to compute ISPS corresponding to any eigenvalue at any operating point. However, at the critical point, where A_{sys} becomes singular, we can further speed up the computation. This is explained in the following sections and appendix B.

4.3.4 ISPS Vs. Eigenvalue Sensitivity

It is numerically verified in [59] that ISPS gives an indirect relation between the eigenvalues and the parameters under consideration. This relation is verified numerically with a well-known eigenvalue sensitivity. The measure of ISPS, namely, the σ_p vector also provides the cluster of parameters that are most sensitive to the corresponding eigenvalue.

However, the following discussion between the σ_p vector and the normal vector leads to further insights about ISPS. Transfer margin estimation becomes possible by further manipulating the information from ISPS.

4.3.5 The σ_p Vector at Saddle Node Bifurcation Vs. the Normal Vector

In power systems, variation of various parameters will often drive the system to bifurcation. The generic bifurcating phenomenon associated with voltage collapse is the so-called saddle node bifurcation (SNB). At a saddle node bifurcation, a stable operating equilibrium disappears and the consequence is that system states dynamically collapse. This explains the dynamic fall of voltage magnitudes in voltage collapse. All the saddle node bifurcation points form the voltage collapse boundary which is a hypersurface in the multi-dimensional parameter space. On this hypersurface, the system state matrix A_{sys} of the following differential system, derived from 3.1 and 3.2 and repeated here for continuity and clarity, has a simple unique zero eigenvalue. It was shown in chapter 3, that the complete system Jacobian J associated with the DAE model becomes singular at the same time when the differential system experiences saddle node bifurcation.

$$\Delta\dot{X} = A_{sys}\Delta X \tag{4.29}$$

This shows that voltage collapse boundary can be equivalently characterized by the singularity of the complete DAE model. For convenience, let us denote the saddle node bifurcation boundary in the R^m parameter space by Σ. Suppose that the system parameters are such that $P_* \in \Sigma$. P is a vector containing all relevant parameters in the DAE model. '*' means evaluation at the current saddle node bifurcation point on Σ. Under standard generic assumptions, Σ is a smooth hypersurface near P_* and a normal vector to the hypersurface at P_* is [34]

$$N(P_*) = \omega H_P \tag{4.30}$$

where ω is the left eigenvector corresponding to the trivial eigenvalue of the total system Jacobian J, and H_P is the Jacobian of F and G with respect to the parameter vector P. In the parameter space, at a particular voltage collapse point on the Σ surface, the normal vector is perpendicular to the tangent plane at that point. This is conceptually illustrated in figure 4.1 when $m = 2$.

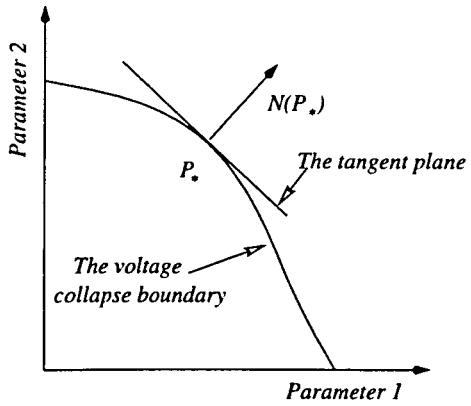

Figure 4.1 The normal vector in the parameter space

Reviewing equations 4.23 to 4.27 and noting the definition of ω, one immediately notices that at saddle node bifurcation, (v_F^T, v_G^T), computed from 4.23 for the zero eigenvalue of A_{sys}, is nothing but ω in equation 4.30. Thus the normal vector can be written as

$$N(P_*) = \begin{bmatrix} v_F^T & v_G^T \end{bmatrix} \begin{bmatrix} F_P \\ G_P \end{bmatrix} \tag{4.31}$$

Consequently, we observe that the normal vector defined with the DAE model is nothing but the σ_P vector corresponding to the zero eigenvalue of the system state matrix A_{sys} at saddle

node bifurcation. The negative sign in 4.28 makes no difference since in the definition of normal vector, the sign of it is chosen such that an increase of the load in the direction of $N(P_*)$ leads to disappearance of the operating equilibrium.

4.4 Transfer Margin Estimation

From the discussion in subsections 4.3.4 and 4.3.5, we get more insights about the measure of ISPS, namely the σ_P vector corresponding to the trivial eigenvalue of A_{sys}. At voltage collapse, it acts as a link between the eigensubspace in which system dynamics is invariant, and the parameter space in which saddle node bifurcation sensitivity can be defined. As such, the measure of ISPS has the potential of giving voltage stability margin sensitivity.

Next it will be shown that the transfer margin sensitivity can be easily obtained by further manipulating the information from ISPS. Referring to section 4.1, we are now trying to derive the sensitivity of a large deviation based index of voltage stability from ISPS.

4.4.1 From ISPS to Bifurcation Parameter Sensitivity

As introduced in section 3.4, a scalar α denoting the system load/generation level is called the bifurcation parameter. The system reaches a state of voltage collapse, when α hits its maximum value (the turning point). For this reason, the system DAE model at equilibrium states is parameterized by this bifurcation parameter α as shown in equations 3.30 to 3.32. When system parameters are changed, the total transfer capability will probably increase or decrease. The change of transfer margin can be determined if the change of α between two bifurcation points on the voltage collapse boundary Σ is known. Since we are interested in estimating the loading margin when some arbitrary parameters are varied, we rewrite the DAE as follows to denote the parameter dependence of the system solution.

$$\dot{X} = F(X(\alpha(P),P),Y(\alpha(P),P),\alpha(P),P) \tag{4.32}$$

$$0 = G(X(\alpha(P),P),Y(\alpha(P),P),\alpha(P),P) \tag{4.33}$$

At a saddle node bifurcation, which is also an equilibrium point (though not asymptotically stable), we take the partial differentiation of the above two equations with respect to the parameter vector P; then

$$0 = \frac{\partial F}{\partial X}\left(\frac{\partial X}{\partial \alpha}\frac{\partial \alpha}{\partial P}+\frac{\partial X}{\partial P}\right)+\frac{\partial F}{\partial Y}\left(\frac{\partial Y}{\partial \alpha}\frac{\partial \alpha}{\partial P}+\frac{\partial Y}{\partial P}\right)+\frac{\partial F}{\partial \alpha}\frac{\partial \alpha}{\partial P}+\frac{\partial F}{\partial P} \tag{4.34}$$

$$0 = \frac{\partial G}{\partial X}\left(\frac{\partial X}{\partial \alpha}\frac{\partial \alpha}{\partial P}+\frac{\partial X}{\partial P}\right)+\frac{\partial G}{\partial Y}\left(\frac{\partial Y}{\partial \alpha}\frac{\partial \alpha}{\partial P}+\frac{\partial Y}{\partial P}\right)+\frac{\partial G}{\partial \alpha}\frac{\partial \alpha}{\partial P}+\frac{\partial G}{\partial P} \tag{4.35}$$

Simplifying the above expressions gives

$$\begin{pmatrix} F_X & F_Y \\ G_X & G_Y \end{pmatrix}\begin{pmatrix} \frac{\partial X}{\partial \alpha}\frac{\partial \alpha}{\partial P}+\frac{\partial X}{\partial P} \\ \frac{\partial Y}{\partial \alpha}\frac{\partial \alpha}{\partial P}+\frac{\partial Y}{\partial P} \end{pmatrix}+\begin{pmatrix} F_\alpha \\ G_\alpha \end{pmatrix}\frac{\partial \alpha}{\partial P}+\begin{pmatrix} F_P \\ G_P \end{pmatrix}=0 \tag{4.36}$$

Premultiplying the above equation by $(v_F^T,\ v_G^T)$ corresponding to the zero eigenvalue of A_{sys} as computed from equation 4.23, the first item will become zero and we get

$$\begin{pmatrix} v_F^T & v_G^T \end{pmatrix}\begin{pmatrix} F_\alpha \\ G_\alpha \end{pmatrix}\frac{\partial \alpha}{\partial P}+\begin{pmatrix} v_F^T & v_G^T \end{pmatrix}\begin{pmatrix} F_P \\ G_P \end{pmatrix}=0 \tag{4.37}$$

Therefore, the bifurcation parameter sensitivity is:

$$\frac{\partial \alpha}{\partial P} = -\frac{\begin{pmatrix} v_F^T & v_G^T \end{pmatrix}\begin{pmatrix} F_P \\ G_P \end{pmatrix}}{\begin{pmatrix} v_F^T & v_G^T \end{pmatrix}\begin{pmatrix} F_\alpha \\ G_\alpha \end{pmatrix}} \tag{4.38}$$

From equations 3.30 to 3.32, using vector notation (the underline sign), we can write the generation and load parameterization equations as

$$\underline{P_{Gs}} = \begin{pmatrix} \cdots P_{Gsi}(\alpha)\cdots \end{pmatrix}^T \tag{4.39}$$

$$\begin{aligned} \underline{L(\alpha)} &= \begin{pmatrix} \cdots P_{Li}(\alpha)\cdots Q_{Li}(\alpha)\cdots \end{pmatrix}^T \\ &= \underline{L_0}+\alpha \underline{K} \\ &= \begin{pmatrix} \underline{P_L} & \underline{Q_L} \end{pmatrix}^T \end{aligned} \tag{4.40}$$

where

$$\begin{aligned} \underline{K} &= \left(\cdots K_{Lp_i} P_{Li0} \cdots K_{Lq_i} Q_{Li0} \cdots \right)^T \\ &\hat{=} \left(\cdots K_{P_i} \cdots K_{Q_i} \cdots \right)^T \\ &\hat{=} \left(\underline{K}_P \quad \underline{K}_Q \right)^T \end{aligned} \tag{4.41}$$

(4.42)

denotes the loading pattern. At saddle node bifurcation, the set of real powers form the voltage instability boundary in the load power space. Using these notations and noting that only L contains α (equations 3.30 to 3.32), by the chain rule, the derivatives of F and G with respect to α can be written as

$$\begin{pmatrix} \frac{\partial F}{\partial \alpha} \\ \frac{\partial G}{\partial \alpha} \end{pmatrix} = \begin{pmatrix} \frac{\partial F}{\partial L} \\ \frac{\partial G}{\partial L} \end{pmatrix} \underline{K} \tag{4.43}$$

From the above discussion, we observe that the bifurcation parameter sensitivity given in equation 4.38 basically comes from the measure of ISPS, namely the σ_P and σ_L vectors corresponding to the zero eigenvalue of A_{sys}. Or equivalently, from the normal vector to the voltage collapse boundary Σ in the extended parameter space (including the load power parameters). This is illustrated by the following equations.

$$\begin{aligned} \frac{\partial \alpha}{\partial P} &= -\frac{\begin{pmatrix} v_F^T & v_G^T \end{pmatrix} \begin{pmatrix} F_P \\ G_P \end{pmatrix}}{\begin{pmatrix} v_F^T & v_G^T \end{pmatrix} \begin{pmatrix} F_\alpha \\ G_\alpha \end{pmatrix}} \\ &= -\frac{\begin{pmatrix} v_F^T & v_G^T \end{pmatrix} \begin{pmatrix} F_P \\ G_P \end{pmatrix}}{\begin{pmatrix} v_F^T & v_G^T \end{pmatrix} \begin{pmatrix} F_L \\ G_L \end{pmatrix} \underline{K}} \\ &= -\frac{\sigma_P}{\sigma_L \underline{K}} \end{aligned} \tag{4.44}$$

This margin sensitivity gives the first order partial derivative in the Taylor series expansion of α as a nonlinear function of P, which describes the hypersurface Σ.

The bifurcation parameter sensitivity will allow us to know, when some parameters are varied, how the system will move along the hypersurface Σ in the vicinity of the current instability point denoted by α_*.

4.4.2 Transfer Margin Estimation

Once $\partial\alpha/\partial P$ is computed, we will first get the bifurcation parameter estimation as

$$\Delta\alpha = \frac{\partial\alpha}{\partial P}\Delta P \tag{4.45}$$

where P contains all the parameters explicitly appearing in the DAE model including the load scenario parameters. If we are only interested in the real power transfer capability, then we define $PLM(\alpha_*)$ as the total power of all the buses at voltage collapse before a parameter variation, and $PLM(\alpha'_*)$ as the total power of all the buses at voltage collapse after a parameter variation. In the case of a non-real-power-load related parameter, we will get the margin change estimate as

$$\begin{aligned} \Delta PLM &= PLM(\alpha'_*) - PLM(\alpha_*) \\ &\doteq \sum_{i=1}^{N} \Delta P_{L_i}(\alpha) \\ &= \Delta\alpha \sum_{i=1}^{N} K_{P_i} \end{aligned} \tag{4.46}$$

And, the new critical powers at all the buses, in vector notation, can be estimated as

$$\underline{P_{L_*}}' = \underline{P_{L_*}} + \Delta\alpha \underline{K_P} \tag{4.47}$$

The above discussion is conceptually illustrated in Figure 4.2 and Figure 4.3.

In the case of a real power load related parameter (K_{Lpi} and P_{Li0}) variation, the loading margin estimation for bus i will be:

$$\Delta P_{L_i}(\alpha, K_{Lpi}, P_{Li0}) = \Delta\alpha K_{Pi} + \frac{\partial P_{L_i}}{\partial K_{Lpi}}|_* \Delta K_{Lpi} + \frac{\partial P_{L_i}}{\partial P_{Li0}}|_* \Delta P_{Li0} \tag{4.48}$$

where

$$\frac{\partial P_{L_i}}{\partial K_{Lpi}}|_* = \alpha_* P_{Li0} \tag{4.49}$$

$$\frac{\partial P_{L_i}}{\partial P_{Li0}}|_* = 1 + \alpha_* K_{Lpi} \tag{4.50}$$

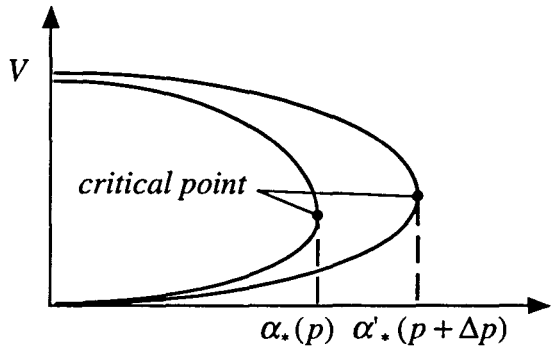

Figure 4.2 Transfer margin as shown on a PV curve

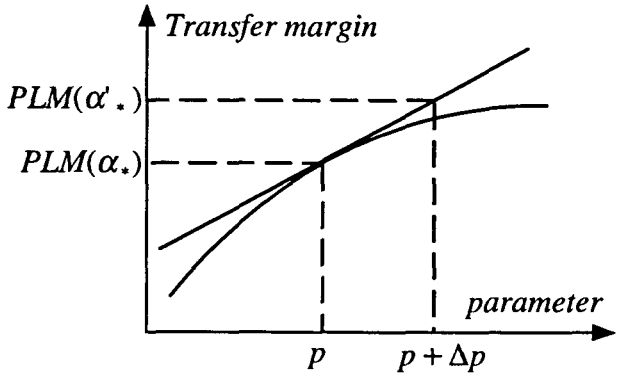

Figure 4.3 Transfer margin estimation

The total margin change estimation will then be modified to include two more terms

$$\Delta PLM = \sum_{i=1}^{N} \Delta P_{L_i} = \Delta\alpha \sum_{i=1}^{N} K_{P_i} + \sum_{i \in Ich} (\frac{\partial P_{L_i}}{\partial K_{Lpi}})|_* \Delta K_{Lpi} + \sum_{i \in Ich} (\frac{\partial P_{L_i}}{\partial P_{Li0}})|_* \Delta P_{Li0} \quad (4.51)$$

where Ich denotes the set which includes all the buses under load parameter variations. When reactive power load parameters (K_{Lqi} and Q_{Li0}) are varied, the real power transfer margin estimation can still be calculated by using equations 4.46 and 4.47. The reactive power transfer margin estimation, however, should be made by using equations similar to 4.48 and 4.51 for bus i and the total.

4.4.3 Multi-parameter Margin Sensitivity

In modern power system operation, coordinated controls are often used to optimize certain performance indices, for instance, to maximize the transfer on a specified transmission interface if possible. Since a first order estimation can be linearly superimposed, we can study the combined parameter influence on stability margin variation by using

$$\Delta\alpha = \frac{\partial\alpha}{\partial P_1}\Delta P_1 + \cdots + \frac{\partial\alpha}{\partial P_m}\Delta P_m \tag{4.52}$$

However, when more than one parameter is varied, the mixed partial derivative term of higher orders also contributes to the margin variation. For instance, when both p_i and p_j are varied, the mixed second order term $\frac{\partial^2\alpha}{\partial p_i \partial p_j}\Delta p_i \Delta p_j$ is also nonzero. Inaccuracy will result from ignoring this term in addition to $\frac{\partial^2\alpha}{\partial p_i^2}\Delta p_i^2$.

4.4.4 Sensitivity Formulas

This subsection will derive the sensitivity formulas with respect to all the parameters studied in this work.

- Sensitivity matrices $\frac{\partial F}{\partial P}$ and $\frac{\partial G}{\partial P}$

  Excitation system parameters

  - Exciter gain K_{Ai}:

$$\frac{\partial f_{g8i}}{\partial K_{Ai}} = \frac{1}{T_{Ai}}(V_{REFi}^{EX} - V_i - R_{Fi}) \tag{4.53}$$

  where f_{g8i} is the right hand side of equation 3.15.

  - Self excitation parameter K_{Ei}:

$$\frac{\partial f_{g7i}}{\partial K_{Ei}} = -\frac{E_{fdi}}{T_{Ei}} \tag{4.54}$$

$$\frac{\partial f_{g9i}}{\partial K_{Ei}} = -\frac{K_{Fi}E_{fdi}}{T_{Ei}T_{Fi}} \tag{4.55}$$

  where f_{g7i} and f_{g9i} are the right hand sides of equation 3.14 and 3.16 respectively.

• Exciter reference voltage V_{REFi}^{EX}:

$$\frac{\partial f_{g8i}}{\partial V_{REFi}^{EX}} = \frac{K_{Ai}}{T_{Ai}} \tag{4.56}$$

Governor parameters

• Governor base case setting P_{Gsi0}:

$$\frac{\partial f_{g6i}}{\partial P_{Gsi0}} = \frac{1}{T_{Gi}} \tag{4.57}$$

where f_{g6i} is the right hand side of equation 3.18.

Network parameters

• Line susceptance B_{ij}:

$$\begin{aligned} \frac{\partial \Delta P_i}{\partial B_{ij}} &= -\frac{\partial P_{Ti}}{\partial B_{ij}} \\ &= -\frac{\partial}{\partial B_{ij}}(V_i \sum_{k=1}^{N} V_k y_{ik} cos(\theta_i - \theta_k - \gamma_{ik})) \\ &= V_i V_j sin(-\theta_i + \theta_j) \end{aligned} \tag{4.58}$$

$$\begin{aligned} \frac{\partial \Delta Q_i}{\partial B_{ij}} &= -\frac{\partial Q_{Ti}}{\partial B_{ij}} \\ &= -\frac{\partial}{\partial B_{ij}}(V_i \sum_{k=1}^{N} V_k y_{ik} sin(\theta_i - \theta_k - \gamma_{ik})) \\ &= V_i V_j cos(\theta_i - \theta_j) \end{aligned} \tag{4.59}$$

where ΔP_i and ΔQ_i are from the real and reactive power mismatch equations as given in 3.4 and 3.5.

• Shunt capacitance B_{i0}:

$$\begin{aligned} \frac{\partial \Delta Q_i}{\partial B_{i0}} &= -\frac{\partial Q_{Ti}}{\partial B_{i0}} \\ &= -\frac{\partial}{\partial B_{i0}}(V_i \sum_{k=1}^{N} V_k y_{ik} sin(\theta_i - \theta_k - \gamma_{ik})) \\ &= V_i^2 \end{aligned} \tag{4.60}$$

Load (scenario) parameters

- Real power load increase speed parameter K_{Lpi}:

$$\frac{\partial f_{g6i}}{\partial K_{Lpj}} = \frac{1}{T_{Gi}} K_{Gpi} P_{Lj0} \tag{4.61}$$

$$\frac{\partial \Delta P_i}{\partial K_{Lpi}} = -\alpha P_{Li0} \tag{4.62}$$

- Reactive power load increase speed parameter K_{Lqi}:

$$\frac{\partial \Delta Q_i}{\partial K_{Lqi}} = -\alpha Q_{Li0} \tag{4.63}$$

- Base case real power load P_{Li0}:

$$\frac{\partial f_{g6i}}{\partial P_{Lj0}} = \frac{1}{T_{Gi}} \alpha K_{Gpi} K_{Lpj} \tag{4.64}$$

$$\frac{\partial \Delta P_i}{\partial P_{Li0}} = -(1 + \alpha K_{Lpi}) \tag{4.65}$$

- Base case reactive power load Q_{Li0}:

$$\frac{\partial \Delta Q_i}{\partial Q_{Li0}} = -(1 + \alpha K_{Lqi}) \tag{4.66}$$

The above formulas are used to construct the sensitivity matrices $\partial F/\partial P$ and $\partial G/\partial P$.

- Sensitivity matrices $\frac{\partial F}{\partial L}$ and $\frac{\partial G}{\partial L}$

$$\frac{\partial f_{g6i}}{\partial P_{Lj}(\alpha)} = \frac{K_{Gpi}}{T_{Gi}} \tag{4.67}$$

$$\frac{\partial \Delta P_i}{\partial P_{Li}(\alpha)} = -1.0 \tag{4.68}$$

$$\frac{\partial \Delta Q_i}{\partial Q_{Li}(\alpha)} = -1.0 \tag{4.69}$$

4.4.5 Computational Issues in Margin Estimation

As we have seen in the last subsection, the bifurcation parameter sensitivity basically comes from the measure of ISPS. Once the measure of ISPS is computed, essentially no further computational cost is needed in getting $\partial\alpha/\partial P$.

In computing the measure of ISPS corresponding to the zero eigenvalue of A_{sys}, we first need to obtain the left eigenvector as computed from equation 4.23. The sensitivity matrices $\partial F/\partial P$, $\partial G/\partial P$, $\partial F/\partial L$ and $\partial G/\partial L$, are extremely sparse and therefore imposes very limited computational burden. Once the bifurcation parameter sensitivity becomes available, margin estimation is simply an evaluation process involving literally no noticeable increase in computing cost.

4.5 Test System Studies

In this section, the proposed sensitivity measure calculated at saddle node bifurcation is applied to estimate the voltage stability margin under system parameter variations. Physical interpretations are given following the test results. The method is tested on the IEEE New England 39-bus system and the reduced Iowa 162-bus network. A large set of parameters are selected to analyze their influence on the voltage stability limited transfer capability.

4.5.1 Parameters of Interest

With the DAE formulation of the power system, we can directly estimate the voltage collapse limited transfer margin with respect to all parameters which explicitly appear in F or G from Eqs.3.1 and 3.2. The parameters studied include:

- Exciter parameters: K_{Ai}, K_{Ei}, and V_{REFi}^{EX}
- Governor parameter and settings: R_{Gi} and P_{Gsi0}
- Network parametrs: B_{i_0} and B_{ij}
- Load (scenario) parameters: K_{Lpi}, P_{Li0}, K_{Lqi} and Q_{Li0}

4.5.2 The New England System

The same scenario as in chapter 3 was used to locate the saddle node bifurcation point. With the nominal parameter settings, the total real power transfer margin between the base case and the critical point is approximately 2466 MW.

4.5.2.1 Exciter parameters

The automatic voltage regulator gain (Fig. 4.4) of the generator at bus 31 affects the voltage collapse limited transfer the most. Obviously, in calibration (parameter estimation), K_{A31} should be given first priority for better accuracy. Otherwise the voltage stability limited transfer evaluation might be in great error.

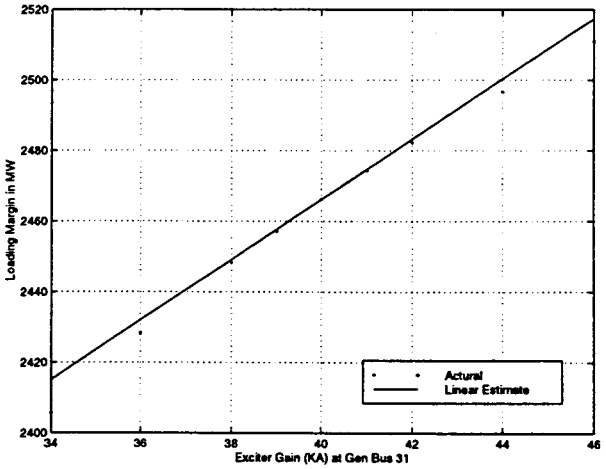

Figure 4.4 Loading margin vs. exciter gain

The parameter K_{Ei} (Fig. 4.5) is related to the exciter self excitation. It is interesting to observe that, in all our test studies, an increase in K_{Ei} results in a reduced voltage stability margin. And we observe that a 20% variation in K_{E32}, with a nominal value 1.0, could give a difference of up to 1000 MW in transfer margin. This shows that it is very important to accurately calibrate K_{Ei}'s.

The exciter reference voltage (Fig. 4.6) is one of the control settings traditionally applied by system operators to control generator terminal voltages. From Fig. 4.6, we can see that V_{REF31}^{EX} is very effective for the increase of the transfer. A 20% increase in V_{REF31}^{EX}, with the nominal setting at 1.0467 pu, makes the system able to transfer an approximately additional 700 MW before causing voltage collapse.

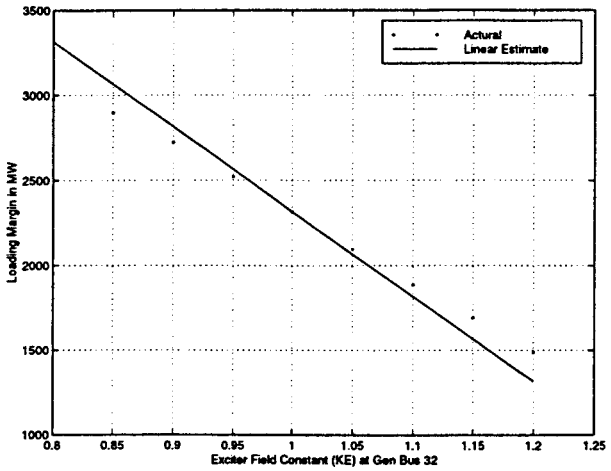

Figure 4.5 Loading margin vs. exciter self excitation

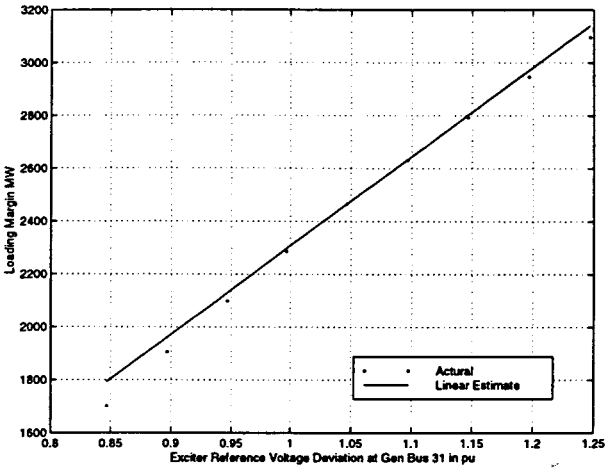

Figure 4.6 Margin vs. exciter reference voltage

4.5.2.2 Governor parameters

Because all the governors hit their limits, the sensitivity of the loading margin with respect to the governor base case settings can not be used to predict the voltage collapse point. In the test case for the Iowa system (next section), where not all governors hit their limits, these sensitivities are valid and thus used.

The steady state governor regulation characteristic, described by R_{Gi}'s, (Figs. 4.7 and 4.8) determines the ultimate contribution of each machine to a change in the load and fixes the resulting system frequency. It gives the slope of the droop characteristic curve of the governor.

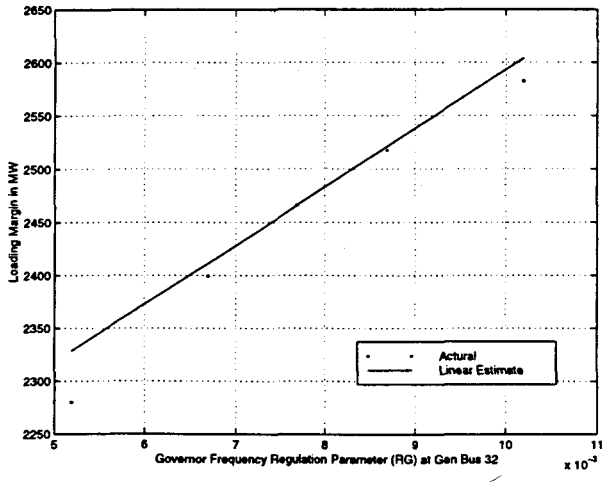

Figure 4.7 Margin vs. governor frequency regulation

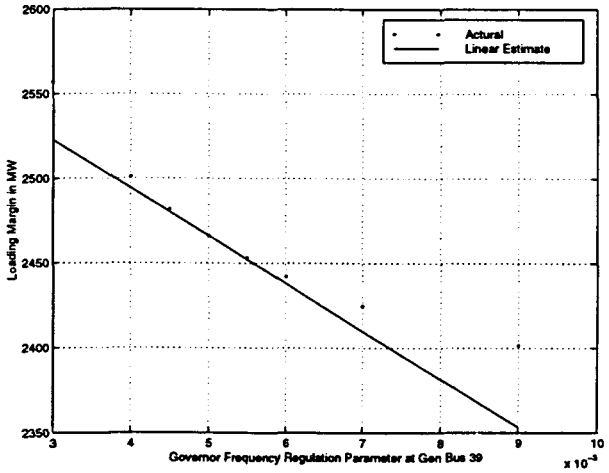

Figure 4.8 Margin vs. governor frequency regulation

The value of R_{Gi} is inversely proportional to the capacity of the generator. From the current test study, we observe that, when we increase R_{Gi}, we get an increase or decrease in total transfer capability.

4.5.2.3 Network parameters

One of the reasons for voltage instability is the lack of reactive power support at critical locations [2]. Supplying enough Vars (Fig. 4.9) locally at or near heavily loaded buses, or at an intermediate point between generation and load centers usually increases the real power

transfer capability. In this test case, the measure of ISPS indicates that bus 10 is one of the best places to put some reactive power support. Bus 10 is linked to the generator bus 32 where this generator is at its limit. Quantitatively, it is shown in Figure 4.9 that a one pu shunt capacitance installation will lead to an increase of approximately 110 MW in total real power transfer. The linear estimate is very accurate over a wide range of shunt values. Selecting the best location for installation of SVC can be analyzed using the same information.

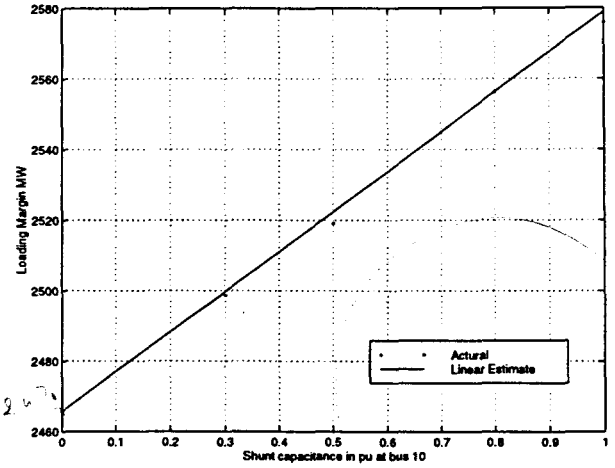

Figure 4.9 Loading margin vs. shunt capacitance

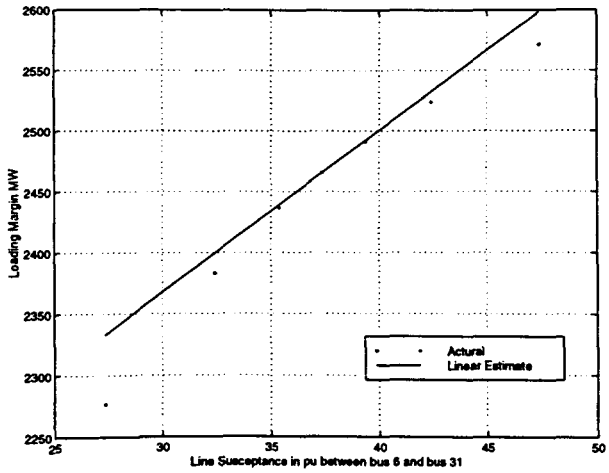

Figure 4.10 Loading margin vs. line susceptance

Line susceptance (Fig. 4.10) is also a critical parameter in transfer capability evaluation. One of the most sensitive line indicated by ISPS is line 6-31. Since the generator at bus 31 is one of the remaining generation sources not hitting the limits, transfer capability can be increased by reducing the reactance of that line. This will enable the network to receive more reactive power from the generator at bus 31. The margin curve becomes nonlinear when ΔB_{6-31} exceeds 10 pu (over 25 percent of its nominal value). Quantitative study of the influence of line susceptances on transmission capability can be extended to analyze the effectiveness of FACTs devices, such as that of TCSC (thyrister controlled series capacitors). Line contingency could also be simulated through this.

4.5.2.4 Load (scenario) parameters

The parameters K_{Lpi} and K_{Lqi} designate the rate of load increase at bus i. If they are zero, the loads will remain at the base case value. By changing these load scenario parameters, the power factors will be varied. At the nominal case, we give 1.0 to both K_{Lpi}'s and K_{Lqi}'s. This will force the load to increase at a constant power factor. For the current scenario, margin sensitivity (Fig. 4.11) indicates that K_{Lp39} is the most sensitive. Forcing the load at bus 39 to remain unchanged (giving 0 to K_{Lp39}) will increase the loading margin of the remaining buses. However, since the load at bus 39 is the largest, the overall margin will decrease by about 100 MW. For the same reason, when we increase the load at this bus at a faster rate by giving K_{Lp39} a value larger than 1.0, the total margin does not increase significantly, rather saturation occurs. Therefore, the linear sensitivity does not work well in this case.

The reactive power load at bus 4 is varied to see how a different load component (power factor) at this bus affects the total transfer margin. From Figure 4.12, we observe that the closer the power factor (lag) is to unity, the more increase of transfer capability will result. This is well predicted by the sensitivity.

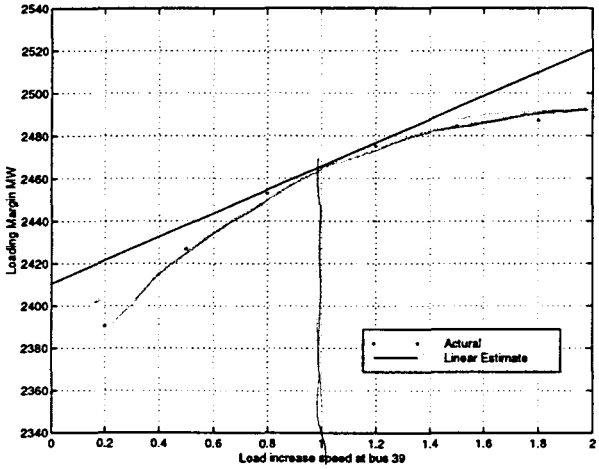

Figure 4.11 Loading margin vs. load parameter K_{Lpi}

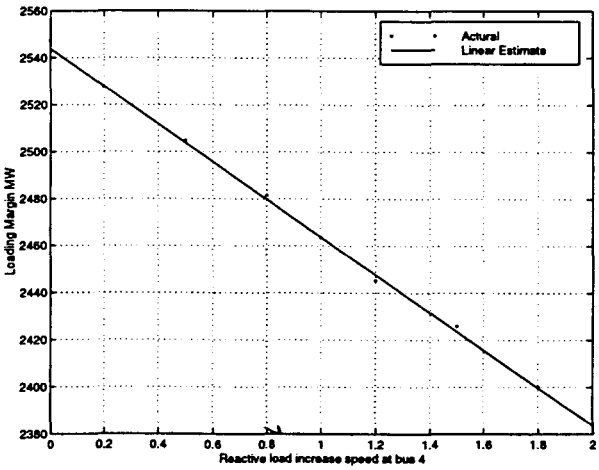

Figure 4.12 Loading margin vs. load parameter K_{Lqi}

The base case real and reactive power loads at bus 3 are 322 MW and 122 MVAR respectively. If we shed up to 3.0 pu load at a constant power factor, the resultant transfer margin (the difference between the base case and the critical point) will increase almost linearly to about 2825 MW. The linear estimate (Fig. 4.13) again works quite well.

4.5.2.5 Multipale-parameter variations

Two parameters (shunt capacitance at bus 10 and exciter reference voltage at bus 31) are changed simultaneously. Equation 4.52 was used to predict the margin. In Figures 4.14 and

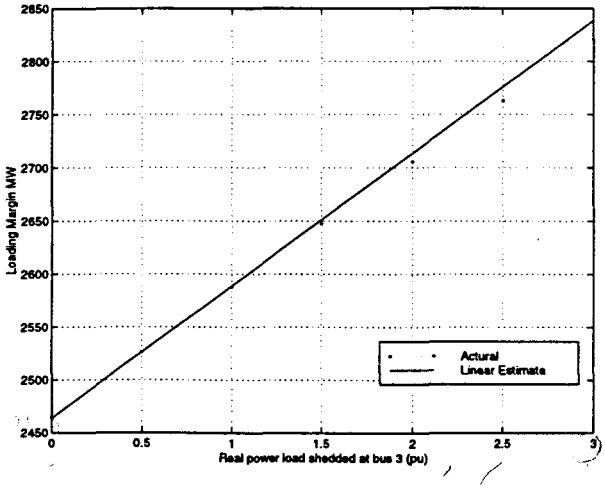

Figure 4.13 Loading margin vs. load shedding

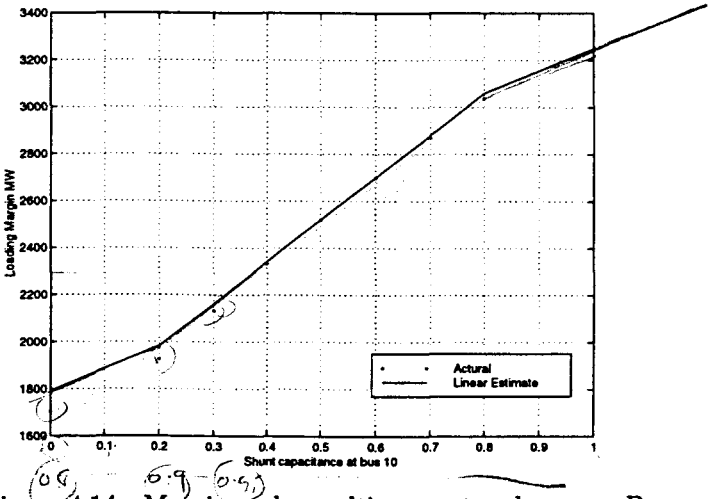

Figure 4.14 Margin under multiparameter changes - B_{i010}

4.15, the transfer margin is plotted against each of the two parameters respectively. The linear prediction is very accurate over the range of parameter variations.

4.5.3 The Iowa System

The same scenario as in chapter 3 was used to locate the nominal case saddle node bifurcation point. With the nominal parameter settings, the total real power transfer margin between the base case and the critical point is approximately 1223 MW.

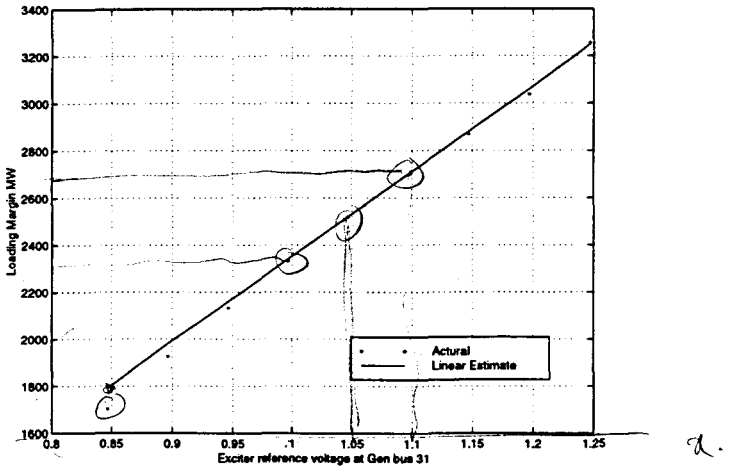

Figure 4.15 Margin under multiparameter changes - V_{REF31}^{EX}

4.5.3.1 Exciter parameters

For the current test case, K_{A27} is the most sensitive excitation gain (Fig. 4.16) in affecting the loading margin. Within 15% change of the parameter, the margin changes almost linearly.

For this test case, the loading margin changes linearly (Fig. 4.17) when the exciter self excitation parameter of generator at bus 27 is varied by ±20%. This makes the sensitivity able to predict with good accuracy.

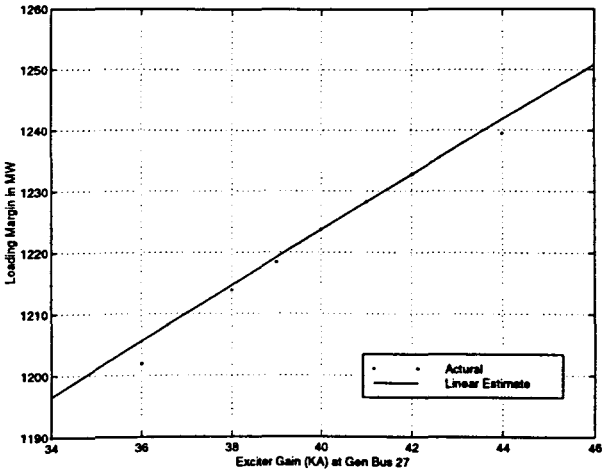

Figure 4.16 Loading margin vs. exciter gain

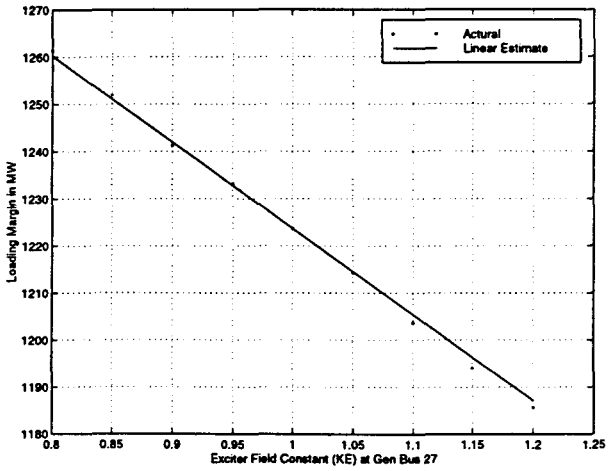

Figure 4.17 Loading margin vs. exciter self excitation

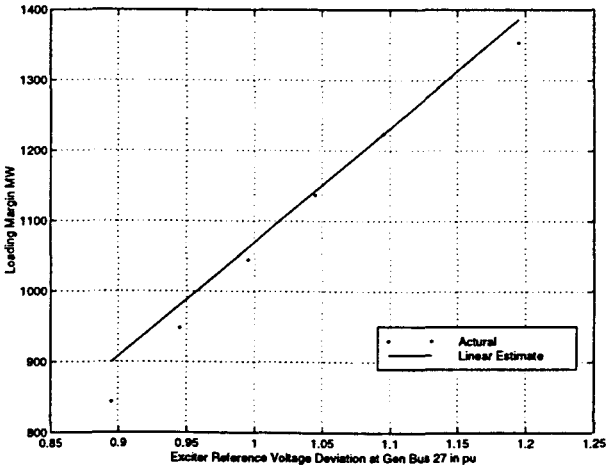

Figure 4.18 Margin vs. exciter reference voltage

From Figure 4.18, we can see that a 20% increase in V_{REF27}^{EX}, with the nominal setting at 1.0951 pu, makes the system able to transfer an approximately additional 150 MW before voltage collapse occurs.

4.5.3.2 Governor parameters

The governor generation/load setting P_{Gsi0} determines the steady state contribution of the machine to the load increase in the system. Changing P_{Gsi} will shift the governor's droop characteristic curve in a parallel direction. From Figure 4.19, we observe that, by increasing

of the governor's setting at generator bus 118, we can get a surplus of transfer margin. This reflects the dependence of the transfer margin on generation sharing scenario. The governor on the generator at bus 125 hits its limit, so like in the New England system, the sensitivity with respect to P_{Gs0125} should not be used for prediction.

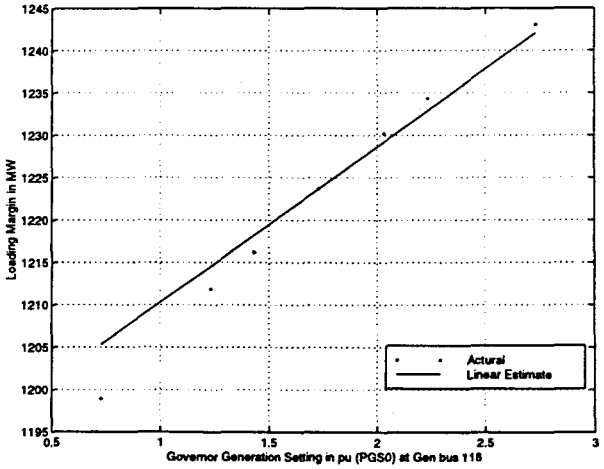

Figure 4.19 Margin vs. governor load settings

4.5.3.3 Network parameters

Bus 30 has lowest voltage when approaching voltage collapse. Margin sensitivity indicates that adding one pu shunt capacitance will lead to an increase of around 90 MW in total real power transfer margin. This is verified as shown in Figure 4.20. The linear estimate is very accurate over the entire range of shunts changes.

The most sensitive line indicated by the margin sensitivity (Fig. 4.21) is line 29-30. Increasing its susceptance will increase the voltage collapse limited transfer, because it will enable the load at bus 30 (the most critical bus) to further receive real power from the generators.

4.5.4 Conclusions

ISPS identifies the cluster of parameters which are responsible for voltage instability. At operating points other than at voltage collapse, with the newly derived sparse formulation of ISPS, we can get the σ_P vector with moderate computing cost. At the critical point, the

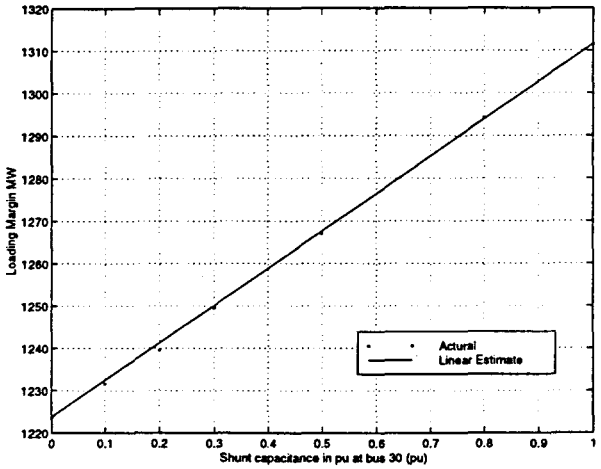

Figure 4.20 Loading margin vs. shunt capacitance

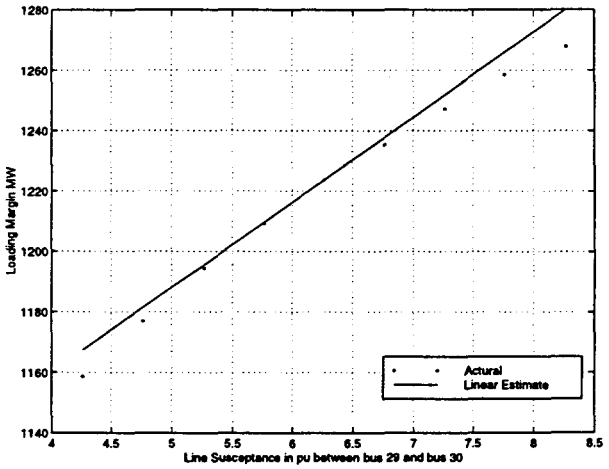

Figure 4.21 Loading margin vs. line susceptance

computation can be further reduced by directly applying the inverse power method on J to compute the left eigenvector and σ_P. With literally no further cost, we can get the margin sensitivity from the measure of ISPS. With the total system equilibria tracing technique introduced in chapter 3, one can identify dynamic voltage collapse without eigenvalue computations. Once the critical point is identified, the voltage collapse limited transfer margin sensitivity can easily be obtained. The DAE formulation also makes it possible to study a wide range of parameters that affect the dynamic voltage collapse limited power transfer. Another approach for margin sensitivity with the power flow model was reported by Dobson in reference [60]. The

methodology given here can be applied to the evaluation of multiarea available transfer capability (ATC) as limited by dynamic voltage collapse. The present competitive power industry environment may lead to frequent violation of transfer capability limits. Voltage security plays an important role in these studies.

5 CONCLUSIONS AND SUGGESTIONS FOR FUTURE WORK

The review given in chapter 2 shows the potential application of homotopy and continuation methods to a wide range of power system problems. Simultaneously solving for the total power system equilibria makes it possible to resolve the problems encountered in the traditional approach. System limits are automatically handled without iterating between the power flow and device equations. Synchronous machines are represented in a consistent manner which is very important in dynamic stability analysis, since we know that the different initial conditions of a dynamic system will result in different stability results. Dynamic voltage collapse identification via simultaneous equilibria tracing, as proposed in this work, helps to avoid forming the system state matrix A_{sys} and computing its eigenvalues, while a complete DAE model makes it possible to capture system dynamics of concern. The AVR and governor limits are explicitly handled. The AVR limits directly control the rotor current and indirectly limit the reactive output of the generator to the network. These system limits have an important impact on the dynamic voltage collapse limited transfer capability. The invariant properties of eigensubspaces are thoroughly exploited by which stability and sensitivity information is combined in a coherent fashion. Further development of ISPS leads to more insights concerning state space and parameter space. Margin sensitivity is derived by intelligently manipulating the information from the measure of ISPS. Test studies with two power systems show the applicability of the methodologies developed in this work.

5.1 Suggestions for Future Work

The limits considered in this work are those of the governor and AVR limits. They are the limits of the synchronous machine control systems. Though they obviously control the

output of the generators, machine capability as affected by the stator current is not explicitly reflected. Only first order sensitivity is considered in this work. Quadratic sensitivity can further be developed for better accuracy. How to alleviate the nonlinear effect caused by the different limits is important in order to more effectively use the margin sensitivity to predict voltage collapse. To this end, one might consider studying the sensitivity of the loading margin with respect to the limits. Further investigation in this aspect is worthwhile. Besides this, implementation of voltage level and other constraints would make the program an even more practical tool in small disturbance voltage stability analysis. Exploiting the capability of quantitative estimation of transfer margin, one could apply the technique to evaluate multi-area power transactions as limited by voltage collapse. Future work can perhaps further extend the simultaneous equilibria tracing technique to identify oscillatory voltage instability problems as caused by *Hopf* bifurcation. Within this framework, it might be possible to still use the sparse total system Jacobian J, escaping the cumbersome eigenvalue computations. Similarly, characterizing the Hopf bifurcation from a parameter space point of view would perhaps produce a sensitivity of voltage stability margin with respect to oscillatory instability.

APPENDIX A NUMERICAL EXAMPLES FOR HOMOTOPY AND CONTINUATION

• Numerical example 1 for homotopy [60]

$$f(y) = \begin{bmatrix} f_1(y) \\ f_2(y) \end{bmatrix} = \begin{bmatrix} y_1^2 - 3y_2^2 + 3 \\ y_1 y_2 + 6 \end{bmatrix} \tag{A.1}$$

Define the homotopy function as:

$$\begin{aligned} H(y,t) &= tf(y) + (1-t)g(y) \\ &= tf(y) + (1-t)(f(y) - f(y_0)) \\ &= f(y) + (t-1)f(y_0) \end{aligned}$$

Then we get a curve (from equation 2.5 in chapter 2) defined by:

$$\begin{bmatrix} y_1'(t) \\ y_2'(t) \end{bmatrix} = -\frac{1}{\Delta} \begin{bmatrix} y_1 & 6y_2 \\ -y_2 & 2y_1 \end{bmatrix} \begin{bmatrix} 1 \\ 7 \end{bmatrix} = -\frac{1}{\Delta} \begin{bmatrix} y_1 + 42y_2 \\ -y_2 + 14y_1 \end{bmatrix} \tag{A.2}$$

where $\Delta = 2y_1^2 + 6y_2^2$, with $y_0 = (1,1)$. After tracing the implicitly-defined curve via some continuation method, we arrive at a solution when $t = 1$: $y^* = (-2.961, 1.978)$. A real root of f is $(-3,2)$. Reasonably we can expect that Newton's method would work well with y^* as the initial guess. After one step of Newton-Raphson iteration, we get $y_1 = (-3.0003, 2.0003)$. However, if we start the Newton's method directly with the initial guess $y_0 = (1,1)$, it takes more than 5 iterations to get the answer y_1. For a more complicated practical nonlinear problem, the conventional Newton's method might not work at all due to the poor selection of the initial values.

• Numerical example 2 for continuation

$$f(y,\alpha) = y^2 - 3y + \alpha = 0 \tag{A.3}$$

with base case known: (y_0, α_0)=(3, 0) and α as the first continuation parameter.

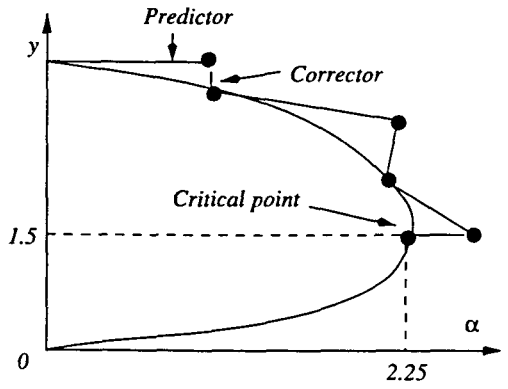

Figure A.1 Continuation process

step 1:

Predictor:

$$-\begin{bmatrix} f_y & f_\alpha \\ 0 & 1 \end{bmatrix}\begin{bmatrix} dy \\ d\alpha \end{bmatrix} = \begin{bmatrix} 0 \\ 1 \end{bmatrix} \tag{A.4}$$

$$\begin{bmatrix} \overline{y}_1 \\ \overline{\alpha}_1 \end{bmatrix} = \begin{bmatrix} 3 \\ 0 \end{bmatrix} + \sigma \begin{bmatrix} dy \\ d\alpha \end{bmatrix} \tag{A.5}$$

The correctors iterations then begin with $(\overline{y}_1, \overline{\alpha}_1)$,

Corrector:

$$-\begin{bmatrix} f_y & f_\alpha \\ 0 & 1 \end{bmatrix}\begin{bmatrix} \Delta y \\ \Delta\alpha \end{bmatrix} = \begin{bmatrix} f(\overline{y}_1, \overline{\alpha}_1) \\ 0 \end{bmatrix} \tag{A.6}$$

$$\begin{bmatrix} y_{1c} \\ \alpha_{1c} \end{bmatrix} = \begin{bmatrix} \overline{y}_1 \\ \overline{\alpha}_1 \end{bmatrix} + \sigma \begin{bmatrix} \Delta y \\ \Delta\alpha \end{bmatrix} \tag{A.7}$$

At the critical point, f_y becomes singular (with a value of 0 in the one-dimensional case). At this point, the continuation parameter should be switched from to y for continuing the curve tracing process beyond the critical point (or sometimes termed as the turning point, or

saddle node bifurcation point) $(1.5, 2.25)$. The augmented Jacobian at this point changes as the continuation parameter is switched from to y:

$$\begin{bmatrix} 0 & 1 \\ 0 & 1 \end{bmatrix} \Rightarrow \begin{bmatrix} 0 & 1 \\ 1 & 0 \end{bmatrix} \tag{A.8}$$

which helps the continuation of the predictor-corrector process.

APPENDIX B EIGENVALUE COMPUTATION USING SPARSITY TECHNIQUES

At any operating point, the following equation (repeated from chapter 4 for clarity and continuity) can be used to compute the eigenvalues of the system state matrix A_{sys}.

$$\begin{bmatrix} v_F^T & v_G^T \end{bmatrix} \begin{bmatrix} F_X & F_Y \\ G_X & G_Y \end{bmatrix} = \begin{bmatrix} \lambda v_F^T & 0 \end{bmatrix} \tag{B.1}$$

The following procedure proposed in [61] is used to illustrate how one may use the sparse formulation to compute selected eigenvalues of A_{sys} sequentially. Selective eigenvalue-analysis also consists of another branch in which the selected eigenvalues are computed in a group. It deals with subspaces. We shall concentrate on the former technique here.

The iteration algorithm involves solving the following linear system:

$$\begin{bmatrix} v_{Fk+1}^T & v_G^T \end{bmatrix} \begin{bmatrix} F_X - \lambda_k I & F_Y \\ G_X & G_Y \end{bmatrix} = \begin{bmatrix} v_{Fk}^T & 0 \end{bmatrix} \tag{B.2}$$

where v_G would not be of direct interest if one is not intended to do sensitivity analysis (chapter 4 and reference [54]). λ_k is the estimate of the eigenvalue at iteration k. We normalize v_{Fk+1} to have unity as its largest element to prevent overflow during the iterations. For the right eigenvector, the linear system of equations to be solved at each iteration can be put in a general form as

$$\begin{bmatrix} F_X - \lambda I & F_Y \\ G_X & G_Y \end{bmatrix} \begin{bmatrix} z_1 \\ z_2 \end{bmatrix} = \begin{bmatrix} \omega \\ u \end{bmatrix} \tag{B.3}$$

where z_1 is the right eigenvector of A_{sys} corresponding to the its eigenvalue λ. Again, z_2 is not of direct interest if only eigenvalue and eigenvector are of concern. ω and u are the intermediate results from previous iterations. Semlyn [61] proposed the following procedure to obtain z_1 and z_2.

- Calculate

$$J_{Deq} \hat{=} G_Y - G_X(F_X - \lambda I)^{-1} F_Y \tag{B.4}$$

  We note that $(F_X - \lambda I)$ is block diagonal and very sparse;

- Solve for z_2 from

$$J_{Deq} z_2 = u - G_X(F_X - \lambda I)^{-1}\omega \tag{B.5}$$

- Solve for z_1 from

$$(F_X - \lambda I)z_1 = \omega - F_Y z_2 \tag{B.6}$$

At the saddle node bifurcation point, if we are only interested in the zero crossing eigenvalue and the corresponding left eigenvector, we can directly apply the inverse power method on the total system Jacobian J.

- *step 0* Initialize V_k, $k = 0$. Set tolerance ϵ;

- *step 1* Perform LU decomposition on J;

- *step 2* Solve for V_{k+1} from

$$V_{k+1} J = V_k \tag{B.7}$$

- *step 3* Estimate the eigenvalue

$$\lambda_{k+1} = \frac{V_{k+1} e_l}{V_k e_l} \tag{B.8}$$

  where e_l is a unit column vector with 1 on the lth position and 0 elsewhere;

- *step 4* If $\|\lambda_{k+1} - \lambda_k\| \leq \epsilon$ done; else go to step 2.

When the solution converges, $V_{k+1} = (v_F, v_G)$ will be the vector used for margin sensitivity (4.28). v_F is the left eigenvector of A_{sys} corresponding to its minimum eigenvalue at saddle node bifurcation, i.e. the zero crossing eigenvalue. Since the total Jacobian J is already LU decomposed for the tangent vector calculation at the end of the continuation, step 1 can be saved.

APPENDIX C GENERATOR CAPABILITY

The capability diagram for a synchronous generator describes the allowed region of operation under steady state conditions. When the armature resistance and saliency are ignored, the following two equations can be used to construct the so-called capability diagram for the generator.

$$P_E^2 + Q_E^2 = V^2 I_a^2 \tag{C.1}$$

$$P_E^2 + (Q_E + \frac{V^2}{X_s})^2 = (V I_{fd} \frac{X_{ad}}{X_s})^2 \tag{C.2}$$

which lead to the following diagram plotted in Figure C.1.

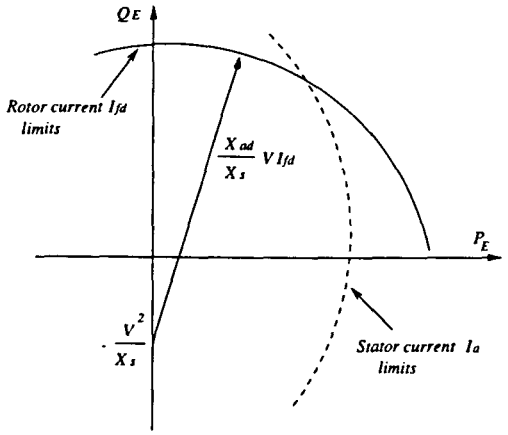

Figure C.1 Generator capability diagram

C.1 Reactive Power Limits Vs. AVR limits

In the new framework, the rotor current is directly limited by imposing AVR limits. The stator current limit is not directly limited by this. However, as usually done in power flow studies, an approximation of the actual (voltage dependent) capability digram can be made by setting fixed reactive power limits. In chapter 3, we stated that the automatic voltage

regulator (AVR) indirectly controls the reactive power output by regulating the AVR output voltage V_R. Therefore, at each loading level, we may use the following equations (from section 3.4) to calculate another limit V_{Rm} which may be imposed on the AVR output voltage in order to control the machine's reactive power generation to stay below the constant maximum.

$$Q_{Emax} = \frac{VE_{qmax}}{X_d} cos(\delta - \theta) - V^2(\frac{cos^2(\delta - \theta)}{X_d} + \frac{sin^2(\delta - \theta)}{X_q}) \tag{C.3}$$

From Q_{Emax} we get E_{qmax} from the above equation, then

$$V_{Rm} = (K_E + S_E)E_{qm} \tag{C.4}$$

If the current V_R value is larger than this, we then set it to this limit. Then the machine's reactive power output will stay below this constant limit Q_{Emax}. The above procedure was also implemented and tested using the New England system. The scenario is the same as that used in section 3.5.

C.1.1 General description of test results

The system experiences a voltage collapse (saddle node bifurcation) at a loading level of 8683 MW. All governors hit limits before reaching voltage instability. Generators at buses 30 and 35 hit their Q limits, generators at buses 33 and 39 hit their AVR limits, while the generator at bus 32 first reached its reactive power generation limit, and then at a higher loading level hit its AVR voltage limit. The buses which experienced lowest voltages at various loading levels are nodes 8, 12, and 15.

C.1.2 Automatic voltage regulator responses

We observed that, for all the generators which hit the reactive power limits or AVR output voltage limits, the terminal voltage, the AVR output voltage, reactive power generation, and exciter reference voltage have similar response profiles. Therefore we take generator at bus 30 as the example for analysis. Figure C.2 shows that, before hitting its reactive power limit, the voltage regulator can maintain a fairly high and steady terminal voltage. When the system total load exceeds 8201 MW, Q_{E30} hits the maximum 380 MVAR capacity, the AVR

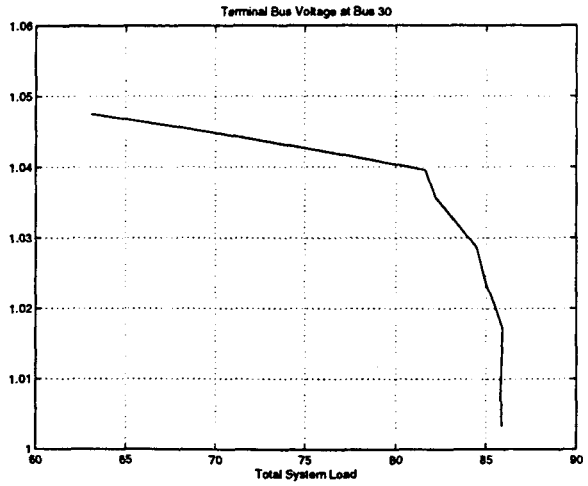

Figure C.2 Voltage at bus 30

output voltage is fixed then to make the generator stay within this reactive capacity. The terminal voltage experiences a noticeable voltage drop there. When the system approaches voltage collapse, other generators also hit their limits which cause some more abrupt changes of the terminal voltage at generator bus 30.

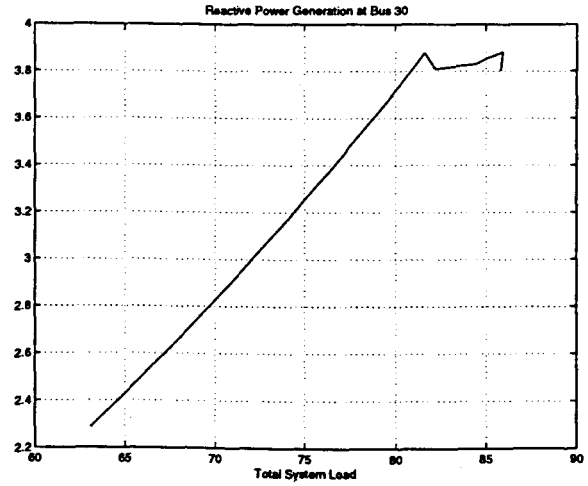

Figure C.3 Reactive power generation at bus 30

Figure C.3 shows the profile of reactive generation at bus 30. There are two abrupt changes. The first one occurs at a system load level of 8201 MW. From this point on, fixing the AVR output voltage can well control the terminal reactive power generation to stay within capacity with a tolerable deviation (less than 2 percent). When the system approaches instability, the

generator at bus 30 exceeds this tolerable maximum again. Then AVR output voltage is reset again to reduce reactive generation.

Figures C.4 and C.5 are the AVR output and exciter reference voltages of the generator at bus 30. The two drops correspond to the twice hitting of the machine's reactive power capability.

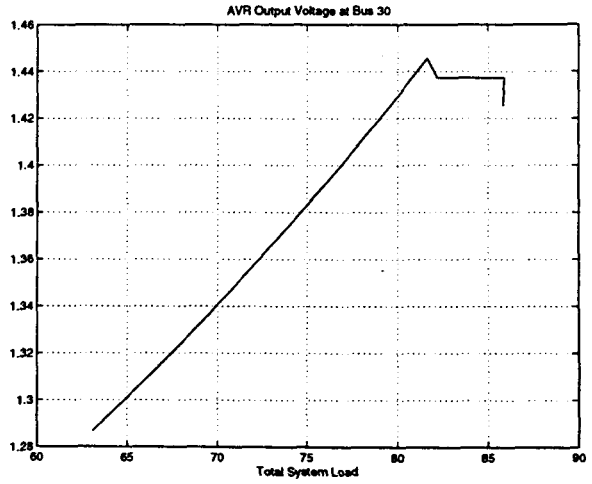

Figure C.4 AVR output voltage V_R at bus 30

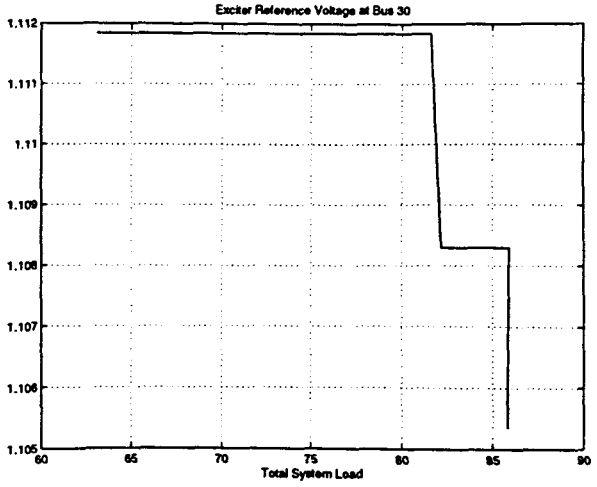

Figure C.5 Exciter reference voltage V_{REF}^{EX} at bus 30

APPENDIX D REDUCED FORMULATION FOR TOTAL POWER SYSTEM EQUILIBRIA TRACING

At steady state, some of the device equations from $F = 0$ can be eliminated without changing the solution. This is shown below. At an equilibrium state, we have

$$
\begin{aligned}
0 &= (\omega_i - \omega_s)\omega_B && \text{(D.1)}\\
0 &= M_{Gi}^{-1}(P_{Mi} - D_{Gi}(\omega_i - \omega_s) - (E'_{qi} - X'_{di}I_{di})I_{qi} - (E'_{di} + X'_{qi}I_{qi})I_{di}) && \text{(D.2)}\\
0 &= \frac{1}{T'_{d0i}}(E_{fdi} - E'_{qi} - (X_{di} - X'_{di})I_{di}) && \text{(D.3)}\\
0 &= \frac{1}{T'_{q0i}}(-E'_{di} + (X_{qi} - X'_{qi})I_{qi}) && \text{(D.4)}\\
0 &= \frac{1}{T_{Ei}}(V_{Ri} - (K_{Ei} + S_{Ei}(E_{fdi}))E_{fdi}) && \text{(D.5)}\\
0 &= \frac{1}{T_{Ai}}(-V_{Ri} + K_{Ai}(V^{EX}_{REFi} - V_i - R_{Fi}), \quad V_{pss} = 0 && \text{(D.6)}\\
0 &= \frac{1}{T_{Fi}}(-R_{Fi} - (K_{Ei} + S_{Ei}(E_{fdi}))K_{Fi}E_{fdi}/T_{Ei} + K_{Fi}V_{Ri}/T_{Ei}) && \text{(D.7)}\\
0 &= \frac{1}{T_{CHi}}(\mu_i - P_{Mi}) && \text{(D.8)}\\
0 &= \frac{1}{T_{Gi}}(P_{Gsi} - (\omega_i - \omega_{ref})/R_{Gi} - \mu_i) && \text{(D.9)}\\
i &= 1, \cdots, N_G
\end{aligned}
$$

Substituting equations D.1, D.2 and D.8 into equation D.9 leads to

$$0 = T_{Gi}^{-1}(P_{Gsi} - \frac{1}{R_{Gi}}(\omega_s - \omega_0) - (E'_{qi} - X'_{di}I_{di})I_{qi} - (E'_{di} + X'_{qi}I_{qi})I_{di}) \qquad \text{(D.10)}$$

Substituting equations D.5 and D.7 into equation D.6 gives

$$0 = \frac{1}{T_{Ai}}(-(K_{Ei} + S_{Ei}(E_{fdi}))E_{fdi} + K_{Ai}(V^{EX}_{REFi} - V_i)) \qquad \text{(D.11)}$$

These two equations together with Eqs. D.3 and D.4 constitute the reduced formulation of the system. The variables ω_i, P_{Mi}, μ_i, V_{Ri} and R_{Fi} then are eliminated. Reviewing the

above procedure, we observe that, as far as the linearized Jacobian (for Newton iterative solutions) is concerned, it is equivalent to the elementary row operations on the original total system Jacobian J. From matrix theory, we know that this will not affect the determinant of the Jacobian matrix. Corresponding to this reduced system of equations we have a reduced Jacobian denoted here as J_{red}.

$$J_{red} = \begin{bmatrix} \frac{\partial \overline{F_1}}{\partial X_1} & \frac{\partial \overline{F_1}}{\partial Y} \\ \frac{\partial G}{\partial X_1} & \frac{\partial G}{\partial Y} \end{bmatrix} \tag{D.12}$$

The above analysis is illustrated as follows.

$$\begin{bmatrix} \frac{\partial F_1}{\partial X_1} & \frac{\partial F_1}{\partial X_2} & \frac{\partial F_1}{\partial Y} \\ \frac{\partial F_2}{\partial X_1} & \frac{\partial F_2}{\partial X_2} & \frac{\partial F_2}{\partial Y} \\ \frac{\partial G}{\partial X_1} & \frac{\partial G}{\partial X_2} & \frac{\partial G}{\partial Y} \end{bmatrix} \Rightarrow \begin{bmatrix} \frac{\partial \overline{F_1}}{\partial X_1} & \frac{\partial \overline{F_1}}{\partial X_2} & \frac{\partial \overline{F_1}}{\partial Y} \\ \frac{\partial F_2}{\partial X_1} & \frac{\partial F_2}{\partial X_2} & \frac{\partial F_2}{\partial Y} \\ \frac{\partial G}{\partial X_1} & \frac{\partial G}{\partial X_2} & \frac{\partial G}{\partial Y} \end{bmatrix} = \begin{bmatrix} \frac{\partial \overline{F_1}}{\partial X_1} & 0 & \frac{\partial \overline{F_1}}{\partial Y} \\ \frac{\partial F_2}{\partial X_1} & \frac{\partial F_2}{\partial X_2} & \frac{\partial F_2}{\partial Y} \\ \frac{\partial G}{\partial X_1} & 0 & \frac{\partial G}{\partial Y} \end{bmatrix}$$

where the right arrow denotes elementary row operations. F_1 denotes equations D.3, D.4, D.9 and D.6. F_2 corresponds to equations D.1, D.2, D.8, D.5 and D.7. $\overline{F_1}$ gives all four equations (for one generator) in the reduced formulation. X_1 variables are those left in the reduced formulation, and X_2 variables are those eliminated. Therefore, it is obvious that the singularity of J indicates the singularity of J_{red} and vice versa, since $\partial F_2/\partial X_2$ is a square nonsingular matrix.

The reduced formulation is also implemented (limits not considered). Because there is a reduction of 5 equations for each generator, it may be more efficient in simultaneous equilibria tracing when there is a large number of generators with detailed modeling. We tested the reduced and the complete formulation using the New England test system. (A description of the system and scenario is given in chapter 3). With the same scenario, they produced two identical solution trajectories and transfer margins. This verifies our previous statement about their equivalence in detecting the saddle node bifurcation (see figure D.1). Because the tangent vectors are different, the same step size will result in different total steps in continuation and also different intermediate solution points. For the test case, the CPU time for the complete formulation is 3.4 seconds (16 steps, step size is 1.8) while 1.4 seconds (15 steps, step size is 0.6) for the reduced formulation.

In regard to margin sensitivity, those parameters which do not appear in the reduced formulation, such as the machine inertia constant M_G, damping D_G and the excitation system soft feedback gain K_{Fi} obviously will have zero sensitivity.

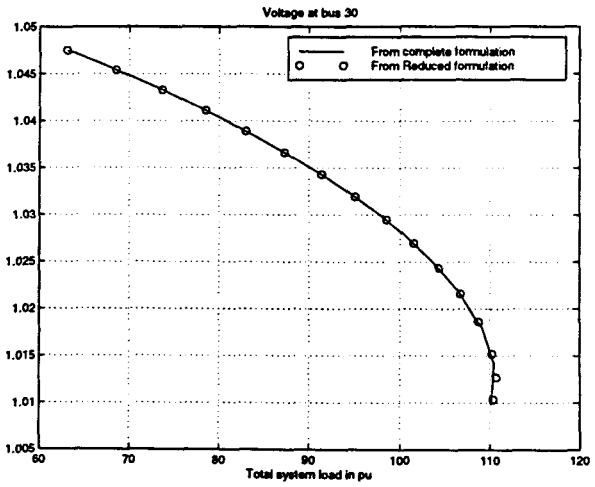

Figure D.1 Trajectory comparison

APPENDIX E DATA OF SAMPLE TEST SYSTEMS

E.1 Data Files of the New England System

- The IEEE format base case power flow data of the New England System

BUS DATA FOLLOWS 39 ITEMS

1 BUS31 1 1 2 0.9820 0.00 9.20 4.60 732.00 280.66 0.00 0.9820 900.000-9999.00 0.0000 0.0000 0 1
2 BUS2 1 1 0 1.0376 -11.22 0.00 0.00 0.00 0.00 0.00 0.0000 0.0000 0.0000 0.0000 0.0000 0 2
3 BUS3 1 1 0 1.0050 -13.88 322.00 122.40 0.00 0.00 0.00 0.0000 0.0000 0.0000 0.0000 0.0000 0 3
4 BUS4 1 1 0 0.9858 -14.02 500.00 184.00 0.00 0.00 0.00 0.0000 0.0000 0.0000 0.0000 0.0000 0 4
5 BUS5 1 1 0 0.9920 -12.25 0.00 0.00 0.00 0.00 0.00 0.0000 0.0000 0.0000 0.0000 0.0000 0 5
6 BUS6 1 1 0 0.9952 -11.41 0.00 0.00 0.00 0.00 0.00 0.0000 0.0000 0.0000 0.0000 0.0000 0 6
7 BUS7 1 1 0 0.9847 -13.76 233.80 84.00 0.00 0.00 0.00 0.0000 0.0000 0.0000 0.0000 0.0000 0 7
8 BUS8 1 1 0 0.9839 -14.33 522.00 176.00 0.00 0.00 0.00 0.0000 0.0000 0.0000 0.0000 0.0000 0 8
9 BUS9 1 1 0 1.0232 -14.60 0.00 0.00 0.00 0.00 0.00 0.0000 0.0000 0.0000 0.0000 0.0000 0 9
10 BUS10 1 1 0 1.0056 -9.42 0.00 0.00 0.00 0.00 0.00 0.0000 0.0000 0.0000 0.0000 0.0000 0 10
11 BUS11 1 1 0 1.0009 -10.10 0.00 0.00 0.00 0.00 0.00 0.0000 0.0000 0.0000 0.0000 0.0000 0 11
12 BUS12 1 1 0 0.9872 -10.24 8.50 88.00 0.00 0.00 0.00 0.0000 0.0000 0.0000 0.0000 0.0000 0 12
13 BUS13 1 1 0 1.0009 -10.23 0.00 0.00 0.00 0.00 0.00 0.0000 0.0000 0.0000 0.0000 0.0000 0 13
14 BUS14 1 1 0 0.9940 -12.19 0.00 0.00 0.00 0.00 0.00 0.0000 0.0000 0.0000 0.0000 0.0000 0 14
15 BUS15 1 1 0 0.9896 -13.34 320.00 153.00 0.00 0.00 0.00 0.0000 0.0000 0.0000 0.0000 0.0000 0 15
16 BUS16 1 1 0 1.0028 -12.16 329.40 132.30 0.00 0.00 0.00 0.0000 0.0000 0.0000 0.0000 0.0000 0 16
17 BUS17 1 1 0 1.0065 -13.12 0.00 0.00 0.00 0.00 0.00 0.0000 0.0000 0.0000 0.0000 0.0000 0 17
18 BUS18 1 1 0 1.0045 -13.86 158.00 30.00 0.00 0.00 0.00 0.0000 0.0000 0.0000 0.0000 0.0000 0 18
19 BUS19 1 1 0 1.0395 -7.87 0.00 0.00 0.00 0.00 0.00 0.0000 0.0000 0.0000 0.0000 0.0000 0 19
20 BUS20 1 1 0 0.9853 -9.48 680.00 103.00 0.00 0.00 0.00 0.0000 0.0000 0.0000 0.0000 0.0000 0 20
21 BUS21 1 1 0 1.0112 -9.83 274.00 115.00 0.00 0.00 0.00 0.0000 0.0000 0.0000 0.0000 0.0000 0 21
22 BUS22 1 1 0 1.0381 -5.44 0.00 0.00 0.00 0.00 0.00 0.0000 0.0000 0.0000 0.0000 0.0000 0 22
23 BUS23 1 1 0 1.0316 -5.65 247.50 84.60 0.00 0.00 0.00 0.0000 0.0000 0.0000 0.0000 0.0000 0 23
24 BUS24 1 1 0 1.0015 -12.07 308.60 92.20 0.00 0.00 0.00 0.0000 0.0000 0.0000 0.0000 0.0000 0 24
25 BUS25 1 1 0 1.0458 -10.02 224.00 47.20 0.00 0.00 0.00 0.0000 0.0000 0.0000 0.0000 0.0000 0 25
26 BUS26 1 1 0 1.0294 -11.40 139.00 47.00 0.00 0.00 0.00 0.0000 0.0000 0.0000 0.0000 0.0000 0 26
27 BUS27 1 1 0 1.0128 -13.40 281.00 75.50 0.00 0.00 0.00 0.0000 0.0000 0.0000 0.0000 0.0000 0 27
28 BUS28 1 1 0 1.0305 -8.01 206.00 27.60 0.00 0.00 0.00 0.0000 0.0000 0.0000 0.0000 0.0000 0 28
29 BUS29 1 1 0 1.0316 -5.23 283.50 126.90 0.00 0.00 0.00 0.0000 0.0000 0.0000 0.0000 0.0000 0 29
30 BUS30 1 1 2 1.0475 -8.97 20.00 20.00 250.00 228.51 0.00 1.0475 380.00 -100.00 0.0000 0.0000 0 30
31 BUS1 1 1 0 1.0435 -13.41 0.00 0.00 0.00 0.00 0.00 0.0000 0.0000 0.0000 0.0000 0.0000 0 31
32 BUS32 1 1 2 0.9831 -1.58 20.00 20.00 650.00 275.85 0.00 0.9831 500.00 -300.00 0.0000 0.0000 0 32
33 BUS33 1 1 2 0.9972 -2.80 20.00 20.00 632.00 197.36 0.00 0.9972 500.00 -300.00 0.0000 0.0000 0 33
34 BUS34 1 1 2 1.0123 -4.49 20.00 20.00 508.00 217.74 0.00 1.0123 450.00 -250.00 0.0000 0.0000 0 34
35 BUS35 1 1 2 1.0493 -0.58 20.00 20.00 650.00 314.70 0.00 1.0493 600.00 -250.00 0.0000 0.0000 0 35
36 BUS36 1 1 2 1.0635 2.01 20.00 20.00 560.00 170.64 0.00 1.0635 500.00 -220.00 0.0000 0.0000 0 36
37 BUS37 1 1 2 1.0278 -3.43 20.00 20.00 540.00 69.56 0.00 1.0278 500.00 -220.00 0.0000 0.0000 0 37
38 BUS38 1 1 2 1.0265 1.73 20.00 20.00 830.00 159.60 0.00 1.0265 500.00 -300.00 0.0000 0.0000 0 38
39 BUS39 1 1 3 1.0300 -14.69 1104.00 250.00 1000.00 124.37 0.00 1.0300 900.00 -800.00 0.0000 0.0000 0 39

-999

BRANCH DATA FOLLOWS 48 ITEMS

31 2 1 1 1 0 0.003500 0.041100 0.69870 0. 0. 0. 0 0 0.0000 0.00 0.0000 0.00000.00000 0.0000 0.0000 1

31 39 1 1 1 0 0.002000 0.050000 0.37500 0. 0. 0. 0 0 0.0000 0.00 0.0000 0.00000.00000 0.0000 0.0000 2

31 39 1 1 2 0 0.002000 0.050000 0.37500 0. 0. 0. 0 0 0.0000 0.00 0.0000 0.00000.00000 0.0000 0.0000 3

2 3 1 1 1 0 0.001300 0.015100 0.25720 0. 0. 0. 0 0 0.0000 0.00 0.0000 0.00000.00000 0.0000 0.0000 4

2 25 1 1 1 0 0.007000 0.008600 0.14600 0. 0. 0. 0 0 0.0000 0.00 0.0000 0.00000.00000 0.0000 0.0000 5

3 4 1 1 1 0 0.001300 0.021300 0.22140 0. 0. 0. 0 0 0.0000 0.00 0.0000 0.00000.00000 0.0000 0.0000 6

3 18 1 1 1 0 0.001100 0.013300 0.21380 0. 0. 0. 0 0 0.0000 0.00 0.0000 0.00000.00000 0.0000 0.0000 7

4 5 1 1 1 0 0.000800 0.012800 0.13420 0. 0. 0. 0 0 0.0000 0.00 0.0000 0.00000.00000 0.0000 0.0000 8

4 14 1 1 1 0 0.000800 0.012900 0.13820 0. 0. 0. 0 0 0.0000 0.00 0.0000 0.00000.00000 0.0000 0.0000 9

5 6 1 1 1 0 0.000200 0.002600 0.04340 0. 0. 0. 0 0 0.0000 0.00 0.0000 0.00000.00000 0.0000 0.0000 10

5 8 1 1 1 0 0.000800 0.011200 0.14760 0. 0. 0. 0 0 0.0000 0.00 0.0000 0.00000.00000 0.0000 0.0000 11

6 7 1 1 1 0 0.000600 0.009200 0.11300 0. 0. 0. 0 0 0.0000 0.00 0.0000 0.00000.00000 0.0000 0.0000 12

6 11 1 1 1 0 0.000700 0.008200 0.13890 0. 0. 0. 0 0 0.0000 0.00 0.0000 0.00000.00000 0.0000 0.0000 13

7 8 1 1 1 0 0.000400 0.004600 0.07800 0. 0. 0. 0 0 0.0000 0.00 0.0000 0.00000.00000 0.0000 0.0000 14

8 9 1 1 1 0 0.002300 0.036300 0.38040 0. 0. 0. 0 0 0.0000 0.00 0.0000 0.00000.00000 0.0000 0.0000 15

9 39 1 1 1 0 0.001000 0.025000 1.20000 0. 0. 0. 0 0 0.0000 0.00 0.0000 0.00000.00000 0.0000 0.0000 16

10 11 1 1 1 0 0.000400 0.004300 0.07290 0. 0. 0. 0 0 0.0000 0.00 0.0000 0.00000.00000 0.0000 0.0000 17

10 13 1 1 1 0 0.000400 0.004300 0.07290 0. 0. 0. 0 0 0.0000 0.00 0.0000 0.00000.00000 0.0000 0.0000 18

13 14 1 1 1 0 0.000900 0.010100 0.17230 0. 0. 0. 0 0 0.0000 0.00 0.0000 0.00000.00000 0.0000 0.0000 19

14 15 1 1 1 0 0.001800 0.021700 0.36600 0. 0. 0. 0 0 0.0000 0.00 0.0000 0.00000.00000 0.0000 0.0000 20

15 16 1 1 1 0 0.000900 0.009400 0.17100 0. 0. 0. 0 0 0.0000 0.00 0.0000 0.00000.00000 0.0000 0.0000 21

16 17 1 1 1 0 0.000700 0.008900 0.13420 0. 0. 0. 0 0 0.0000 0.00 0.0000 0.00000.00000 0.0000 0.0000 22

16 19 1 1 1 0 0.001600 0.019500 0.30400 0. 0. 0. 0 0 0.0000 0.00 0.0000 0.00000.00000 0.0000 0.0000 23

16 21 1 1 1 0 0.000800 0.013500 0.25480 0. 0. 0. 0 0 0.0000 0.00 0.0000 0.00000.00000 0.0000 0.0000 24

16 24 1 1 1 0 0.000300 0.005900 0.06800 0. 0. 0. 0 0 0.0000 0.00 0.0000 0.00000.00000 0.0000 0.0000 25

17 18 1 1 1 0 0.000700 0.008200 0.13190 0. 0. 0. 0 0 0.0000 0.00 0.0000 0.00000.00000 0.0000 0.0000 26

17 27 1 1 1 0 0.001300 0.017300 0.32160 0. 0. 0. 0 0 0.0000 0.00 0.0000 0.00000.00000 0.0000 0.0000 27

21 22 1 1 1 0 0.000800 0.014000 0.25650 0. 0. 0. 0 0 0.0000 0.00 0.0000 0.00000.00000 0.0000 0.0000 28

22 23 1 1 1 0 0.000600 0.009600 0.18460 0. 0. 0. 0 0 0.0000 0.00 0.0000 0.00000.00000 0.0000 0.0000 29

23 24 1 1 1 0 0.002200 0.035000 0.36100 0. 0. 0. 0 0 0.0000 0.00 0.0000 0.00000.00000 0.0000 0.0000 30

25 26 1 1 1 0 0.003200 0.032300 0.51300 0. 0. 0. 0 0 0.0000 0.00 0.0000 0.00000.00000 0.0000 0.0000 31

26 27 1 1 1 0 0.001400 0.014700 0.23960 0. 0. 0. 0 0 0.0000 0.00 0.0000 0.00000.00000 0.0000 0.0000 32

26 28 1 1 1 0 0.004300 0.047400 0.78020 0. 0. 0. 0 0 0.0000 0.00 0.0000 0.00000.00000 0.0000 0.0000 33

26 29 1 1 1 0 0.005700 0.062500 1.02900 0. 0. 0. 0 0 0.0000 0.00 0.0000 0.00000.00000 0.0000 0.0000 34

28 29 1 1 1 0 0.001400 0.015100 0.24900 0. 0. 0. 0 0 0.0000 0.00 0.0000 0.00000.00000 0.0000 0.0000 35

2 30 1 1 1 1 0.000000 0.018100 0.00000 0. 0. 0. 0 0 1.0250 0.00 0.0000 0.00000.00000 0.0000 0.0000 36

6 1 1 1 1 1 0.000000 0.050000 0.00000 0. 0. 0. 0 0 1.0700 0.00 0.0000 0.00000.00000 0.0000 0.0000 37

6 1 1 1 2 1 0.000000 0.050000 0.00000 0. 0. 0. 0 0 1.0700 0.00 0.0000 0.00000.00000 0.0000 0.0000 38

10 32 1 1 1 1 0.000000 0.020000 0.00000 0. 0. 0. 0 0 1.0700 0.00 0.0000 0.00000.00000 0.0000 0.0000 39

12 11 1 1 1 1 0.001600 0.043500 0.00000 0. 0. 0. 0 0 1.0060 0.00 0.0000 0.00000.00000 0.0000 0.0000 40

12 13 1 1 1 1 0.001600 0.043500 0.00000 0. 0. 0. 0 0 1.0060 0.00 0.0000 0.00000.00000 0.0000 0.0000 41

19 20 1 1 1 1 0.000700 0.013800 0.00000 0. 0. 0. 0 0 1.0600 0.00 0.0000 0.00000.00000 0.0000 0.0000 42

19 33 1 1 1 1 0.000700 0.014200 0.00000 0. 0. 0. 0 0 1.0700 0.00 0.0000 0.00000.00000 0.0000 0.0000 43

20 34 1 1 1 1 0.000900 0.018000 0.00000 0. 0. 0. 0 0 1.0090 0.00 0.0000 0.00000.00000 0.0000 0.0000 44

22 35 1 1 1 1 0.000000 0.014300 0.00000 0. 0. 0. 0 0 1.0250 0.00 0.0000 0.00000.00000 0.0000 0.0000 45

23 36 1 1 1 1 0.000500 0.027200 0.00000 0. 0. 0. 0 0 1.0000 0.00 0.0000 0.00000.00000 0.0000 0.0000 46

25 37 1 1 1 1 0.000600 0.023200 0.00000 0. 0. 0. 0 0 1.0250 0.00 0.0000 0.00000.00000 0.0000 0.0000 47

29 38 1 1 1 1 0.000800 0.015600 0.00000 0. 0. 0. 0 0 1.0250 0.00 0.0000 0.00000.00000 0.0000 0.0000 48

-999

LOSS ZONES FOLLOWS 2 ITEMS

-99

INTERCHANGE DATA FOLLOWS 1 ITEMS

-9
TIE LINES FOLLOW 0 ITEMS
-999

- The ISU format of the dynamic data of the New England System

Generator transient parameter follows
Num Gen_name Xd Xq X'd X'q Rs T'do T'qo Mg Dg
1 BUS31 0.2590 0.2820 0.0700 0.1700 0.0002 6.5600 1.5000 60.600 5.000
30 BUS30 0.1000 0.0690 0.0310 0.0690 0.0002 10.2000 0.0010 84.000 5.000
32 BUS32 0.2500 0.2370 0.0530 0.0880 0.0002 5.7000 1.5000 71.600 5.000
33 BUS33 0.2620 0.2580 0.0440 0.1660 0.0002 5.6900 1.5000 57.200 5.000
34 BUS34 0.6700 0.6200 0.1320 0.1660 0.0002 5.4000 0.4400 52.000 5.000
35 BUS35 0.2540 0.2410 0.0500 0.0810 0.0060 7.3000 0.4000 69.600 5.000
36 BUS36 0.2950 0.2920 0.0490 0.1860 0.0002 5.6600 1.5000 52.800 5.000
37 BUS37 0.2900 0.2800 0.0570 0.0910 0.0010 6.7000 0.4100 48.600 5.000
38 BUS38 0.2110 0.2050 0.0570 0.0590 0.0002 4.7900 1.9600 69.000 5.000
39 BUS39 0.0200 0.0190 0.0060 0.0080 0.0002 7.0000 0.7000 1000.000 10.000
-999
Generator control system (exciter + AVR + governor) parameter follows
Num Gen_name Ke Te Se Ka Ta Kf Tf Tch Tg Rg
1 BUS31 1.0000 0.4100 0.0000 40.0000 0.0500 0.0600 0.5000 54.1000 0.4500 0.0500
30 BUS30 1.0000 0.2500 0.0000 20.0000 0.0600 0.0400 1.0000 1.6000 0.2000 0.0500
32 BUS32 1.0000 0.5000 0.0000 40.0000 0.0600 0.0800 1.0000 10.0000 3.0000 0.0500
33 BUS33 1.0000 0.5000 0.0000 40.0000 0.0600 0.0800 1.0000 10.1800 0.2400 0.0500
34 BUS34 1.0000 0.7900 0.0000 30.0000 0.0200 0.0300 1.0000 9.7900 0.1200 0.0500
35 BUS35 1.0000 0.4700 0.0000 40.0000 0.0200 0.0800 1.2500 10.0000 3.0000 0.0500
36 BUS36 1.0000 0.7300 0.0000 30.0000 0.0200 0.0300 1.0000 7.6800 0.2000 0.0500
37 BUS37 1.0000 0.5300 0.0000 40.0000 0.0200 0.0900 1.2600 7.0000 3.0000 0.0500
38 BUS38 1.0000 1.4000 0.0000 20.0000 0.0200 0.0300 1.0000 6.1000 0.3800 0.0500
39 BUS39 1.0000 1.0000 0.0000 20.0000 0.0200 0.0300 1.0000 10.0000 2.0000 0.0500
-999
Dynamic loads data follows
Num Bus_name TpL TqL ALd BLd ALph Beta
-999
Static var compensator data follows
Num Bus_name Ksvs Tsvs Vsvsr
-999
On load tap-changer data follows
S_N Secondary_Bus P_N Prime_Bus Tr Vrr
-999

- The ISU format of the governor and AVR limits data file for the New England System

IEEE NEW ENGLAND 39 BUS SYSTEM

THE AVR VOLTAGE LIMITS-FIELD CURRENT

---

1 4.9000
30 1.4500
32 3.2500
33 4.2500
34 8.2300
35 3.4000
36 3.6500

```
37 3.7500
38 3.4500
39 1.5000
-999
------------------------------
THE GOVERNOR LIMITS-PGSMAX
------------------------------
1 9.1500
30 3.1250
32 8.1250
33 7.9000
34 6.3500
35 8.1250
36 7.0000
37 6.7500
38 10.3750
39 12.5000
-999
```

- The ISU format of the scenario control file for the New England System

```
TOTAL POWER SYSTEM EQUILIBRIA TRACING - VOLTAGE STABILITY ANALYSIS
BO LONG AND V. AJJARAPU
DEPARTMENT OF ELECTRICAL AND COMPUTER ENGINEERING
IOWA STATE UNIVERSITY
COMPANY: ISU
BASE CASE: NEW ENGLAND 39 BUS 10 MACHINE TEST SYSTEM
OUTAGES: none
-999
LINE RATING TO USE IN ANALYSIS (1,2, OR 3)
2
C************************************************************
LOCATION OF LOAD INCREASE FOR LOAD/GENERATION INCREASE SCENARIO
------------------------------
INITIAL LOAD
BUS NAME P(MW) Q(MVAR)
--- ------ ------ ------
C******KLP***KLQ**********************************************
BUS NUMBERS WHERE LOAD IS TO BE INCREASED
3 1.0 1.0
4 1.0 1.0
7 1.0 1.0
8 1.0 1.0
15 1.0 1.0
16 1.0 1.0
18 1.0 1.0
20 1.0 1.0
21 1.0 1.0
23 1.0 1.0
24 1.0 1.0
25 1.0 1.0
26 1.0 1.0
27 1.0 1.0
28 1.0 1.0
29 1.0 1.0
39 1.0 1.0
```

```
-999
C*****************************************************************
LOCATION OF GENERATION INCREASE FOR LOAD/GENERATION INCREASE SCENARIO
------------------------------------
BUS NAME AREA OUTPUT(MW) + —- ------- —- ------. --------
C*****************************************************************
BUS NUMBER, SCALING FACTOR
1
30
32
33
34
35
36
37
38
39
-999
C*********************************************************
LOCATION OF INCREASE FOR REACTIVE LOAD INCREASE SCENARIO
-------------------------------
INITIAL LOAD
BUS NAME P(MW) Q(MVAR)
—- ------- ------ ------
C*********************************************************
BUS NUMBERS WHERE REACTIVE LOAD IS TO BE ADDED
-999
C*********************************************************
LOCATION OF EXPORTING UNITS FOR IMPORT/EXPORT SCENARIO
-----------------------------
BUS NAME AREA OUTPUT(MW) + —- ------- —- ------. --------
C*********************************************************
BUS NUMBER, SCALING FACTOR
-999
C*********************************************************
LOCATION OF IMPORTING UNITS FOR IMPORT/EXPORT SCENARIO
-------------------------------
BUS NAME AREA OUTPUT(MW) - —- ------- —- ------. --------
C*********************************************************
BUS NUMBER, SCALING FACTOR
-999
C*****************************************************************
LOCATION OF LOAD INCREASE FOR LOAD/IMPORT SCENARIO
-------------------------
INITIAL LOAD
BUS NAME P(MW) Q(MVAR)
—- ------- ------ ------
C*****************************************************************
BUS NUMBERS WHERE LOAD IS TO BE INCREASED AND SERVED FROM OUTSIDE
-999
C*********************************************************
LOCATION OF GENERATION INCREASE FOR LOAD/IMPORT SCENARIO
-------------------------------
BUS NAME AREA OUTPUT(MW) + —- ------- —- ------. --------
```

```
C*******************************************************
BUS NUMBER, SCALING FACTOR
-999 0
C************************
BUSES TO MONITER
————————
BUS NAME AREA
—- ——— —-
C************************
BUS NUMBERS
1
30
32
33
34
35
36
37
38
39
-999
CONVERGENCE TOLERANCE FOR POWER FLOW
0.00001
MAXIMUM NUMBER OF ITERATIONS ALLOWED
30
NUMBER OF WEAK BUSES TO MONITER
10
```

- The load participation factors of the generators

```
1 .115239
30 .039358
32 .102330
33 .099496
34 .079975
35 .102330
36 .088161
37 .085013
38 .130668
39 .157430
```

E.2 Data Files of the Iowa System

- The IEEE format base case power flow data of the Iowa System

```
100.0 1980 S MODIFIED IOWA SYSTEM
BUS DATA FOLLOWS 162 ITEMS (HEADER)
1 COOPR 3 1 12 0 1.0327 -25.33 0.00 0.00 0.00 0.00 3.00 0.0000 0.0000 0.0000 0.0000 -1.0000 0 1
2 MOOR 3 1 12 0 1.0226 -29.99 0.00 0.00 0.00 0.00 3.00 0.0000 0.0000 0.0000 0.0000 0.0000 0 2
3 STJO 712 1 5 2 1.0000 -32.49 2370.00 96.90 2000.00 0.00 712.00 0.0000 800.00 0.0000 0.0000 0.0000 0 3
4 BOONIL 3 1 6 0 1.0191 -33.74 0.00 0.00 0.00 0.00 3.00 0.0000 0.0000 0.0000 0.0000 0.0000 0 4
5 NEBCY 3 1 11 0 1.0340 -24.51 0.00 0.00 0.00 0.00 3.00 0.0000 0.0000 0.0000 0.0000 -0.5000 0 5
6 COOPR1G 100 1 12 2 1.0000 -19.15 0.00 0.00 794.00 180.78 100.00 1.0000 400.00 -200.00 0.0000 0.0000 0 6
7 LINCLN 3 1 12 0 1.0188 -30.38 0.00 0.00 0.00 0.00 3.00 0.0000 0.0000 0.0000 0.0000 0.0000 0 7
```

8 WAGEER 7 1 5 0 1.0346 -33.81 398.00 19.20 0.00 0.00 7.00 0.0000 0.0000 0.0000 0.0000 0.0000 0 8
9 S345 403 1 11 0 1.0264 -27.76 0.00 0.00 0.00 0.00 403.00 0.0000 0.0000 0.0000 0.0000 0.0000 0 9
10 TWINCH 4 1 5 0 0.9931 -35.68 226.00 11.50 0.00 0.00 4.00 0.0000 0.0000 0.0000 0.0000 0.0000 0 10
11 SX CY 4 1 1 0 0.9998 -31.83 0.00 0.00 0.00 0.00 4.00 0.0000 0.0000 0.0000 0.0000 0.0000 0 11
12 SHELON 7 1 5 0 1.0380 -33.65 193.00 5.90 0.00 0.00 7.00 0.0000 0.0000 0.0000 0.0000 0.0000 0 12
13 GR ILD 3 1 5 0 1.0149 -30.67 204.00 37.30 0.00 0.00 3.00 0.0000 0.0000 0.0000 0.0000 0.0000 0 13
14 S12 605 1 5 0 1.0282 -31.03 381.00 56.30 0.00 0.00 605.00 0.0000 0.0000 0.0000 0.0000 0.0000 0 14
15 FTRAD 4 1 5 2 1.0188 -24.52 1420.00 0.00 1500.00 5.90 4.00 0.0000 800.00 0.0000 0.0000 0.0000 0 15
16 ROCHTR 5 1 5 0 1.0143 -29.58 -54.20 26.700 .00 0.00 5.00 0.0000 0.0000 0.0000 0.0000 0.0000 0 16
17 HARMNY 5 1 5 0 1.0061 -28.80 -116.50 44.700 .00 0.00 5.00 0.0000 0.0000 0.0000 0.0000 0.0000 0 17
18 ADAM 5 1 9 0 1.0354 -33.75 34.40 11.67 0.00 0.00 5.00 0.0000 0.0000 0.0000 0.0000 0.0000 0 18
19 DUBUUE 5 1 5 0 1.0000 -38.06 64.40 3.12 0.00 0.00 5.00 1.0000 9.79 -66.20 0.0000 0.0000 0 19
20 HINTON 8 1 1 0 0.9796 -32.69 37.90 12.50 0.00 0.00 8.00 0.0000 0.0000 0.0000 0.0000 0.0000 0 20
21 POSTIL 5 1 5 0 1.0083 -30.42 -69.80 23.20 0.00 0.00 5.00 0.0000 0.0000 0.0000 0.0000 0.0000 0 21
22 HAZLON 5 1 9 0 1.0338 -37.63 17.39 5.27 0.00 0.00 5.00 0.0000 0.0000 0.0000 0.0000 0.0000 0 22
23 HRN K 5 1 5 0 0.9884 -34.85 63.50 0.00 0.00 0.00 5.00 0.0000 0.0000 0.0000 0.0000 0.0000 0 23
24 LAKFD 5 1 9 0 1.0095 -33.32 0.00 0.00 0.00 0.00 5.00 0.0000 0.0000 0.0000 0.0000 0.0000 0 24
25 LAKFD 3 1 9 0 1.0013 -29.37 0.00 0.00 0.00 0.00 3.00 0.0000 0.0000 0.0000 0.0000 -0.5000 0 25
26 RAUN 3 1 2 0 1.0324 -21.49 0.00 0.00 0.00 0.00 3.00 0.0000 0.0000 0.0000 0.0000 -0.5000 0 26
27 WILMRT 3 1 5 2 0.9980 -30.39 1824.00 57.90 1500.00 0.00 3.00 0.0000 0.0000 0.0000 0.0000 0.0000 0 27
28 FOX K 5 1 9 0 0.9885 -36.13 38.47 13.17 0.00 0.00 5.00 0.0000 0.0000 0.0000 0.0000 0.0000 0 28
29 WINBGO 5 1 9 0 0.9882 -37.93 28.31 9.03 0.00 0.00 5.00 0.0000 0.0000 0.0000 0.0000 0.0000 0 29
30 HAYWD 5 1 9 0 0.9981 -39.80 101.20 32.52 0.00 0.00 5.00 0.0000 0.0000 0.0000 0.0000 0.1500 0 30
31 RAPIAN 5 1 5 0 0.9904 -37.07 72.50 -3.100 0.00 0.00 5.00 0.0000 0.0000 0.0000 0.0000 0.0000 0 31
32 LIMECK 5 1 9 0 1.0049 -41.08 52.70 15.06 0.00 0.00 5.00 0.0000 0.0000 0.0000 0.0000 0.2000 0 32
33 MASNTY 5 1 9 0 0.9983 -43.01 45.17 15.16 0.00 0.00 5.00 0.0000 0.0000 0.0000 0.0000 0.2000 0 33
34 FRANKN 5 1 2 0 0.9986 -42.99 14.18 5.25 0.00 0.00 5.00 0.0000 0.0000 0.0000 0.0000 0.0320 0 34
35 FLOY 5 1 2 0 0.9894 -44.44 54.48 14.63 0.00 0.00 5.00 0.0000 0.0000 0.0000 0.0000 0.0500 0 35
36 GARNR 5 1 4 0 0.9960 -43.16 31.96 8.68 0.00 0.00 5.00 0.0000 0.0000 0.0000 0.0000 0.0300 0 36
37 ADAM 3 1 3 0 0.9870 -30.58 0.00 0.00 0.00 0.00 3.00 0.0000 0.0000 0.0000 0.0000 0.0000 0 37
38 DUNDE 5 1 4 0 1.0188 -38.15 14.76 4.08 0.00 0.00 5.00 0.0000 0.0000 0.0000 0.0000 0.0150 0 38
39 HAZLON 3 1 9 0 0.9875 -33.22 0.00 0.00 0.00 0.00 3.00 0.0000 0.0000 0.0000 0.0000 0.0000 0 39
40 BLKHK 5 1 2 0 0.9999 -42.06 52.88 17.60 0.00 0.00 5.00 0.0000 0.0000 0.0000 0.0000 0.0000 0 40
41 WSHBN 5 1 2 0 1.0076 -40.21 39.20 12.80 0.00 0.00 5.00 0.0000 0.0000 0.0000 0.0000 0.0000 0 41
42 ARNOD 3 1 4 0 1.0036 -33.02 0.00 0.00 0.00 0.00 3.00 0.0000 0.0000 0.0000 0.0000 0.0000 0 42
43 CLINON 5 1 5 0 1.0120 -35.64 41.50 -17.20 0.00 0.00 5.00 0.0000 0.0000 0.0000 0.0000 0.0000 0 43
44 CALUS 5 1 4 0 1.0072 -36.16 16.32 3.71 0.00 0.00 5.00 0.0000 0.0000 0.0000 0.0000 0.0000 0 44
45 TRIBJI 5 1 4 0 0.9958 -36.21 20.02 5.41 0.00 0.00 5.00 0.0000 0.0000 0.0000 0.0000 0.0190 0 45
46 DENIN 5 1 1 0 0.9991 -38.96 65.31 22.30 0.00 0.00 5.00 0.0000 0.0000 0.0000 0.0000 0.2620 0 46
47 ANITTP 5 1 4 0 0.9910 -41.68 4.82 1.56 0.00 0.00 5.00 0.0000 0.0000 0.0000 0.0000 0.0000 0 47
48 CRESN 5 1 1 0 1.0000 -40.59 33.76 -8.00 0.00 0.00 5.00 1.0000 40.00 -20.00 0.0000 0.0000 0 48
49 ANIT 5 1 4 0 0.9889 -41.99 6.82 1.78 0.00 0.00 5.00 0.0000 0.0000 0.0000 0.0000 0.0000 0 49
50 MARY 12 1 5 0 0.9963 -39.50 99.70 -23.40 0.00 0.00 12.00 0.0000 0.0000 0.0000 0.0000 0.0000 0 50
51 CLRNA 5 1 6 0 0.9917 -38.23 0.00 0.00 0.00 0.00 5.00 0.0000 0.0000 0.0000 0.0000 0.0000 0 51
52 D.MON 5 1 6 0 1.0150 -39.33 218.20 42.80 0.00 0.00 5.00 0.0000 0.0000 0.0000 0.0000 0.0000 0 52
53 SX CY 5 1 1 0 0.9957 -30.68 0.00 0.00 0.00 0.00 5.00 0.0000 0.0000 0.0000 0.0000 0.0000 0 53
54 WISDM 5 1 1 0 0.9889 -37.87 70.34 20.57 0.00 0.00 5.00 0.0000 0.0000 0.0000 0.0000 0.0000 0 54
55 PLYMH 5 1 2 0 0.9963 -30.39 0.00 0.00 0.00 0.00 5.00 0.0000 0.0000 0.0000 0.0000 0.0000 0 55
56 OSGOD 5 1 10 0 0.9917 -40.50 25.29 7.26 0.00 0.00 5.00 0.0000 0.0000 0.0000 0.0000 0.0320 0 56
57 SAC 5 1 2 0 0.9978 -37.54 48.48 -4.39 0.00 0.00 5.00 1.0000 20.00 -0.10 0.0000 0.0000 0 57
58 UTICJC 4 1 1 0 1.0088 -28.69 0.00 0.00 0.00 0.00 4.00 0.0000 0.0000 0.0000 0.0000 0.0000 0 58
59 EAGL 4 1 1 0 0.9846 -33.03 84.43 27.05 0.00 0.00 4.00 0.0000 0.0000 0.0000 0.0000 0.0000 0 59
60 SX FLL 7 1 5 0 0.9924 -34.01 244.00 26.00 0.00 0.00 7.00 0.0000 0.0000 0.0000 0.0000 0.0000 0 60
61 SIOXLS 4 1 1 0 0.9837 -31.43 0.00 0.00 0.00 0.00 4.00 0.0000 0.0000 0.0000 0.0000 0.0000 0 61

62 FTTHMP 4 1 5 0 1.0238 -18.48 -865.60 -70.80 0.00 0.00 4.00 0.0000 0.0000 0.0000 0.0000 0.0000 0 62
63 HANLN 4 1 5 0 0.9886 -29.77 59.10 -2.90 0.00 0.00 4.00 0.0000 0.0000 0.0000 0.0000 0.0000 0 63
64 SIOXLS 100 1 1 0 1.0155 -28.89 0.00 0.00 0.00 0.00 100.00 0.0000 0.0000 0.0000 0.0000 0.0000 0 64
65 WTRTWN 3 1 5 0 0.9968 -25.33 -26.30 116.00 0.00 0.00 3.00 0.0000 0.0000 0.0000 0.0000 0.0000 0 65
66 SX CY 3 1 1 0 1.0007 -31.12 0.00 0.00 0.00 0.00 3.00 0.0000 0.0000 0.0000 0.0000 -0.5000 0 66
67 BURT 5 1 10 0 1.0001 -41.74 22.54 7.03 0.00 0.00 5.00 0.0000 0.0000 0.0000 0.0000 0.0600 0 67
68 HOPE 5 1 10 0 1.0137 -40.24 40.42 12.68 0.00 0.00 5.00 0.0000 0.0000 0.0000 0.0000 0.1200 0 68
69 HOPET 5 1 2 0 1.0205 -38.92 0.00 0.00 0.00 0.00 5.00 0.0000 0.0000 0.0000 0.0000 0.0000 0 69
70 NEAL 5 1 2 0 1.0264 -23.58 0.00 0.00 0.00 0.00 5.00 0.0000 0.0000 0.0000 0.0000 0.0000 0 70
71 MONOA 5 1 2 0 0.9925 -31.78 29.87 11.93 0.00 0.00 5.00 0.0000 0.0000 0.0000 0.0000 0.1200 0 71
72 S12 905 1 5 0 1.0168 -30.78 427.00 110.00 0.00 0.00 905.00 0.0000 0.0000 0.0000 0.0000 0.0000 0 72
73 NEAL12G 100 1 2 2 1.0000 -18.46 0.00 0.00 447.00 86.14 100.00 1.0000 267.00 -72.00 0.0000 0.0000 0 73
74 LEHIH 3 1 8 0 1.0117 -33.57 0.00 0.00 0.00 0.00 3.00 0.0000 0.0000 0.0000 0.0000 0.0000 0 74
75 FT.CL 3 1 11 0 1.0301 -25.43 0.00 0.00 0.00 0.00 3.00 0.0000 0.0000 0.0000 0.0000 -0.5000 0 75
76 NEAL34G 100 1 2 2 1.0000 -16.49 0.00 0.00 1055.00 135.45 100.00 1.0000 605.00 -170.00 0.0000 0.0000 0 76
77 WRIGT 5 1 2 0 1.0114 -40.49 26.41 8.88 0.00 0.00 5.00 0.0000 0.0000 0.0000 0.0000 0.0470 0 77
78 FT.DDG 5 1 8 0 1.0232 -38.24 79.12 0.00 0.00 0.00 5.00 0.0000 0.0000 0.0000 0.0000 0.0000 0 78
79 LEHIH 5 1 8 0 1.0320 -36.19 0.00 0.00 0.00 0.00 5.00 0.0000 0.0000 0.0000 0.0000 0.0000 0 79
80 POMEOY 5 1 2 0 1.0101 -38.36 15.76 5.25 0.00 0.00 5.00 0.0000 0.0000 0.0000 0.0000 0.0280 0 80
81 WATELO 8 1 2 0 1.0011 -46.42 50.88 16.80 0.00 0.00 8.00 0.0000 0.0000 0.0000 0.0000 0.2210 0 81
82 WATELO 5 1 2 0 0.9990 -42.03 62.28 20.26 0.00 0.00 5.00 0.0000 0.0000 0.0000 0.0000 0.1040 0 82
83 WTR OGT 100 1 2 0 1.0033 -41.13 0.00 0.00 0.00 0.00 100.00 0.0000 0.0000 0.0000 0.0000 0.0000 0 83
84 DYSAT 5 1 4 0 1.0098 -37.77 37.90 9.49 0.00 0.00 5.00 0.0000 0.0000 0.0000 0.0000 0.0260 0 84
85 CARRLL 5 1 2 0 0.9709 -41.07 40.52 11.36 0.00 0.00 5.00 0.0000 0.0000 0.0000 0.0000 0.1200 0 85
86 GR JT 5 1 4 0 0.9699 -44.99 50.73 13.35 0.00 0.00 5.00 0.0000 0.0000 0.0000 0.0000 0.1200 0 86
87 GUTHIE 7 1 4 0 0.9802 -43.54 16.91 4.23 0.00 0.00 7.00 0.0000 0.0000 0.0000 0.0000 0.0000 0 87
88 JASPR 8 1 7 0 0.9892 -44.76 60.60 4.44 0.00 0.00 8.00 0.0000 0.0000 0.0000 0.0000 0.0000 0 88
89 GR JT 7 1 4 0 0.9911 -46.16 0.00 0.00 0.00 0.00 7.00 0.0000 0.0000 0.0000 0.0000 0.0000 0 89
90 BOON 7 1 4 0 0.9613 -48.65 50.21 16.76 0.00 0.00 7.00 0.0000 0.0000 0.0000 0.0000 0.1000 0 90
91 CDRPS 5 1 4 0 1.0122 -36.55 51.24 12.83 0.00 0.00 5.00 0.0000 0.0000 0.0000 0.0000 0.0000 0 91
92 WYOMG 5 1 4 0 1.0024 -37.52 36.12 9.05 0.00 0.00 5.00 0.0000 0.0000 0.0000 0.0000 0.0000 0 92
93 ARNOD 5 1 4 0 1.0290 -32.66 103.80 34.56 0.00 0.00 5.00 0.0000 0.0000 0.0000 0.0000 0.0000 0 93
94 HILL 5 1 8 0 1.0264 -36.94 164.00 6.49 0.00 0.00 5.00 0.0000 0.0000 0.0000 0.0000 0.0000 0 94
95 PRARCK 7 1 4 0 1.0301 -36.55 117.20 39.01 0.00 0.00 7.00 0.0000 0.0000 0.0000 0.0000 0.0000 0 95
96 MTOW 7 1 4 0 1.0014 -45.07 119.20 0.00 0.00 0.00 7.00 0.0000 0.0000 0.0000 0.0000 0.0000 0 96
97 CALUS 7 1 4 0 1.0266 -37.22 22.84 5.71 0.00 0.00 7.00 0.0000 0.0000 0.0000 0.0000 0.0000 0 97
98 SIX T 7 1 4 0 1.0441 -35.31 151.10 20.35 0.00 0.00 7.00 1.0450 30.00 -0.10 0.0000 0.0000 0 98
99 PRARK4G 100 1 4 2 1.0000 -31.41 0.00 0.00 130.90 5.69 100.00 1.0000 75.60 -60.60 0.0000 0.0000 0 99
100 WELSRG 7 1 4 0 0.9874 -45.83 23.21 6.90 0.00 0.00 7.00 0.0000 0.0000 0.0000 0.0000 0.0300 0 100
101 MTOW 3G 100 1 4 2 1.0000 -40.09 0.00 0.00 82.00 30.47 100.00 1.0000 38.60 -24.40 0.0000 0.0000 0 101
102 MQOKTA 5 1 4 0 1.0034 -37.02 16.54 4.08 0.00 0.00 5.00 0.0000 0.0000 0.0000 0.0000 0.0000 0 102
103 DAVNRT 5 1 5 0 1.0151 -34.68 322.00 -45.80 0.00 0.00 5.00 0.0000 0.0000 0.0000 0.0000 0.0000 0 103
104 IA FS 7 1 4 0 0.9930 -44.63 31.52 10.56 0.00 0.00 7.00 0.0000 0.0000 0.0000 0.0000 0.0560 0 104
105 DUNDE 7 1 4 0 1.0339 -38.59 24.84 6.23 0.00 0.00 7.00 0.0000 0.0000 0.0000 0.0000 0.0170 0 105
106 MONRE 5 1 7 0 0.9948 -43.01 0.00 0.00 0.00 0.00 5.00 0.0000 0.0000 0.0000 0.0000 0.0000 0 106
107 POWAHK 5 1 7 0 0.9911 -43.89 35.41 5.41 0.00 0.00 5.00 0.0000 0.0000 0.0000 0.0000 0.0000 0 107
108 AROL 1G 100 1 4 3 1.0000 -27.69 0.00 0.00 551.05 154.08 100.00 1.0000 9999.00-9999.00 0.0000 0.0000 0 108
109 HILL 3 1 8 0 1.0134 -33.05 0.00 0.00 0.00 0.00 3.00 0.0000 0.0000 0.0000 0.0000 0.0000 0 109
110 CBLUFS 5 1 6 0 1.0275 -29.52 0.00 0.00 0.00 0.00 5.00 0.0000 0.0000 0.0000 0.0000 0.0000 0 110
111 AVOC 5 1 6 0 1.0055 -33.93 65.41 16.72 0.00 0.00 5.00 0.0000 0.0000 0.0000 0.0000 0.0000 0 111
112 CBLUFS 3 1 6 0 1.0274 -27.01 0.00 0.00 0.00 0.00 3.00 0.0000 0.0000 0.0000 0.0000 -0.5000 0 112
113 S121 105 1 5 0 1.0253 -30.95 32.70 -95.20 0.00 0.00 105.00 0.0000 0.0000 0.0000 0.0000 0.0000 0 113
114 C.BL12G 100 1 6 2 1.0000 -23.67 0.00 0.00 131.00 22.39 100.00 1.0000 33.00 -25.00 0.0000 0.0000 0 114
115 BOONIL 5 1 6 0 1.0176 -36.05 17.32 3.34 0.00 0.00 5.00 0.0000 0.0000 0.0000 0.0000 0.0000 0 115

116 SYCAOR 5 1 6 0 1.0243 -37.29 56.08 11.20 0.00 0.00 5.00 0.0000 0.0000 0.0000 0.0000 0.0000 0 116
117 ASHAA 5 1 6 0 1.0142 -37.95 101.90 20.06 0.00 0.00 5.00 0.0000 0.0000 0.0000 0.0000 0.0000 0 117
118 DPS 57G 100 1 6 2 1.0000 -34.03 0.00 0.00 173.00 59.61 100.00 1.0000 100.00 -44.00 0.0000 0.0000 0 118
119 SYCAOR 3 1 6 0 1.0098 -35.25 0.00 0.00 0.00 0.00 3.00 0.0000 0.0000 0.0000 0.0000 0.0000 0 119
120 S345 603 1 11 0 1.0239 -27.37 0.00 0.00 0.00 0.00 603.00 0.0000 0.0000 0.0000 0.0000 0.0000 0 120
121 C.BL 3G 100 1 6 2 1.0000 -20.10 0.00 0.00 620.00 150.96 100.00 1.0000 250.00 -120.00 0.0000 0.0000 0 121
122 OSKLOS 5 1 6 0 0.9888 -45.83 47.28 9.36 0.00 0.00 5.00 0.0000 0.0000 0.0000 0.0000 0.0000 0 122
123 WAPELO 5 1 5 0 1.0000 -46.19 165.00 -54.89 0.00 0.00 5.00 1.0000 66.59 6.49 0.0000 0.0000 0 123
124 DVNPT 3 1 5 2 1.0090 -31.02 2000.00 90.90 2571.00 0.00 3.00 0.0000 0.0000 0.0000 0.0000 0.0000 0 124
125 PALM 710 1 5 2 1.0200 -29.34 2000.00 0.00 2388.00 -23.48 710.00 1.0200 9900.00-1099.00 0.0000 0.0000 0 125
126 PR ILD 3 1 5 2 1.0111 -26.59 2000.00 0.00 2467.00 63.80 3.00 0.0000 9900.00 0.0000 0.0000 0.0000 0 126
127 LACRSS 3 1 5 0 0.9851 -29.54 -52.60 65.00 0.00 0.00 3.00 0.0000 0.0000 0.0000 0.0000 0.0000 0 127
128 S345 903 1 11 0 1.0240 -27.27 0.00 0.00 0.00 0.00 903.00 0.0000 0.0000 0.0000 0.0000 0.0000 0 128
129 S345 503 1 11 0 1.0244 -27.49 0.00 0.00 0.00 0.00 503.00 0.0000 0.0000 0.0000 0.0000 0.0000 0 129
130 FT.CL1G 100 1 11 2 1.0300 -19.35 0.00 0.00 455.00 123.23 100.00 1.0300 288.00 -144.00 0.0000 0.0000 0 130
131 NEBCY1G 100 1 11 2 1.0180 -20.43 0.00 0.00 575.00 94.26 100.00 1.0180 320.00 -265.00 0.0000 0.0000 0 131
132 S125 505 1 5 0 1.0200 -30.36 159.00 36.10 0.00 0.00 505.00 0.0000 0.0000 0.0000 0.0000 0.0000 0 132
133 S701 8 1 6 0 1.0354 -32.19 30.10 6.02 0.00 0.00 8.00 0.0000 0.0000 0.0000 0.0000 0.0000 0 133
134 S701 5 1 6 0 1.0232 -30.86 17.46 3.34 0.00 0.00 5.00 0.0000 0.0000 0.0000 0.0000 0.0000 0 134
135 S702 8 1 6 0 1.0322 -32.23 20.06 4.01 0.00 0.00 8.00 0.0000 0.0000 0.0000 0.0000 0.0000 0 135
136 S703 8 1 6 0 1.0256 -32.50 20.06 4.01 0.00 0.00 8.00 0.0000 0.0000 0.0000 0.0000 0.0000 0 136
137 S704 8 1 6 0 1.0292 -32.46 20.06 4.01 0.00 0.00 8.00 0.0000 0.0000 0.0000 0.0000 0.0000 0 137
138 CBLUFS 8 1 6 0 1.0317 -31.28 0.00 0.00 0.00 0.00 8.00 0.0000 0.0000 0.0000 0.0000 0.0000 0 138
139 S706 8 1 6 0 1.0267 -32.05 10.10 2.01 0.00 0.00 8.00 0.0000 0.0000 0.0000 0.0000 0.0000 0 139
140 S705 8 1 6 0 1.0287 -32.38 13.58 2.68 0.00 0.00 8.00 0.0000 0.0000 0.0000 0.0000 0.0000 0 140
141 HSTNGS 5 1 6 0 1.0028 -33.91 0.00 0.00 0.00 0.00 5.00 0.0000 0.0000 0.0000 0.0000 0.0000 0 141
142 CLRNDA 8 1 6 0 1.0278 -40.63 27.09 5.35 0.00 0.00 8.00 0.0000 0.0000 0.0000 0.0000 0.0000 0 142
143 R.OAK 8 1 6 0 1.0058 -39.42 21.07 4.01 0.00 0.00 8.00 0.0000 0.0000 0.0000 0.0000 0.0000 0 143
144 HSTNGS 8 1 6 0 1.0222 -36.16 12.37 2.01 0.00 0.00 8.00 0.0000 0.0000 0.0000 0.0000 0.0000 0 144
145 GWOOD 8 1 6 0 1.0191 -34.40 10.83 2.21 0.00 0.00 8.00 0.0000 0.0000 0.0000 0.0000 0.0000 0 145
146 SHENDO 8 1 6 0 1.0101 -39.89 21.33 4.01 0.00 0.00 8.00 0.0000 0.0000 0.0000 0.0000 0.0000 0 146
147 WABASH 5 1 6 0 1.0104 -38.98 216.40 42.80 0.00 0.00 5.00 0.0000 0.0000 0.0000 0.0000 0.0000 0 147
148 SYCAOR 8 1 6 0 1.0134 -40.01 120.00 24.00 0.00 0.00 8.00 0.0000 0.0000 0.0000 0.0000 0.0000 0 148
149 RAUN 5 1 2 0 1.0259 -23.76 0.00 0.00 0.00 0.00 5.00 0.0000 0.0000 0.0000 0.0000 0.0000 0 149
150 NEAL 405 1 2 0 1.0234 -24.41 4.80 1.60 0.00 0.00 405.00 0.0000 0.0000 0.0000 0.0000 0.0000 0 150
151 INTRCG 5 1 2 0 1.0100 -26.70 24.00 8.00 0.00 0.00 5.00 0.0000 0.0000 0.0000 0.0000 0.0000 0 151
152 TEKAMA 5 1 5 0 1.0234 -26.79 6.00 -2.80 0.00 0.00 5.00 0.0000 0.0000 0.0000 0.0000 0.0000 0 152
153 NEAL 8 1 2 0 1.0178 -25.80 4.00 1.60 0.00 0.00 8.00 0.0000 0.0000 0.0000 0.0000 0.0000 0 153
154 KELLOG 8 1 2 0 0.9751 -32.10 28.00 9.60 0.00 0.00 8.00 0.0000 0.0000 0.0000 0.0000 0.0600 0 154
155 M SIDE 8 1 2 0 0.9855 -30.27 12.00 4.00 0.00 0.00 8.00 0.0000 0.0000 0.0000 0.0000 0.0000 0 155
156 E SIDE 8 1 2 0 0.9788 -31.79 8.00 2.40 0.00 0.00 8.00 0.0000 0.0000 0.0000 0.0000 0.0000 0 156
157 PLYMTH 8 1 2 0 0.9803 -32.55 32.00 10.40 0.00 0.00 8.00 0.0000 0.0000 0.0000 0.0000 0.0000 0 157
158 LOGANP 8 1 2 0 0.9683 -33.49 16.00 5.60 0.00 0.00 8.00 0.0000 0.0000 0.0000 0.0000 0.0300 0 158
159 MCCOOK 8 1 2 0 0.9687 -33.32 8.00 2.40 0.00 0.00 8.00 0.0000 0.0000 0.0000 0.0000 0.0000 0 159
160 SC WST 8 1 2 0 0.9715 -32.76 14.40 4.80 0.00 0.00 8.00 0.0000 0.0000 0.0000 0.0000 0.0300 0 160
161 KELOG 5 1 2 0 1.0040 -28.10 32.00 10.40 0.00 0.00 5.00 0.0000 0.0000 0.0000 0.0000 0.0000 0 161
162 LEEDS 5 1 2 0 1.0004 -28.97 20.00 6.40 0.00 0.00 5.00 0.0000 0.0000 0.0000 0.0000 0.0000 0 162
-999
BRANCH DATA FOLLOWS 284 ITEMS (HEADER)
1 2 1 12 1 0 0.003500 0.032100 0.54372 52. 0. 0. 0 0 0.0000 0.00 0.0000 0.0000 .00000 0.0000 0.0000 1
1 3 1 12 1 0 0.003400 0.032600 0.72240 52. 0. 0. 0 0 0.0000 0.00 0.0000 0.0000 .00000 0.0000 0.0000 2
1 4 1 12 1 0 0.006400 0.062100 0.98700 52. 0. 0. 0 0 0.0000 0.00 0.0000 0.0000 .00000 0.0000 0.0000 3
1 5 1 12 1 0 0.001100 0.011900 0.20120 52. 0. 0. 0 0 0.0000 0.00 0.0000 0.0000 .00000 0.0000 0.0000 4
1 6 1 12 1 1 0.000000 0.013300 0.00000 900. 0. 0. 0 0 1.0520 0.00 0.0000 0.0000 .00000 0.0000 0.0000 5

2 7 1 12 1 0 0.001400 0.012500 0.21210 52. 0. 0. 0 0 0.0000 0.00 0.0000 0.0000 .00000 0.0000 0.0000 6
2 13 1 12 1 0 0.004600 0.041700 0.70586 52. 0. 0. 0 0 0.0000 0.00 0.0000 0.0000 .00000 0.0000 0.0000 7
3 14 1 5 1 0 0.236100 1.012200 0.00000 0. 0. 0. 0 0 0.0000 0.00 0.0000 0.0000 .00000 0.0000 0.0000 8
3 50 1 5 1 0 0.038900 0.169900 0.00000 0. 0. 0. 0 0 0.0000 0.00 0.0000 0.0000 .00000 0.0000 0.0000 9
3 103 1 5 1 0 0.107400 1.802300 0.00000 0. 0. 0. 0 0 0.0000 0.00 0.0000 0.0000 .00000 0.0000 0.0000 10
3 123 1 5 1 0 0.288300 1.671900 0.00000 0. 0. 0. 0 0 0.0000 0.00 0.0000 0.0000 .00000 0.0000 0.0000 11
3 124 1 5 1 0 0.014000 0.648300 0.00000 0. 0. 0. 0 0 0.0000 0.00 0.0000 0.0000 .00000 0.0000 0.0000 12
3 125 1 5 1 0 0.008400 0.113900 0.00000 0. 0. 0. 0 0 0.0000 0.00 0.0000 0.0000 .00000 0.0000 0.0000 13
4 112 1 6 1 0 0.005900 0.056800 0.92500 52. 0. 0. 0 0 0.0000 0.00 0.0000 0.0000 .00000 0.0000 0.0000 14
4 115 1 6 1 1 0.000000 0.018500 0.00000 500. 0. 0. 0 0 1.0000 0.00 0.0000 0.0000 .00000 0.0000 0.0000 15
4 119 1 6 1 0 0.001400 0.011900 0.20500 52. 0. 0. 0 0 0.0000 0.00 0.0000 0.0000 .00000 0.0000 0.0000 16
5 120 1 11 1 0 0.002200 0.022400 0.37930 52. 0. 0. 0 0 0.0000 0.00 0.0000 0.0000 .00000 0.0000 0.0000 17
5 129 1 11 1 0 0.002200 0.026800 0.46120 52. 0. 0. 0 0 0.0000 0.00 0.0000 0.0000 .00000 0.0000 0.0000 18
5 131 1 11 1 1 0.000000 0.012700 0.00000 710. 0. 0. 0 0 1.0250 0.00 0.0000 0.0000 .00000 0.0000 0.0000 19
7 8 1 12 1 1 0.000400 0.018900 0.00000 672. 0. 0. 0 0 0.9750 0.00 0.0000 0.0000 .00000 0.0000 0.0000 20
7 9 1 12 1 0 0.001700 0.016900 0.28726 52. 0. 0. 0 0 0.0000 0.00 0.0000 0.0000 .00000 0.0000 0.0000 21
8 10 1 5 1 0 0.459100 1.070300 0.00000 0. 0. 0. 0 0 0.0000 0.00 0.0000 0.0000 .00000 0.0000 0.0000 22
8 12 1 5 1 0 0.010600 0.057400 0.00000 0. 0. 0. 0 0 0.0000 0.00 0.0000 0.0000 .00000 0.0000 0.0000 23
8 13 1 5 1 0 0.127400 0.478400 0.00000 0. 0. 0. 0 0 0.0000 0.00 0.0000 0.0000 .00000 0.0000 0.0000 24
8 14 1 5 1 0 0.047300 0.395600 0.00000 0. 0. 0. 0 0 0.0000 0.00 0.0000 0.0000 .00000 0.0000 0.0000 25
8 15 1 5 1 0 0.503500 1.743300 0.00000 0. 0. 0. 0 0 0.0000 0.00 0.0000 0.0000 .00000 0.0000 0.0000 26
8 132 1 5 1 0 0.025200 0.288000 0.00000 0. 0. 0. 0 0 0.0000 0.00 0.0000 0.0000 .00000 0.0000 0.0000 27
9 75 1 11 1 0 0.001300 0.015000 0.26828 717. 0. 0. 0 0 0.0000 0.00 0.0000 0.0000 .00000 0.0000 0.0000 28
10 11 1 5 1 0 0.005100 0.037000 0.07160 69. 0. 0. 0 0 0.0000 0.00 0.0000 0.0000 .00000 0.0000 0.0000 29
10 13 1 5 1 0 0.129900 0.622000 0.00000 0. 0. 0. 0 0 0.0000 0.00 0.0000 0.0000 .00000 0.0000 0.0000 30
10 15 1 5 1 0 0.127500 0.703300 0.00000 0. 0. 0. 0 0 0.0000 0.00 0.0000 0.0000 .00000 0.0000 0.0000 31
10 60 1 5 1 0 0.252500 1.224200 0.00000 0. 0. 0. 0 0 0.0000 0.00 0.0000 0.0000 .00000 0.0000 0.0000 32
11 15 1 1 1 0 0.028500 0.179300 0.34840 0. 0. 0. 0 0 0.0000 0.00 0.0000 0.0000 .00000 0.0000 0.0000 33
11 46 1 1 1 0 0.014200 0.122500 0.18760 69. 0. 0. 0 0 0.0000 0.00 0.0000 0.0000 .00000 0.0000 0.0000 34
11 58 1 1 1 0 0.017000 0.107000 0.20740 0. 0. 0. 0 0 0.0000 0.00 0.0000 0.0000 .00000 0.0000 0.0000 35
11 59 1 1 1 0 0.007100 0.047100 0.08520 0. 0. 0. 0 0 0.0000 0.00 0.0000 0.0000 .00000 0.0000 0.0000 36
12 2 1 5 1 1 0.000800 0.037700 0.00000 336. 0. 0. 0 0 1.0250 0.00 0.0000 0.0000 .00000 0.0000 0.0000 37
12 13 1 5 1 0 0.103800 0.313700 0.00000 0. 0. 0. 0 0 0.0000 0.00 0.0000 0.0000 .00000 0.0000 0.0000 38
12 14 1 5 1 0 0.159800 0.641500 0.00000 0. 0. 0. 0 0 0.0000 0.00 0.0000 0.0000 .00000 0.0000 0.0000 39
12 132 1 5 1 0 0.448600 1.577300 0.00000 0. 0. 0. 0 0 0.0000 0.00 0.0000 0.0000 .00000 0.0000 0.0000 40
13 15 1 5 1 0 0.044000 0.322700 0.00000 0. 0. 0. 0 0 0.0000 0.00 0.0000 0.0000 .00000 0.0000 0.0000 41
13 62 1 5 1 0 0.009800 0.122100 0.00000 0. 0. 0. 0 0 0.0000 0.00 0.0000 0.0000 .00000 0.0000 0.0000 42
14 72 1 5 1 0 0.010700 0.082800 0.00000 0. 0. 0. 0 0 0.0000 0.00 0.0000 0.0000 .00000 0.0000 0.0000 43
14 113 1 5 1 0 0.006300 0.038200 0.00000 0. 0. 0. 0 0 0.0000 0.00 0.0000 0.0000 .00000 0.0000 0.0000 44
14 132 1 5 1 0 0.005700 0.037400 0.00000 0. 0. 0. 0 0 0.0000 0.00 0.0000 0.0000 .00000 0.0000 0.0000 45
15 58 1 5 1 0 0.011500 0.073200 0.14200 0. 0. 0. 0 0 0.0000 0.00 0.0000 0.0000 .00000 0.0000 0.0000 46
15 60 1 5 1 0 0.390700 1.675300 0.00000 0. 0. 0. 0 0 0.0000 0.00 0.0000 0.0000 .00000 0.0000 0.0000 47
15 62 1 5 1 0 0.008400 0.058800 0.00000 0. 0. 0. 0 0 0.0000 0.00 0.0000 0.0000 .00000 0.0000 0.0000 48
15 63 1 5 1 0 0.170400 1.455500 0.00000 0. 0. 0. 0 0 0.0000 0.00 0.0000 0.0000 .00000 0.0000 0.0000 49
16 17 1 5 1 0 0.601700 1.437300 0.00000 0. 0. 0. 0 0 0.0000 0.00 0.0000 0.0000 .00000 0.0000 0.0000 50
16 18 1 5 1 0 0.029700 0.107000 0.05460 87. 0. 0. 0 0 0.0000 0.00 0.0000 0.0000 .00000 0.0000 0.0000 51
16 27 1 5 1 0 0.157400 0.887100 0.00000 0. 0. 0. 0 0 0.0000 0.00 0.0000 0.0000 .00000 0.0000 0.0000 52
16 126 1 5 1 0 0.105300 0.513200 0.00000 0. 0. 0. 0 0 0.0000 0.00 0.0000 0.0000 .00000 0.0000 0.0000 53
16 127 1 5 1 0 0.095800 0.527600 0.00000 0. 0. 0. 0 0 0.0000 0.00 0.0000 0.0000 .00000 0.0000 0.0000 54
17 18 1 5 1 0 0.021300 0.101300 0.06410 87. 0. 0. 0 0 0.0000 0.00 0.0000 0.0000 .00000 0.0000 0.0000 55
17 19 1 5 1 0 0.231400 0.767800 0.00000 0. 0. 0. 0 0 0.0000 0.00 0.0000 0.0000 .00000 0.0000 0.0000 56
17 21 1 5 1 0 0.047100 0.266500 0.00000 0. 0. 0. 0 0 0.0000 0.00 0.0000 0.0000 .00000 0.0000 0.0000 57
17 127 1 5 1 0 0.028700 0.263700 0.00000 0. 0. 0. 0 0 0.0000 0.00 0.0000 0.0000 .00000 0.0000 0.0000 58
18 30 1 9 1 0 0.020700 0.108800 0.05200 87. 0. 0. 0 0 0.0000 0.00 0.0000 0.0000 .00000 0.0000 0.0000 59

18 32 1 9 1 0 0.023400 0.122000 0.05830 87. 0. 0. 0 0 0.0000 0.00 0.0000 0.0000 .00000 0.0000 0.0000 60
18 37 1 9 1 1 0.000000 0.045600 0.00000 225. 0. 0. 0 0 1.1190 0.00 0.0000 0.0000 .00000 0.0000 0.0000 61
19 21 1 5 1 0 0.386700 1.900500 0.00000 0. 0. 0. 0 0 0.0000 0.00 0.0000 0.0000 .00000 0.0000 0.0000 62
19 38 1 5 1 0 0.023900 0.125000 0.05960 87. 0. 0. 0 0 0.0000 0.00 0.0000 0.0000 .00000 0.0000 0.0000 63
19 43 1 5 1 0 0.060300 0.257200 0.00000 0. 0. 0. 0 0 0.0000 0.00 0.0000 0.0000 .00000 0.0000 0.0000 64
19 127 1 5 1 0 0.107400 0.680900 0.00000 0. 0. 0. 0 0 0.0000 0.00 0.0000 0.0000 .00000 0.0000 0.0000 65
20 53 1 1 1 1 0.000000 0.114000 0.00000 75. 0. 0. 0 0 1.0000 0.00 0.0000 0.0000 .00000 0.0000 0.0000 66
20 157 1 1 1 0 0.011300 0.027900 0.00050 64. 0. 0. 0 0 0.0000 0.00 0.0000 0.0000 .00000 0.0000 0.0000 67
21 22 1 5 1 0 0.031200 0.162900 0.07780 87. 0. 0. 0 0 0.0000 0.00 0.0000 0.0000 .00000 0.0000 0.0000 68
21 127 1 5 1 0 0.010500 0.641400 0.00000 0. 0. 0. 0 0 0.0000 0.00 0.0000 0.0000 .00000 0.0000 0.0000 69
22 38 1 9 1 0 0.014000 0.054000 0.02500 87. 0. 0. 0 0 0.0000 0.00 0.0000 0.0000 .00000 0.0000 0.0000 70
22 39 1 9 1 1 0.000000 0.049300 0.00000 225. 0. 0. 0 0 1.1080 0.00 0.0000 0.0000 .00000 0.0000 0.0000 71
22 40 1 9 1 0 0.018800 0.071700 0.03280 87. 0. 0. 0 0 0.0000 0.00 0.0000 0.0000 .00000 0.0000 0.0000 72
22 41 1 9 1 0 0.017200 0.085000 0.04046 87. 0. 0. 0 0 0.0000 0.00 0.0000 0.0000 .00000 0.0000 0.0000 73
23 24 1 5 1 0 0.017400 0.051100 0.02300 87. 0. 0. 0 0 0.0000 0.00 0.0000 0.0000 .00000 0.0000 0.0000 74
23 60 1 5 1 0 0.066000 0.309300 0.00000 0. 0. 0. 0 0 0.0000 0.00 0.0000 0.0000 .00000 0.0000 0.0000 75
24 25 1 9 1 1 0.000000 0.034000 0.00000 225. 0. 0. 0 0 1.0220 0.00 0.0000 0.0000 .00000 0.0000 0.0000 76
24 28 1 9 1 0 0.024900 0.072500 0.02020 87. 0. 0. 0 0 0.0000 0.00 0.0000 0.0000 .00000 0.0000 0.0000 77
24 45 1 9 1 0 0.013700 0.072500 0.03400 87. 0. 0. 0 0 0.0000 0.00 0.0000 0.0000 .00000 0.0000 0.0000 78
25 26 1 9 1 0 0.005900 0.058300 0.93016 52. 0. 0. 0 0 0.0000 0.00 0.0000 0.0000 .00000 0.0000 0.0000 79
25 27 1 9 1 0 0.004400 0.041000 0.83840 52. 0. 0. 0 0 0.0000 0.00 0.0000 0.0000 .00000 0.0000 0.0000 80
26 74 1 2 1 0 0.006300 0.060700 0.93000 52. 0. 0. 0 0 0.0000 0.00 0.0000 0.0000 .00000 0.0000 0.0000 81
26 75 1 2 1 0 0.003000 0.032200 0.50388 52. 0. 0. 0 0 0.0000 0.00 0.0000 0.0000 .00000 0.0000 0.0000 82
26 76 1 2 1 1 0.000000 0.008200 0.00000 1250. 0. 0. 0 0 1.0400 0.00 0.0000 0.0000 .00000 0.0000 0.0000 83
27 31 1 5 1 0 0.010100 0.127300 0.00000 0. 0. 0. 0 0 0.0000 0.00 0.0000 0.0000 .00000 0.0000 0.0000 84
27 62 1 5 1 0 0.017300 0.581000 0.00000 0. 0. 0. 0 0 0.0000 0.00 0.0000 0.0000 .00000 0.0000 0.0000 85
27 65 1 5 1 0 0.010500 0.276400 0.00000 0. 0. 0. 0 0 0.0000 0.00 0.0000 0.0000 .00000 0.0000 0.0000 86
27 125 1 5 1 0 0.035000 1.684500 0.00000 0. 0. 0. 0 0 0.0000 0.00 0.0000 0.0000 .00000 0.0000 0.0000 87
27 126 1 5 1 0 0.002200 0.022500 0.00000 0. 0. 0. 0 0 0.0000 0.00 0.0000 0.0000 .00000 0.0000 0.0000 88
27 127 1 5 1 0 0.150600 1.435500 0.00000 0. 0. 0. 0 0 0.0000 0.00 0.0000 0.0000 .00000 0.0000 0.0000 89
28 29 1 9 1 0 0.024000 0.096500 0.04440 87. 0. 0. 0 0 0.0000 0.00 0.0000 0.0000 .00000 0.0000 0.0000 90
29 30 1 9 1 0 0.038000 0.150000 0.06960 87. 0. 0. 0 0 0.0000 0.00 0.0000 0.0000 .00000 0.0000 0.0000 91
29 31 1 9 1 0 0.020600 0.083300 0.03850 87. 0. 0. 0 0 0.0000 0.00 0.0000 0.0000 .00000 0.0000 0.0000 92
30 32 1 9 1 0 0.024900 0.100500 0.04580 87. 0. 0. 0 0 0.0000 0.00 0.0000 0.0000 .00000 0.0000 0.0000 93
32 33 1 9 1 0 0.011400 0.044800 0.02078 87. 0. 0. 0 0 0.0000 0.00 0.0000 0.0000 .00000 0.0000 0.0000 94
33 34 1 9 1 0 0.028000 0.114000 0.05200 87. 0. 0. 0 0 0.0000 0.00 0.0000 0.0000 .00000 0.0000 0.0000 95
33 35 1 9 1 0 0.021600 0.107000 0.05100 87. 0. 0. 0 0 0.0000 0.00 0.0000 0.0000 .00000 0.0000 0.0000 96
33 36 1 9 1 0 0.010200 0.053600 0.02550 87. 0. 0. 0 0 0.0000 0.00 0.0000 0.0000 .00000 0.0000 0.0000 97
34 40 1 2 1 0 0.039700 0.151700 0.06898 87. 0. 0. 0 0 0.0000 0.00 0.0000 0.0000 .00000 0.0000 0.0000 98
34 77 1 2 1 0 0.023500 0.089600 0.04072 87. 0. 0. 0 0 0.0000 0.00 0.0000 0.0000 .00000 0.0000 0.0000 99
35 40 1 2 1 0 0.027100 0.134100 0.06382 87. 0. 0. 0 0 0.0000 0.00 0.0000 0.0000 .00000 0.0000 0.0000 100
36 67 1 4 1 0 0.017600 0.092400 0.04400 87. 0. 0. 0 0 0.0000 0.00 0.0000 0.0000 .00000 0.0000 0.0000 101
37 39 1 3 1 0 0.003900 0.037900 0.67000 52. 0. 0. 0 0 0.0000 0.00 0.0000 0.0000 .00000 0.0000 0.0000 102
37 126 1 3 1 0 0.004000 0.038100 0.67000 52. 0. 0. 0 0 0.0000 0.00 0.0000 0.0000 .00000 0.0000 0.0000 103
37 127 1 3 1 0 0.004000 0.040300 0.68320 52. 0. 0. 0 0 0.0000 0.00 0.0000 0.0000 .00000 0.0000 0.0000 104
39 42 1 9 1 0 0.002000 0.018600 0.32000 52. 0. 0. 0 0 0.0000 0.00 0.0000 0.0000 .00000 0.0000 0.0000 105
40 81 1 2 1 0 0.030000 0.345000 0.00390 50. 0. 0. 0 0 0.0000 0.00 0.0000 0.0000 .00000 0.0000 0.0000 106
40 82 1 2 1 0 0.004000 0.019000 0.01080 87. 0. 0. 0 0 0.0000 0.00 0.0000 0.0000 .00000 0.0000 0.0000 107
41 81 1 2 1 0 0.037000 0.372000 0.00580 50. 0. 0. 0 0 0.0000 0.00 0.0000 0.0000 .00000 0.0000 0.0000 108
41 83 1 2 1 0 0.005200 0.025600 0.01234 0. 0. 0. 0 0 0.0000 0.00 0.0000 0.0000 .00000 0.0000 0.0000 109
41 84 1 2 1 0 0.005700 0.058000 0.02910 87. 0. 0. 0 0 0.0000 0.00 0.0000 0.0000 .00000 0.0000 0.0000 110
42 109 1 4 1 0 0.001900 0.019600 0.33300 52. 0. 0. 0 0 0.0000 0.00 0.0000 0.0000 .00000 0.0000 0.0000 111
43 44 1 5 1 0 0.018800 0.075100 0.03490 87. 0. 0. 0 0 0.0000 0.00 0.0000 0.0000 .00000 0.0000 0.0000 112
43 103 1 5 1 0 0.032400 0.170200 0.00000 0. 0. 0. 0 0 0.0000 0.00 0.0000 0.0000 .00000 0.0000 0.0000 113

43 124 1 5 1 0 0.029300 0.176600 0.00000 0. 0. 0. 0 0 0.0000 0.00 0.0000 0.0000 .00000 0.0000 0.0000 114
43 125 1 5 1 0 0.144900 0.650900 0.00000 0. 0. 0. 0 0 0.0000 0.00 0.0000 0.0000 .00000 0.0000 0.0000 115
44 102 1 4 1 0 0.013000 0.050000 0.02370 87. 0. 0. 0 0 0.0000 0.00 0.0000 0.0000 .00000 0.0000 0.0000 116
44 103 1 4 1 0 0.012700 0.051000 0.02450 87. 0. 0. 0 0 0.0000 0.00 0.0000 0.0000 .00000 0.0000 0.0000 117
45 54 1 4 1 0 0.010800 0.057000 0.02720 87. 0. 0. 0 0 0.0000 0.00 0.0000 0.0000 .00000 0.0000 0.0000 118
46 47 1 1 1 0 0.031000 0.137800 0.06220 87. 0. 0. 0 0 0.0000 0.00 0.0000 0.0000 .00000 0.0000 0.0000 119
47 48 1 4 1 0 0.025100 0.111400 0.05020 87. 0. 0. 0 0 0.0000 0.00 0.0000 0.0000 .00000 0.0000 0.0000 120
47 49 1 4 1 0 0.003000 0.012000 0.00540 0. 0. 0. 0 0 0.0000 0.00 0.0000 0.0000 .00000 0.0000 0.0000 121
48 50 1 1 1 0 0.033600 0.166000 0.07800 0. 0. 0. 0 0 0.0000 0.00 0.0000 0.0000 .00000 0.0000 0.0000 122
48 51 1 1 1 0 0.042000 0.130000 0.05700 0. 0. 0. 0 0 0.0000 0.00 0.0000 0.0000 .00000 0.0000 0.0000 123
48 52 1 1 1 0 0.054000 0.168000 0.07400 87. 0. 0. 0 0 0.0000 0.00 0.0000 0.0000 .00000 0.0000 0.0000 124
49 87 1 4 1 0 0.014000 0.068000 0.02660 0. 0. 0. 0 0 0.0000 0.00 0.0000 0.0000 .00000 0.0000 0.0000 125
50 51 1 5 1 0 0.030000 0.090000 0.04100 0. 0. 0. 0 0 0.0000 0.00 0.0000 0.0000 .00000 0.0000 0.0000 126
50 123 1 5 1 0 0.407100 1.854300 0.00000 0. 0. 0. 0 0 0.0000 0.00 0.0000 0.0000 .00000 0.0000 0.0000 127
50 125 1 5 1 0 0.133700 0.603100 0.00000 0. 0. 0. 0 0 0.0000 0.00 0.0000 0.0000 .00000 0.0000 0.0000 128
51 141 1 6 1 0 0.032300 0.100000 0.04428 87. 0. 0. 0 0 0.0000 0.00 0.0000 0.0000 .00000 0.0000 0.0000 129
52 79 1 6 1 0 0.062300 0.212600 0.09400 87. 0. 0. 0 0 0.0000 0.00 0.0000 0.0000 .00000 0.0000 0.0000 130
52 106 1 6 1 0 0.023100 0.071700 0.03150 87. 0. 0. 0 0 0.0000 0.00 0.0000 0.0000 .00000 0.0000 0.0000 131
52 116 1 6 1 0 0.006000 0.048700 0.02570 87. 0. 0. 0 0 0.0000 0.00 0.0000 0.0000 .00000 0.0000 0.0000 132
52 117 1 6 1 0 0.011700 0.049300 0.02300 87. 0. 0. 0 0 0.0000 0.00 0.0000 0.0000 .00000 0.0000 0.0000 133
52 118 1 6 1 1 0.000000 0.052000 0.00000 200. 0. 0. 0 0 1.0430 0.00 0.0000 0.0000 .00000 0.0000 0.0000 134
53 11 1 1 1 1 0.000500 0.020000 0.00000 375. 0. 0. 0 0 1.0000 0.00 0.0000 0.0000 .00000 0.0000 0.0000 135
53 54 1 1 1 0 0.027500 0.196100 0.09560 87. 0. 0. 0 0 0.0000 0.00 0.0000 0.0000 .00000 0.0000 0.0000 136
53 55 1 1 1 0 0.000500 0.002600 0.00230 87. 0. 0. 0 0 0.0000 0.00 0.0000 0.0000 .00000 0.0000 0.0000 137
54 56 1 1 1 0 0.017400 0.091000 0.04300 87. 0. 0. 0 0 0.0000 0.00 0.0000 0.0000 .00000 0.0000 0.0000 138
54 57 1 1 1 0 0.025000 0.123700 0.05886 87. 0. 0. 0 0 0.0000 0.00 0.0000 0.0000 .00000 0.0000 0.0000 139
55 57 1 2 1 0 0.046200 0.176300 0.08012 87. 0. 0. 0 0 0.0000 0.00 0.0000 0.0000 .00000 0.0000 0.0000 140
55 149 1 2 1 0 0.015300 0.067100 0.03126 87. 0. 0. 0 0 0.0000 0.00 0.0000 0.0000 .00000 0.0000 0.0000 141
55 162 1 2 1 0 0.004000 0.018900 0.00976 87. 0. 0. 0 0 0.0000 0.00 0.0000 0.0000 .00000 0.0000 0.0000 142
56 67 1 10 1 0 0.017000 0.089400 0.04250 87. 0. 0. 0 0 0.0000 0.00 0.0000 0.0000 .00000 0.0000 0.0000 143
57 80 1 2 1 0 0.027200 0.103700 0.04714 87. 0. 0. 0 0 0.0000 0.00 0.0000 0.0000 .00000 0.0000 0.0000 144
58 61 1 1 1 0 0.013300 0.101800 0.18420 69. 0. 0. 0 0 0.0000 0.00 0.0000 0.0000 .00000 0.0000 0.0000 145
59 61 1 1 1 0 0.010600 0.070600 0.12100 0. 0. 0. 0 0 0.0000 0.00 0.0000 0.0000 .00000 0.0000 0.0000 146
60 61 1 5 1 1 0.002700 0.065300 -0.00220 100. 0. 0. 0 0 1.0250 0.00 0.0000 0.0000 .00000 0.0000 0.0000 147
60 61 1 5 2 1 0.002000 0.039300 0.00000 200. 0. 0. 0 0 1.0250 0.00 0.0000 0.0000 .00000 0.0000 0.0000 148
60 62 1 5 1 0 0.367400 0.964000 0.00000 0. 0. 0. 0 0 0.0000 0.00 0.0000 0.0000 .00000 0.0000 0.0000 149
60 65 1 5 1 0 0.104100 0.414400 0.00000 0. 0. 0. 0 0 0.0000 0.00 0.0000 0.0000 .00000 0.0000 0.0000 150
60 126 1 5 1 0 0.536700 1.829500 0.00000 0. 0. 0. 0 0 0.0000 0.00 0.0000 0.0000 .00000 0.0000 0.0000 151
61 62 1 1 1 0 0.029600 0.227500 0.39960 69. 0. 0. 0 0 0.0000 0.00 0.0000 0.0000 .00000 0.0000 0.0000 152
61 63 1 1 1 0 0.004300 0.042200 0.07640 69. 0. 0. 0 0 0.0000 0.00 0.0000 0.0000 .00000 0.0000 0.0000 153
62 63 1 5 1 0 0.015800 0.170200 0.00000 0. 0. 0. 0 0 0.0000 0.00 0.0000 0.0000 .00000 0.0000 0.0000 154
62 65 1 5 1 0 0.004000 0.074000 0.00000 0. 0. 0. 0 0 0.0000 0.00 0.0000 0.0000 .00000 0.0000 0.0000 155
62 126 1 5 1 0 0.004400 0.296900 0.00000 0. 0. 0. 0 0 0.0000 0.00 0.0000 0.0000 .00000 0.0000 0.0000 156
63 65 1 5 1 0 0.240900 1.960000 0.00000 0. 0. 0. 0 0 0.0000 0.00 0.0000 0.0000 .00000 0.0000 0.0000 157
64 65 1 1 1 0 0.005000 0.057100 0.90984 1200. 0. 0. 0 0 0.0000 0.00 0.0000 0.0000 .00000 0.0000 0.0000 158
64 66 1 1 1 0 0.003300 0.038100 0.60656 1200. 0. 0. 0 0 0.0000 0.00 0.0000 0.0000 .00000 0.0000 0.0000 159
65 126 1 5 1 0 0.003100 0.153600 0.00000 0. 0. 0. 0 0 0.0000 0.00 0.0000 0.0000 .00000 0.0000 0.0000 160
66 11 1 1 1 1 0.000000 0.011800 0.00000 500. 0. 0. 0 0 1.0000 0.00 0.0000 0.0000 .00000 0.0000 0.0000 161
67 68 1 10 1 0 0.019300 0.101300 0.04820 87. 0. 0. 0 0 0.0000 0.00 0.0000 0.0000 .00000 0.0000 0.0000 162
68 69 1 10 1 0 0.006800 0.035300 0.01690 87. 0. 0. 0 0 0.0000 0.00 0.0000 0.0000 .00000 0.0000 0.0000 163
69 77 1 2 1 0 0.009800 0.037400 0.01698 87. 0. 0. 0 0 0.0000 0.00 0.0000 0.0000 .00000 0.0000 0.0000 164
69 78 1 2 1 0 0.011400 0.043400 0.01970 87. 0. 0. 0 0 0.0000 0.00 0.0000 0.0000 .00000 0.0000 0.0000 165
69 79 1 2 1 0 0.005200 0.043300 0.02206 87. 0. 0. 0 0 0.0000 0.00 0.0000 0.0000 .00000 0.0000 0.0000 166
70 73 1 2 1 1 0.000000 0.019700 0.00000 495. 0. 0. 0 0 1.0400 0.00 0.0000 0.0000 .00000 0.0000 0.0000 167

70 149 1 2 1 0 0.000200 0.001800 0.00090 87. 0. 0. 0 0 0.0000 0.00 0.0000 0.0000 .00000 0.0000 0.0000 168
70 149 1 2 2 0 0.000200 0.001800 0.00090 87. 0. 0. 0 0 0.0000 0.00 0.0000 0.0000 .00000 0.0000 0.0000 169
71 85 1 2 1 0 0.030400 0.150600 0.07166 87. 0. 0. 0 0 0.0000 0.00 0.0000 0.0000 .00000 0.0000 0.0000 170
71 150 1 2 1 0 0.019600 0.097000 0.04616 87. 0. 0. 0 0 0.0000 0.00 0.0000 0.0000 .00000 0.0000 0.0000 171
72 113 1 5 1 0 0.002200 0.013000 0.00000 0. 0. 0. 0 0 0.0000 0.00 0.0000 0.0000 .00000 0.0000 0.0000 172
72 132 1 5 1 0 0.002800 0.016800 0.00000 0. 0. 0. 0 0 0.0000 0.00 0.0000 0.0000 .00000 0.0000 0.0000 173
72 152 1 5 1 0 0.038500 0.180000 0.00000 0. 0. 0. 0 0 0.0000 0.00 0.0000 0.0000 .00000 0.0000 0.0000 174
74 119 1 8 1 0 0.003100 0.031000 0.48210 52. 0. 0. 0 0 0.0000 0.00 0.0000 0.0000 .00000 0.0000 0.0000 175
75 128 1 11 1 0 0.000800 0.008700 0.16592 52. 0. 0. 0 0 0.0000 0.00 0.0000 0.0000 .00000 0.0000 0.0000 176
75 130 1 11 1 1 0.000400 0.024200 0.00000 578. 0. 0. 0 0 1.0250 0.00 0.0000 0.0000 .00000 0.0000 0.0000 177
78 79 1 8 1 0 0.005100 0.033600 0.01824 87. 0. 0. 0 0 0.0000 0.00 0.0000 0.0000 .00000 0.0000 0.0000 178
78 80 1 8 1 0 0.024400 0.093000 0.04228 87. 0. 0. 0 0 0.0000 0.00 0.0000 0.0000 .00000 0.0000 0.0000 179
79 74 1 8 1 1 0.000000 0.018000 0.00000 500. 0. 0. 0 0 1.0250 0.00 0.0000 0.0000 .00000 0.0000 0.0000 180
82 83 1 2 1 0 0.005300 0.024900 0.01300 0. 0. 0. 0 0 0.0000 0.00 0.0000 0.0000 .00000 0.0000 0.0000 181
84 93 1 4 1 0 0.012500 0.082600 0.04150 87. 0. 0. 0 0 0.0000 0.00 0.0000 0.0000 .00000 0.0000 0.0000 182
85 86 1 2 1 0 0.021100 0.104600 0.04978 87. 0. 0. 0 0 0.0000 0.00 0.0000 0.0000 .00000 0.0000 0.0000 183
86 87 1 4 1 0 0.028000 0.112000 0.05370 87. 0. 0. 0 0 0.0000 0.00 0.0000 0.0000 .00000 0.0000 0.0000 184
86 88 1 4 1 0 0.044000 0.228000 0.10902 87. 0. 0. 0 0 0.0000 0.00 0.0000 0.0000 .00000 0.0000 0.0000 185
88 96 1 7 1 0 0.074000 0.250000 0.01428 69. 0. 0. 0 0 0.0000 0.00 0.0000 0.0000 .00000 0.0000 0.0000 186
88 106 1 7 1 0 0.007900 0.046800 0.02314 139. 0. 0. 0 0 0.0000 0.00 0.0000 0.0000 .00000 0.0000 0.0000 187
89 86 1 4 1 1 0.000000 0.057000 0.00000 90. 0. 0. 0 0 1.0250 0.00 0.0000 0.0000 .00000 0.0000 0.0000 188
89 90 1 4 1 0 0.069000 0.134000 0.01400 60. 0. 0. 0 0 0.0000 0.00 0.0000 0.0000 .00000 0.0000 0.0000 189
90 96 1 4 1 0 0.183700 0.359000 0.03700 80. 0. 0. 0 0 0.0000 0.00 0.0000 0.0000 .00000 0.0000 0.0000 190
91 92 1 4 1 0 0.015600 0.081900 0.03760 87. 0. 0. 0 0 0.0000 0.00 0.0000 0.0000 .00000 0.0000 0.0000 191
91 93 1 4 1 0 0.014300 0.089500 0.04496 87. 0. 0. 0 0 0.0000 0.00 0.0000 0.0000 .00000 0.0000 0.0000 192
91 94 1 4 1 0 0.014500 0.095700 0.04800 87. 0. 0. 0 0 0.0000 0.00 0.0000 0.0000 .00000 0.0000 0.0000 193
92 102 1 4 1 0 0.015000 0.061000 0.02920 87. 0. 0. 0 0 0.0000 0.00 0.0000 0.0000 .00000 0.0000 0.0000 194
93 42 1 4 1 1 0.000000 0.026000 0.00000 400. 0. 0. 0 0 1.0250 0.00 0.0000 0.0000 .00000 0.0000 0.0000 195
93 108 1 4 1 1 0.000000 0.015400 0.00000 600. 0. 0. 0 0 1.0500 0.00 0.0000 0.0000 .00000 0.0000 0.0000 196
94 103 1 8 1 0 0.022700 0.133300 0.06600 87. 0. 0. 0 0 0.0000 0.00 0.0000 0.0000 .00000 0.0000 0.0000 197
94 107 1 8 1 0 0.061300 0.189100 0.08366 87. 0. 0. 0 0 0.0000 0.00 0.0000 0.0000 .00000 0.0000 0.0000 198
94 109 1 8 1 1 0.000000 0.035000 0.00000 300. 0. 0. 0 0 1.0250 0.00 0.0000 0.0000 .00000 0.0000 0.0000 199
95 91 1 4 1 1 0.005400 0.045800 -0.00360 250. 0. 0. 0 0 1.0200 0.00 0.0000 0.0000 .00000 0.0000 0.0000 200
95 96 1 4 1 0 0.087000 0.212000 0.08600 118. 0. 0. 0 0 0.0000 0.00 0.0000 0.0000 .00000 0.0000 0.0000 201
95 97 1 4 1 0 0.128900 0.280900 0.03348 50. 0. 0. 0 0 0.0000 0.00 0.0000 0.0000 .00000 0.0000 0.0000 202
95 98 1 4 1 0 0.007100 0.043000 0.02246 121. 0. 0. 0 0 0.0000 0.00 0.0000 0.0000 .00000 0.0000 0.0000 203
95 99 1 4 1 1 0.000000 0.068500 0.00000 150. 0. 0. 0 0 1.0300 0.00 0.0000 0.0000 .00000 0.0000 0.0000 204
96 100 1 4 1 0 0.069000 0.161000 0.01850 60. 0. 0. 0 0 0.0000 0.00 0.0000 0.0000 .00000 0.0000 0.0000 205
96 101 1 4 1 1 0.000000 0.103100 0.00000 96. 0. 0. 0 0 1.0300 0.00 0.0000 0.0000 .00000 0.0000 0.0000 206
97 44 1 4 1 1 0.005100 0.100700 -0.00251 84. 0. 0. 0 0 1.0250 0.00 0.0000 0.0000 .00000 0.0000 0.0000 207
98 93 1 4 1 1 0.000600 0.021400 -0.03406 504. 0. 0. 0 0 1.0250 0.00 0.0000 0.0000 .00000 0.0000 0.0000 208
98 105 1 4 1 0 0.148500 0.293000 0.03100 60. 0. 0. 0 0 0.0000 0.00 0.0000 0.0000 .00000 0.0000 0.0000 209
100 104 1 4 1 0 0.062000 0.145000 0.01660 60. 0. 0. 0 0 0.0000 0.00 0.0000 0.0000 .00000 0.0000 0.0000 210
103 123 1 5 1 0 0.182000 0.751000 0.00000 0. 0. 0. 0 0 0.0000 0.00 0.0000 0.0000 .00000 0.0000 0.0000 211
103 124 1 5 1 0 0.000200 0.016700 0.00000 0. 0. 0. 0 0 0.0000 0.00 0.0000 0.0000 .00000 0.0000 0.0000 212
103 125 1 5 1 0 0.027900 0.197200 0.00000 0. 0. 0. 0 0 0.0000 0.00 0.0000 0.0000 .00000 0.0000 0.0000 213
104 34 1 4 1 1 0.008000 0.063700 -0.00330 106. 0. 0. 0 0 1.0000 0.00 0.0000 0.0000 .00000 0.0000 0.0000 214
105 38 1 4 1 1 0.000000 0.116000 0.00000 45. 0. 0. 0 0 1.0250 0.00 0.0000 0.0000 .00000 0.0000 0.0000 215
106 107 1 7 1 0 0.019600 0.061100 0.02684 87. 0. 0. 0 0 0.0000 0.00 0.0000 0.0000 .00000 0.0000 0.0000 216
107 122 1 7 1 0 0.013000 0.062100 0.02960 87. 0. 0. 0 0 0.0000 0.00 0.0000 0.0000 .00000 0.0000 0.0000 217
109 119 1 8 1 0 0.006000 0.057700 0.92900 52. 0. 0. 0 0 0.0000 0.00 0.0000 0.0000 .00000 0.0000 0.0000 218
109 124 1 8 1 0 0.002000 0.022200 0.37820 52. 0. 0. 0 0 0.0000 0.00 0.0000 0.0000 .00000 0.0000 0.0000 219
109 125 1 8 1 0 0.007000 0.062000 1.00000 52. 0. 0. 0 0 0.0000 0.00 0.0000 0.0000 .00000 0.0000 0.0000 220
110 111 1 6 1 0 0.023000 0.099000 0.04600 87. 0. 0. 0 0 0.0000 0.00 0.0000 0.0000 .00000 0.0000 0.0000 221

110 112 1 6 1 1 0.000000 0.018500 0.00000 500. 0. 0. 0 0 1.0000 0.00 0.0000 0.0000 .00000 0.0000 0.0000 222
110 114 1 6 1 1 0.000000 0.076800 0.00000 150. 0. 0. 0 0 1.0400 0.00 0.0000 0.0000 .00000 0.0000 0.0000 223
110 134 1 6 1 0 0.003200 0.025600 0.01346 87. 0. 0. 0 0 0.0000 0.00 0.0000 0.0000 .00000 0.0000 0.0000 224
110 141 1 6 1 0 0.021000 0.064900 0.02872 87. 0. 0. 0 0 0.0000 0.00 0.0000 0.0000 .00000 0.0000 0.0000 225
111 115 1 6 1 0 0.052700 0.221500 0.10300 87. 0. 0. 0 0 0.0000 0.00 0.0000 0.0000 .00000 0.0000 0.0000 226
112 120 1 6 1 0 0.000500 0.004400 0.07200 52. 0. 0. 0 0 0.0000 0.00 0.0000 0.0000 .00000 0.0000 0.0000 227
112 121 1 6 1 1 0.000000 0.019000 0.00000 720. 0. 0. 0 0 1.0500 0.00 0.0000 0.0000 .00000 0.0000 0.0000 228
113 132 1 5 1 0 0.045900 0.291100 0.00000 0. 0. 0. 0 0 0.0000 0.00 0.0000 0.0000 .00000 0.0000 0.0000 229
113 134 1 5 1 0 0.000800 0.007200 0.00380 323. 0. 0. 0 0 0.0000 0.00 0.0000 0.0000 .00000 0.0000 0.0000 230
115 117 1 6 1 0 0.001900 0.015400 0.03300 87. 0. 0. 0 0 0.0000 0.00 0.0000 0.0000 .00000 0.0000 0.0000 231
116 117 1 6 1 0 0.004800 0.039100 0.02144 87. 0. 0. 0 0 0.0000 0.00 0.0000 0.0000 .00000 0.0000 0.0000 232
116 119 1 6 1 1 0.000000 0.009000 0.00000 1000. 0. 0. 0 0 1.0250 0.00 0.0000 0.0000 .00000 0.0000 0.0000 233
116 147 1 6 1 0 0.003500 0.028600 0.01558 87. 0. 0. 0 0 0.0000 0.00 0.0000 0.0000 .00000 0.0000 0.0000 234
117 147 1 6 1 0 0.002200 0.017500 0.01006 87. 0. 0. 0 0 0.0000 0.00 0.0000 0.0000 .00000 0.0000 0.0000 235
120 14 1 11 1 1 0.000300 0.018800 0.00000 500. 0. 0. 0 0 0.9750 0.00 0.0000 0.0000 .00000 0.0000 0.0000 236
120 128 1 11 1 0 0.000400 0.005100 0.10008 718. 0. 0. 0 0 0.0000 0.00 0.0000 0.0000 .00000 0.0000 0.0000 237
120 129 1 11 1 0 0.000300 0.003800 0.06518 718. 0. 0. 0 0 0.0000 0.00 0.0000 0.0000 .00000 0.0000 0.0000 238
122 123 1 6 1 0 0.017500 0.083500 0.03970 87. 0. 0. 0 0 0.0000 0.00 0.0000 0.0000 .00000 0.0000 0.0000 239
123 125 1 5 1 0 0.042300 0.244100 0.00000 0. 0. 0. 0 0 0.0000 0.00 0.0000 0.0000 .00000 0.0000 0.0000 240
124 125 1 5 1 0 0.011300 0.158500 0.00000 0. 0. 0. 0 0 0.0000 0.00 0.0000 0.0000 .00000 0.0000 0.0000 241
124 126 1 5 1 0 0.057700 0.825600 0.00000 0. 0. 0. 0 0 0.0000 0.00 0.0000 0.0000 .00000 0.0000 0.0000 242
125 126 1 5 1 0 0.020100 0.591500 0.00000 0. 0. 0. 0 0 0.0000 0.00 0.0000 0.0000 .00000 0.0000 0.0000 243
126 127 1 5 1 0 0.087700 0.704900 0.00000 0. 0. 0. 0 0 0.0000 0.00 0.0000 0.0000 .00000 0.0000 0.0000 244
128 72 1 11 1 1 0.000400 0.018000 0.00000 500. 0. 0. 0 0 1.0000 0.00 0.0000 0.0000 .00000 0.0000 0.0000 245
129 132 1 11 1 1 0.000400 0.019800 0.00000 500. 0. 0. 0 0 1.0000 0.00 0.0000 0.0000 .00000 0.0000 0.0000 246
133 134 1 6 1 1 0.000000 0.041000 0.00000 160. 0. 0. 0 0 1.0250 0.00 0.0000 0.0000 .00000 0.0000 0.0000 247
133 135 1 6 1 0 0.010900 0.025900 0.00048 63. 0. 0. 0 0 0.0000 0.00 0.0000 0.0000 .00000 0.0000 0.0000 248
133 136 1 6 1 0 0.039000 0.099000 0.00164 57. 0. 0. 0 0 0.0000 0.00 0.0000 0.0000 .00000 0.0000 0.0000 249
133 137 1 6 1 0 0.013400 0.050400 0.00100 87. 0. 0. 0 0 0.0000 0.00 0.0000 0.0000 .00000 0.0000 0.0000 250
135 138 1 6 1 0 0.046600 0.118200 0.00196 57. 0. 0. 0 0 0.0000 0.00 0.0000 0.0000 .00000 0.0000 0.0000 251
136 139 1 6 1 0 0.026000 0.065000 0.00110 57. 0. 0. 0 0 0.0000 0.00 0.0000 0.0000 .00000 0.0000 0.0000 252
137 140 1 6 1 0 0.004100 0.015600 0.00032 87. 0. 0. 0 0 0.0000 0.00 0.0000 0.0000 .00000 0.0000 0.0000 253
138 110 1 6 1 1 0.000000 0.041000 0.00000 160. 0. 0. 0 0 1.0000 0.00 0.0000 0.0000 .00000 0.0000 0.0000 254
138 139 1 6 1 0 0.026000 0.065000 0.00110 57. 0. 0. 0 0 0.0000 0.00 0.0000 0.0000 .00000 0.0000 0.0000 255
138 140 1 6 1 0 0.025100 0.094100 0.00184 87. 0. 0. 0 0 0.0000 0.00 0.0000 0.0000 .00000 0.0000 0.0000 256
138 145 1 6 1 0 0.092300 0.233800 0.00386 57. 0. 0. 0 0 0.0000 0.00 0.0000 0.0000 .00000 0.0000 0.0000 257
142 51 1 6 1 1 0.000000 0.172800 0.00000 83. 0. 0. 0 0 1.0700 0.00 0.0000 0.0000 .00000 0.0000 0.0000 258
142 143 1 6 1 0 0.158200 0.391900 0.00674 63. 0. 0. 0 0 0.0000 0.00 0.0000 0.0000 .00000 0.0000 0.0000 259
142 146 1 6 1 0 0.161800 0.386100 0.00696 63. 0. 0. 0 0 0.0000 0.00 0.0000 0.0000 .00000 0.0000 0.0000 260
143 144 1 6 1 0 0.092700 0.232200 0.00210 63. 0. 0. 0 0 0.0000 0.00 0.0000 0.0000 .00000 0.0000 0.0000 261
144 141 1 6 1 1 0.000000 0.082000 0.00000 80. 0. 0. 0 0 1.0250 0.00 0.0000 0.0000 .00000 0.0000 0.0000 262
144 145 1 6 1 0 0.089000 0.221000 0.00314 57. 0. 0. 0 0 0.0000 0.00 0.0000 0.0000 .00000 0.0000 0.0000 263
144 146 1 6 1 0 0.068000 0.290600 0.00584 87. 0. 0. 0 0 0.0000 0.00 0.0000 0.0000 .00000 0.0000 0.0000 264
148 116 1 6 1 1 0.000000 0.041000 0.00000 160. 0. 0. 0 0 1.0000 0.00 0.0000 0.0000 .00000 0.0000 0.0000 265
149 26 1 2 1 1 0.000000 0.038600 0.00000 300. 0. 0. 0 0 1.0000 0.00 0.0000 0.0000 .00000 0.0000 0.0000 266
149 26 1 2 2 1 0.000000 0.038600 0.00000 300. 0. 0. 0 0 1.0000 0.00 0.0000 0.0000 .00000 0.0000 0.0000 267
149 150 1 2 1 0 0.001000 0.008500 0.00198 87. 0. 0. 0 0 0.0000 0.00 0.0000 0.0000 .00000 0.0000 0.0000 268
149 151 1 2 1 0 0.003900 0.026200 0.01384 87. 0. 0. 0 0 0.0000 0.00 0.0000 0.0000 .00000 0.0000 0.0000 269
149 152 1 2 1 0 0.025300 0.116800 0.05444 87. 0. 0. 0 0 0.0000 0.00 0.0000 0.0000 .00000 0.0000 0.0000 270
151 161 1 2 1 0 0.002100 0.013800 0.00750 87. 0. 0. 0 0 0.0000 0.00 0.0000 0.0000 .00000 0.0000 0.0000 271
153 70 1 2 1 1 0.000000 0.091600 0.00000 93. 0. 0. 0 0 1.0000 0.00 0.0000 0.0000 .00000 0.0000 0.0000 272
153 70 1 2 2 1 0.000000 0.091600 0.00000 93. 0. 0. 0 0 1.0000 0.00 0.0000 0.0000 .00000 0.0000 0.0000 273
153 154 1 2 1 0 0.071000 0.284100 0.00536 72. 0. 0. 0 0 0.0000 0.00 0.0000 0.0000 .00000 0.0000 0.0000 274
153 155 1 2 1 0 0.043000 0.185600 0.00388 96. 0. 0. 0 0 0.0000 0.00 0.0000 0.0000 .00000 0.0000 0.0000 275

154 156 1 2 1 0 0.015500 0.037900 0.00072 72. 0. 0. 0 0 0.0000 0.00 0.0000 0.0000 .00000 0.0000 0.0000 276
154 160 1 2 1 0 0.010200 0.042900 0.00094 72. 0. 0. 0 0 0.0000 0.00 0.0000 0.0000 .00000 0.0000 0.0000 277
155 156 1 2 1 0 0.017600 0.082200 0.00150 96. 0. 0. 0 0 0.0000 0.00 0.0000 0.0000 .00000 0.0000 0.0000 278
156 157 1 2 1 0 0.053000 0.127300 0.00218 48. 0. 0. 0 0 0.0000 0.00 0.0000 0.0000 .00000 0.0000 0.0000 279
157 55 1 2 1 1 0.000000 0.082700 0.00000 150. 0. 0. 0 0 1.0000 0.00 0.0000 0.0000 .00000 0.0000 0.0000 280
157 158 1 2 1 0 0.048900 0.140400 0.00282 72. 0. 0. 0 0 0.0000 0.00 0.0000 0.0000 .00000 0.0000 0.0000 281
158 159 1 2 1 0 0.033900 0.066400 0.00120 72. 0. 0. 0 0 0.0000 0.00 0.0000 0.0000 .00000 0.0000 0.0000 282
159 160 1 2 1 0 0.019000 0.081100 0.01200 72. 0. 0. 0 0 0.0000 0.00 0.0000 0.0000 .00000 0.0000 0.0000 283
161 162 1 2 1 0 0.002200 0.010300 0.00534 87. 0. 0. 0 0 0.0000 0.00 0.0000 0.0000 .00000 0.0000 0.0000 284
-999
LOSS ZONES FOLLOWS 12 ITEMS
-99
INTERCHANGE DATA FOLLOWS 0 ITEMS (HEADER)
-9
TIE LINES FOLLOW 0 ITEMS (HEADER)
-999

- The ISU format of the dynamic data of the Iowa System

MODIFIED IOWA SYSTEM STABILITY RELATED PARAMETERS OF GENERATOR
& EXCITATION & GOVERNOR & SVC & OLTC & DYNAMIC LOADS
Generator transient parameter follows
1 2 3 4 5 6 7 8 9 10 11
Num Gen_name Xd Xq X'd X'q Rs T'do T'qo Mg Dg
3 STJO 712 0.1000 0.0690 0.0040 0.0690 0.0002 10.2000 0.010 1000.000 5.000
6 COOPR1G 100 0.2590 0.2820 0.0437 0.1700 0.0002 6.5600 1.5000 69.120 5.000
15 FTRAD 4 0.2590 0.2820 0.0100 0.1700 0.0002 6.5600 1.5000 800.000 5.000
27 WILMRT 3 0.2500 0.2370 0.0050 0.0880 0.0002 5.7000 1.5000 800.000 5.000
73 NEAL12G 100 0.2540 0.2410 0.0507 0.0810 0.0060 7.3000 0.4000 33.580 5.000
76 NEAL34G 100 0.2950 0.2920 0.0206 0.1860 0.0002 5.6600 1.5000 64.980 5.000
99 PRARK4G 100 0.2900 0.2800 0.1131 0.0910 0.0010 6.7000 0.4100 13.300 5.000
101 MTOW 3G 100 0.2110 0.2050 0.3115 0.0590 0.0002 4.7900 1.9600 5.320 5.000
108 AROL 1G 100 0.0200 0.0190 0.0535 0.0080 0.0002 7.0000 0.7000 59.200 10.000
114 C.BL12G 100 0.0200 0.0190 0.1770 0.0080 0.0002 7.0000 0.7000 10.000 10.000
118 DPS 57G 100 0.0200 0.0190 0.1049 0.0080 0.0002 7.0000 0.7000 22.620 10.000
121 C.BL 3G 100 0.0200 0.0190 0.0297 0.0080 0.0002 7.0000 0.7000 39.580 10.000
124 DVNPT 3 0.0200 0.0190 0.0020 0.0080 0.0002 7.0000 0.7000 2000.000 10.000
125 PALM 710 0.0200 0.0190 0.0020 0.0080 0.0002 7.0000 0.7000 2000.000 10.000
126 PR ILD 3 0.0200 0.0190 0.0040 0.0080 0.0002 7.0000 0.7000 1000.000 10.000
130 FT.CL1G 100 0.0200 0.0190 0.0559 0.0080 0.0002 7.0000 0.7000 57.200 10.000
131 NEBCY1G 100 0.0200 0.0190 0.0544 0.0080 0.0002 7.0000 0.7000 41.320 10.000
-999
Generator control system (exciter + AVR + governor) parameter follows
Num Gen_name Ke Te Se Ka Ta Kf Tf Tch Tg Rg
3 STJO 712 1.0000 0.2500 0.0000 20.0000 0.0600 0.0400 1.0000 1.6000 0.2000 0.0500
6 COOPR1G 100 1.0000 0.4100 0.0000 40.0000 0.0500 0.0600 0.5000 54.1000 0.4500 0.0500
15 FTRAD 4 1.0000 0.5000 0.0000 40.0000 0.0600 0.0800 1.0000 10.0000 3.0000 0.0500
27 WILMRT 3 1.0000 0.5000 0.0000 40.0000 0.0600 0.0800 1.0000 10.1800 0.2400 0.0500
73 NEAL12G 100 1.0000 0.7900 0.0000 30.0000 0.0200 0.0300 1.0000 9.7900 0.1200 0.0500
76 NEAL34G 100 1.0000 0.4700 0.0000 40.0000 0.0200 0.0800 1.2500 10.0000 3.0000 0.0500
99 PRARK4G 100 1.0000 0.7300 0.0000 30.0000 0.0200 0.0300 1.0000 7.6800 0.2000 0.0500
101 MTOW 3G 100 1.0000 0.5300 0.0000 40.0000 0.0200 0.0900 1.2600 7.0000 3.0000 0.0500
108 AROL 1G 100 1.0000 1.4000 0.0000 20.0000 0.0200 0.0300 1.0000 6.1000 0.3800 0.0500
114 C.BL12G 100 1.0000 1.0000 0.0000 20.0000 0.0200 0.0300 1.0000 10.0000 2.0000 0.0500
118 DPS 57G 100 1.0000 1.0000 0.0000 20.0000 0.0200 0.0300 1.0000 10.0000 2.0000 0.0500

121 C.BL 3G 100 1.0000 1.0000 0.0000 20.0000 0.0200 0.0300 1.0000 10.0000 2.0000 0.0500
124 DVNPT 3 1.0000 1.0000 0.0000 20.0000 0.0200 0.0300 1.0000 10.0000 2.0000 0.0500
125 PALM 710 1.0000 1.0000 0.0000 20.0000 0.0200 0.0300 1.0000 10.0000 2.0000 0.0500
126 PR ILD 3 1.0000 1.0000 0.0000 20.0000 0.0200 0.0300 1.0000 10.0000 2.0000 0.0500
130 FT.CL1G 100 1.0000 1.0000 0.0000 20.0000 0.0200 0.0300 1.0000 10.0000 2.0000 0.0500
131 NEBCY1G 100 1.0000 1.0000 0.0000 20.0000 0.0200 0.0300 1.0000 10.0000 2.0000 0.0500
-999
Dynamic loads data follows
Num Bus_name TpL TqL ALd BLd ALph Beta
-999
Static var compensator data follows
Num Bus_name Ksvs Tsvs Vsvsr
-999
On load tap-changer data follows
S_N Secondary_Bus P_N Prime_Bus Tr Vrr
-999

- The ISU format of the governor and AVR limits data file for the Iowa System

IOWA SYSTEM

THE AVR VOLTAGE LIMITS-FIELD CURRENT

---

3 4.9000
6 4.9000
15 6.4500
27 8.2500
73 8.2300
76 3.9000
99 3.7500
101 1.1400
108 1.0600
114 3.4500
118 1.0500
121 3.4000
124 3.6500
125 3.7500
126 1.2000
130 3.4500
131 3.2500
-999

THE GOVERNOR LIMITS-PGSMAX

---

3 25.0000
6 10.0000
15 18.0000
27 18.0000
73 6.0000
76 13.5000
99 2.0000
101 2.0000
108 7.0000
114 1.7000
118 3.2000

```
121 7.8000
124 33.0000
125 25.0000
126 31.0000
130 6.0000
131 7.2500
-999
```

- The ISU format of the scenario control file for the Iowa System

```
POWER SYSTEM EQUILIBRIA TRACING - VOLTAGE STABILITY ANALYSIS
BO LONG AND V. AJJARAPU
DEPARTMENT OF ELECTRICAL AND COMPUTER ENGINEERING
IOWA STATE UNIVERSITY
COMPANY: IOWA STATE UNIVERSITY
BASE CASE: IOWA SYSTEM
OUTAGES: none
-999
LINE RATING TO USE IN ANALYSIS (1,2, OR 3)
2
C************************************************************
LOCATION OF LOAD INCREASE FOR LOAD/GENERATION INCREASE SCENARIO
----------------------------------------
INITIAL LOAD
BUS NAME P(MW) Q(MVAR)
--- ------ ------ ------
C************************************************************
BUS NUMBERS WHERE LOAD IS TO BE INCREASED
18 1.0 1.0
20 1.0 1.0
22 1.0 1.0
30 1.0 1.0
32 1.0 1.0
52 1.0 1.0
59 1.0 1.0
80 1.0 1.0
82 1.0 1.0
87 1.0 1.0
89 1.0 1.0
-999
C************************************************************
LOCATION OF GENERATION INCREASE FOR LOAD/GENERATION INCREASE SCENARIO
----------------------------------------
BUS NAME AREA OUTPUT(MW) + --- ------- --- ------ --------
C************************************************************
BUS NUMBER, SCALING FACTOR
3
6
15
27
73
76
99
101
108
```

```
114
118
121
124
125
126
130
131
-999
C*******************************************************
LOCATION OF INCREASE FOR REACTIVE LOAD INCREASE SCENARIO
————————————————————————
INITIAL LOAD
BUS NAME P(MW) Q(MVAR)
—. ———— ———— ————-
C*******************************************************
BUS NUMBERS WHERE REACTIVE LOAD IS TO BE ADDED
-999
C*******************************************************
LOCATION OF EXPORTING UNITS FOR IMPORT/EXPORT SCENARIO
————————————————————
BUS NAME AREA OUTPUT(MW) + —. ———— —. ———. ————————
C*******************************************************
BUS NUMBER, SCALING FACTOR
-999
C*******************************************************
LOCATION OF IMPORTING UNITS FOR IMPORT/EXPORT SCENARIO
————————————————————
BUS NAME AREA OUTPUT(MW) - —. ———— —. ———. ————————
C*******************************************************
BUS NUMBER, SCALING FACTOR
-999
C*************************************************************
LOCATION OF LOAD INCREASE FOR LOAD/IMPORT SCENARIO
————————————————————
INITIAL LOAD
BUS NAME P(MW) Q(MVAR)
—. ———— ———— ————-
C*************************************************************
BUS NUMBERS WHERE LOAD IS TO BE INCREASED AND SERVED FROM OUTSIDE
-999
C*******************************************************
LOCATION OF GENERATION INCREASE FOR LOAD/IMPORT SCENARIO
————————————————————————
BUS NAME AREA OUTPUT(MW) + —. ———— —. ———. ————————
C*******************************************************
BUS NUMBER, SCALING FACTOR
-999 0
C***********************
BUSES TO MONITER
————————-
BUS NAME AREA
—. ———— —.
C***********************
```

BUS NUMBERS
6
19
48
57
73
76
98
99
191
114
118
121
123
125
130
131
-999
CONVERGENCE TOLERANCE FOR POWER FLOW
0.001000
MAXIMUM NUMBER OF ITERATIONS ALLOWED
30
NUMBER OF WEAK BUSES TO MONITER
10

- The load participation factors of the generators

3 .114679
6 .045527
15 .086009
27 .086009
73 .025631
76 .060493
99 .007506
101 .004702
108 .031601
114 .007511
118 .009920
121 .035550
124 .147420
125 .136926
126 .141456
130 .026089
131 .032970

BIBLIOGRAPHY

[1] P. Kundur, *Power System Control and Stability.* New York: McGraw Hill, 1994.

[2] C. Taylor, *Power System Voltage Stability.* New York: McGraw Hill, 1993.

[3] C. Taylor, "Engineering challenges in the new environment," in *invited speech at the 28th North American Power Symposium, MIT, Cambridge, MA, 96,* (Boston), 1996.

[4] *Voltage Stability of Power Systems: Concepts, Analytical Tools, and Industry Experience,* IEEE Working Group on Voltage Stability, 1990.

[5] *Criteria and Counter Measure for Voltage Collapse,* CIGRE Task Force 38.02.12, 1994.

[6] E. Allgower and K. Georg, *Numerical Continuation Methods.* New York: Springer-Verlag, 1990.

[7] R. Kalaba, "Solving nonlinear equations by adaptive homotopy continuation," *Applied Mathematics and Computation,* vol. 42, pp. 99–115, 1991.

[8] A. P. Morgan, *Solving Polynomial Systems Using Continuation for Engineering and Scientific Problems.* Englewood, Cliffs, NJ: Prentice Hall, 1987.

[9] L. T. Watson *et al.*, "Tracing nonlinear equilibrium paths by homotopy method," *Nonlinear Analysis, Theory, Methods and Applications,* vol. 8, no. 11, pp. 1271–1282, 1983.

[10] M. Kubicek and M. Marek, *Computational Methods in Bifurcation Theory and Dissipative Structures.* New York: Springer-Verlag, 1983.

[11] W. C. Rheinboldt and J. Burkardt, "A locally parameterized continuation process," *ACM Trans. of Math. Software,* pp. 215–235, 1983.

[12] R. Seydel, *From Equilibrium to Chaos: Practical Bifurcation and Stability Analysis.* New York: Elsevier, 1988.

[13] R. Seydel, *Practical Bifurcation and Stability Analysis.* New York: Springer-Verlag, 1995.

[14] D. Davidenko, "On a new method of numerically integrating a system of nonlinear equations," *Dokl., Akad. Nauk, USSR*, vol. 88, pp. 601–614, 1953.

[15] R. J. Thomas, R. D. Barnard, and J. Meisel, "The generation of quasi steady-state load-flow trajectories and multiple singular point solutions," *IEEE Trans. on Power Apparatus and Systems*, vol. PAS90, pp. 1967–1974, May 1971.

[16] V. Ajjarapu and N. Jain, "Optimal continuation power flow," *Electric Power Systems Research*, vol. 35, pp. 17–24, 1995.

[17] V. Ajjarapu, P.L.Lau, and S.Battula, "Optimal reactive power planning strategy against voltage collapse," *IEEE Trasactions on Power Systems*, vol. 9, pp. 906–917, May 1994.

[18] V. Ajjarapu, "The role of bifurcation and continuation methods in the analysis of voltage collapse," *Sadhana*, vol. 18, pp. 829–841, September 1993.

[19] V. Ajjarapu and C. Christy, "The continuation power flow: A tool for steady state voltage stability analysis," *IEEE Trasactions on Power Systems*, vol. 7, pp. 417–423, February 1992.

[20] V. Ajjarapu and B. Lee, "Bifurcation and its application to nonlinear dynamical phenomena in an electrical power system," *IEEE Trasactions on Power Systems*, vol. 7, pp. 424–431, February 1992.

[21] V. Ajjarapu, "Identification of steady state voltage stability in power systems," *Int. J. of Energy Systems*, vol. 11, pp. 43–46, 1991.

[22] K. C. Almeida, F. D. Galiana, and S. Soares, "A general parametric optimal power flow," in *IEEE Power Industry Computer Applications (PICA)*, pp. 66–73, 1993.

[23] F. L. Alvarado, I. Dobson, and Y. Hu, "Computation of closest bifurcations in power systems," *IEEE Trans. on Power Systems*, vol. 9, pp. 918–928, May 1994.

[24] C. A. Canizares and F. L. Alvarado, "Point of collapse and continuation methods for large ac/dc systems," *IEEE Trans. on Power Systems*, vol. 8, pp. 1–8, February 1993.

[25] C. A. Canizares, F. L. Alvarado, C. L. Demarco, I. Dobson, and W. F. Long, "Point of collapse methods applied to ac/dc power systems," *IEEE Trans. on Power Systems*, vol. 7, pp. 673–683, May 1992.

[26] Cañizares and F. Alvarado, "Computational experience with the point of collapse method on very large scale ac/dc systems," in *Bulk Power System Voltage Phenomena-Voltage Stability and Security Workshop, Deeplake, MD*, pp. 103–113, August 1991.

[27] H. D. Chiang and R. Jean-Jumeau, "A more efficient formulation for computation of the maximum loading points in electric power systems," *IEEE Trans. on Power Systems*, vol. 10, pp. 584–592, May 1995.

[28] H. D. Chiang, A. J. Flueck, K. S. Shah, and N. Balu, "Cpflow: A practical tool for tracing power system steady-state stationary behavior due to the load and generation variations," *IEEE Trans. on Power Systems*, vol. 10, pp. 623–634, May 1994.

[29] T. V. Cutsem, "An approach to corrective control of voltage instability using simulation and sensitivity," *IEEE Trans. on Power Systems*, vol. 10, pp. 616–622, May 1995.

[30] T. V. Cutsem, Y. Jacquemart, J. Marquet, and P. Pruvot, "A comprehensive analysis of mid-term voltage stability," in *IEEE/PES WM, 511-6 PWRS 1994, San Francisco*, July 1994.

[31] I. Dobson and L. Lu, "New methods for computing a closest saddle node bifurcation and worst case load power margin for voltage collapse," *IEEE Trans. on Power Systems*, vol. 8, pp. 905–913, August 1993.

[32] I. Dobson, "Computing a closest bifurcation instability in multidimensional parameter space," *Journal of Nonlinear Science*, vol. 3, no. 3, pp. 307–327, 1993.

[33] I. Dobson and L. Lu, "Computing an optimum direction in control space to avoid saddle node bifurcations and voltage collapse in electric power systems," *IEEE Trans. on Automatic Control*, vol. 37, pp. 1616–1620, October 1992.

[34] I. Dobson, "Observations on the geometry of saddle node bifurcation and voltage collapse in electrc power systems," *IEEE Trans. on Circuits and Systems Part I*, vol. 39, pp. 240–243, March 1992.

[35] I. Dobson and H. D. Chiang, "Toward a theory of voltage collapse in electric power systems," *Systems and Control Letters*, vol. 13, pp. 253–262, September 1989.

[36] A. Fahmideh-Vojdani and F. Galiana, "The continuation method and its application in system planning and operation," in *CIGRE Symposium*, vol. 39-83, (Florence, Italy), 1983.

[37] A. J. Flueck, H. D. Chiang, and K. S. Shah, "Investigating the installed real power transfer of a large scale power system under a proposed multiarea interchange schdule using cpflow," in *IEEE/PES SPM, 550-4 PWRS 1995*, July 1995.

[38] M. Huneault and F. D. Galiana, "An investigation of the solution of the optimal power flow problem incorporating continuation methods," *IEEE Trans. on Power Systems*, vol. 5, pp. 103–110, February 1990.

[39] M. Huneault, A. R. Fahmideh-Vojdani, M. Juman, R. Calderon, and F. D. Galiana, "The continuation method in power system optimization: Application to economy-security functions," *IEEE Trans. on Power Appar. Syst. PAS-104(1985)*, vol. PAS-104, pp. 114–124, February 1985.

[40] K. Iba *et al.*, "Calculation of critical loading condition with nose curve using homotopy continuation method," *IEEE Trans. on Power Systems*, vol. 6, pp. 584–593, May 1991.

[41] B. Lee and V. Ajjarapu, "Invariant subspace parametric sensitivity (isps) of structure preserving power system models," *IEEE Trans. on Power Systems*, vol. 11, pp. 845–850, May 1996.

[42] J. Lu, C.W.Liu, and J.S.Thorp, "New methods for computing a saddle node bifurcation point for voltage stability analysis," *IEEE Trans. on Power Systems*, vol. 10, pp. 978–989, May 1995.

[43] R. A. Ponrajah and F. Galiana, "The minimum cost optimal power flow problem solver via the restart homotopy continuation method," *IEEE Trans. on Power Systems*, vol. 4, pp. 139–148, February 1989.

[44] N. Yorino, S. Harada, and H. Chen, "A method to approximate a closest loadability limit using multiple load flow solutions," in *IEEE/PES Winter Meeting*, vol. 309-5-PWRS, (Baltimore, MD), 1996.

[45] A. S. G. Moore, "The calculation of turning points of nonlinear equations," *SIAM J. Numer. Anal*, vol. 17, pp. 567–576, May 1980.

[46] P. Sauer and M. Pai, "Power system steady-state stability and the load-flow jacobian," *IEEE Trans. on Power and Systems*, vol. 5, pp. 1374–1381, November 1990.

[47] P. M. Anderson and A. A. Fouad, *Power System Stability and Control.* New York: IEEE PES Press, 1994.

[48] V. Ajjarapu, Z. H. Feng, and B. Long, "A novel approach to trace total power system equilibria," in *Submitted to IEEE Winter Power Meeting 1998*, Jan. 1998.

[49] C. Taylor, ed., *Indices Predicating Voltage Collapse Including Dynamic Phenomena*, CIGRE Task Force 38.02.11, 1994.

[50] Venikov, A. Stroev, I. Idelchick, and I. Tarasov, "Estimation of electric power system steady-state stability in load flow calculation," *IEEE Trans. on Power Appar. Syst. PAS-94(1975)*, vol. PAS-94, pp. 1034–1041, May 1975.

[51] C. A. Canizares, A. C. Z. de Souza, and V. H. Quintana, "Comparison of performance indices for detection of proximity to voltage collapse," in *IEEE Summer Power Meeting, Paper 95 SM 583-5 PWRS*, July 1995.

[52] T. V. Cutsem, "A method to compute the reactive power margins with respect to voltage collapse," *IEEE Trans. on Power Systems*, vol. 6, pp. 145–156, Feb. 1991.

[53] T. J. Overbye, I. Dobson, and C. L. DeMarco, "Q-v curve interpretation of energy measure for voltage security," *IEEE Trans. on Power Systems*, vol. 9, pp. 331–340, February 1994.

[54] T. Smed, "Feasible eigenvalue sensitivity for large power systems," *IEEE Trans. on Power and Systems*, vol. 8, pp. 555–563, May 1990.

[55] Fernandes, P. Sauer, and M. A. Pai, "Quantification of parameter importance in power system steady state stability analysis," in *the 28th North American Power Symposium, MIT, Cambridge, MA, 96*, pp. 131–135, 1996.

[56] L. A. Zadeh and C. A. Desoer, *Linear Systems Theory-The State Space Approach.* New York: McGraw-hill, 1963.

[57] N. Martins, "Efficient eigenvalue and frequency response methods applied to power system small signal stability studies," *IEEE Trans. on Power and Systems*, vol. 1, pp. 217–226, February 1986.

[58] L. Wang and A. Semlyn, "Application of sparse eigenvalue techniques to the small signal stability analysis of large power systems," *IEEE Trans. on Power and Systems*, vol. 5, pp. 635–642, May 1990.

[59] B. Lee, *A Unified Framework to Study the Voltage Stability of the Structure Preserving Power System Model.* PhD thesis, Iowa State University, Ames, Iowa, 1994.

[60] S. Greene, I. Dobson, and F. L. Alvarado, "Sensitivity of the loading margin to voltage collapse with respect to arbitrary parameters," in *IEEE/PES WM, 278-2-PWRS 1996, Baltimore*, Jan. 1996.

[61] D. Kincaid and W. Cheney, *Numerical Analysis.* Pacific Grove, California: Brooks/Cole, 1991.

[62] A. Semlyn and L. Wang, "Sequential computation of the complete eigensystem for the study zone in small signal stability analysis of of large power systems," *IEEE Trans. on Power and Systems*, vol. 3, pp. 715–725, May 1988.

ACKNOWLEDGEMENTS

My sincere appreciation undoubtedly first goes to my major professor - Dr. Venkataramana Ajjarapu. His financial support and academic guidance made this work possible. His constant attention and instructive suggestions were essential during all stages of the research. All these add up to an earnest thanks.

I would also like to express my gratitude to Dr. Vijay Vittal and Dr. James D. McCalley who encouraged me to apply for the power program at ISU. My appreciation is also extended to Dr. John Lamont and Dr. Dragan Mirković who spent time being my committee members.

Dr. Zhihong Feng is yet another person to whom I want to say thank you. His rich experiences in power systems engineering made the many conversations with him always informative and enjoyable.

Finally and most of all, the love, care and moral support from my parents are forever the lights in my life. I thank all my family members including my brother for giving me the strongest motivations for diligent work and great achievements.